Molecular analyses of the Class B synthetic multivulva genes of *Caenorhabditis elegans*

by Xiaowei Lu
B.S. Biochemistry, Beijing University, 1991

Submitted to the Department of Biology
in partial fulfillment of the requirements for the degree of

DOCTOR OF PHILOSOPHY

at the
MASSACHUSETTS INSTITUTE OF TECHNOLOGY

February 1999

Signature of Author: _____
Department of Biology
February 1999

Certified by: _____
H. Robert Horvitz
Professor of Biology
Thesis Supervisor

Accepted by: _____
Alan D. Grossman
Chairman of the Graduate Committee
Department of Biology

Molecular analyses of the class B synthetic multivulva genes of *Caenorhabditis elegans*

Xiaowei Lu

ABSTRACT

Ras signaling during vulval development in *C. elegans* is antagonized by the activity of the synthetic mulitivulva genes. These genes fall into two functionally redundant classes, class A and class B. Inactivation of both A and B activity results in a multivulva phenotype as a consequence of ectopic expression of vulval cell fates. By contrast, mutations in either class alone have no visible vulval phenotypes. To elucidate the molecular mechanisms by which the synthetic multivulva genes antagonize Ras signaling activity, we have characterized the class B synthetic multivulva genes, *lin-35*, *lin-53* and *lin-37*. *lin-35* encodes a protein similar to the retinoblastoma tumor suppressor protein Rb and related p107 and p130. *lin-53* encodes a 7 WD-repeat protein similar to RbAp48 and RbAp46, two related mammalian Rb-binding proteins that are also implicated in chromatin remodeling. *lin-37* encodes a novel protein. We also identified *hda-1*, a *C. elegans* deacetylase gene, as a class B synthetic multivulva gene. We showed that the LIN-35 Rb protein is expressed in the vulval precursor cells and their descendants during vulval development, and that LIN-35 Rb, LIN-53 p48 and HDA-1 physically interact with one another *in vitro*. Taken together, these results led us to propose that the class B synthetic multivulva genes act to repress transcription of vulval cell fate genes mediated by the LIN-35 Rb/LIN-53 p48/HDA-1 repressor complex.

Thesis supervisor: H. Robert Horvitz

Title: Professor of Biology

Acknowledgments

I would like to thank my thesis advisor, Bob Horvitz, for setting a great example to me as a dedicated scientist, and for providing an excellent environment that nurtures intellectual curiosity and critical thinking. I would also like to thank the members of my thesis committee, Tyler Jacks, Monty Krieger, Chris Kaiser and Ed Harlow for their help and encouragement along the way.

I would like to thank all the members of the Horvitz lab for their friendship and their inputs over the course of this work, especially Scott Clark for teaching me *C. elegans* genetics and molecular biology when I first joined the lab, Jeff Thomas, Craig Ceol and Ewa Davison for making this work more fun and exciting, Zheng Zhou, Mark Alkema, Barbara Conradt, Mark Metzstein, Gillian Stanfield, Liz Speliotes, Yi-Chun Wu and Sander van den Heuvel for helpful ideas and discussions, Beth James for her meticulous and skillful deciphering of DNA sequences, and Na An for her numerous helps both in and out of the lab.

I am very grateful to my family, my parents Yongquan Kuang and Derong Lu and my brothers Haifeng Lu and Yungang Lu, who have always been loving and supportive, and my grandaunt Tingyun Kuang, who first led me into the world of science.

Finally, I would like to dedicate this work to my husband and my best friend, Wei Wang. I would never have completed this work without his love, support, patience and the joy he brought to my life.

Table of Contents

Chapter 1

The retinoblastoma protein family

Xiaowei Lu

Howard Hughes Medical Institute, Massachusetts Institute of Technology
Cambridge, MA 02139

Summary

The retinoblastoma tumor suppressor protein Rb has been extensively studied for the past decade. Rb appears to integrate multiple intercellular signals and regulate transcription correspondingly to control proliferation, differentiation and apoptosis. Many Rb-related proteins have been identified, including the mammalian p107 and p130. p107 and p130 have functions distinct from and also partially overlapping with those of Rb. The identification of Rb-related proteins in invertebrates including *Drosophila* and *C. elegans* suggests that the functions of Rb have been well conserved during evolution. Furthermore, genetic studies in *Drosophila* and *C. elegans* have shed light on developmental control of cell cycle in the context of pattern formation and cell fate specification, and promise further insight into pathways implicated in development as well as in disease.

Overview of cell cycle

A cell can sense and respond to extracellular signals and undergo proliferation, differentiation or programmed cell death (apoptosis). These processes are intricately regulated by a vast network of cellular pathways to ensure proper response to the environment and homeostasis of multicellular organisms. Two tumor suppressor pathways mediated by the retinoblastoma protein Rb and p53, respectively, are of fundamental importance. This is underscored by their frequent concurrent inactivation in the development of human cancer. Rb regulates cell cycle progression, as I will describe in more detail in this chapter. p53 functions as a cell cycle checkpoint by activating transcription of genes that induce cell cycle arrest or apoptosis in response to stress such as DNA damage (reviewed by Levine, 1997). Inactivation of these two pathways lead to uncontrolled proliferation and escape from cell cycle arrest/apoptosis following DNA damage, which have been proposed to be critical events that lead to malignancy (reviewed by Sherr, 1996).

The cell cycle serves to ensure that DNA is faithfully replicated once and that identical chromosomal copies are segregated equally into two daughter cells (Heichman and Roberts, 1994). It is typically composed of G1 (for Gap 1), S (for DNA Synthesis), G2 (for Gap 2) and M (for mitosis) phases. The mammalian cell cycle is driven by the sequential formation, activation, and subsequent inactivation of a series of cyclin/cyclin-dependent kinase (CDK) complexes. The D-type cyclins (cyclin D1, D2, D3) complexed with CDK4 or CDK6 regulate progression through G1 phase, cyclin E-CDK2 regulates entry into S phase, cyclin A-CDK2 regulates progression through S phase, and cyclins A or B-cdc2 complexes regulate entry into M phase (Figure 1). The activities of CDKs are regulated by their respective partner cyclins, by phosphorylation and dephosphorylation, and by the CDK inhibitor (CKI) proteins in a cell-cycle dependent manner (reviewed by Lees, 1995; Morgan, 1995; Sherr and Roberts, 1995). There are two families of CKIs: the INK4 inhibitors, which include p16, p15 and p18, specifically inactivate cyclin D-CDK4/6, while the CIP/KIP inhibitors, which include p21, p27 and p57, inhibit a broad spectrum of cyclin-CDK complexes (reviewed by Sherr and Roberts, 1995). The

G1 to S and G2 to M transitions represent two checkpoints where a number of surveillance systems operate to prevent premature entry into the next phase of the cell cycle.

Restriction point and G1 to S transition

Passage through the Restriction (R) point (Pardee, 1989), a time point in G1 beyond which cells become irreversibly committed to progression through the cell cycle, is regulated by the retinoblastoma tumor suppressor protein Rb (reviewed by Bartek et al., 1996; Weinberg, 1995). Active, hypophosphorylated Rb associates with the E2F transcription factors to repress transcription of E2F responsive genes, many of which are involved in DNA synthesis or cell cycle control (see below). Hyperphosphorylation of Rb dissociates Rb/E2F complexes, resulting in expression of E2F genes and G1 to S transition.

Inactivation of Rb is mediated by the sequential, cooperative phosphorylation first by cyclin D-CDK4/6 and then cyclin E-CDK2 complexes (Hatakeyama et al., 1994; Lundberg and Weinberg, 1998). Thus, cell cycle progression is controlled by a negative regulatory pathway composed of p16 CKI, cyclin D-CDK4 and Rb. This growth control pathway is frequently targeted in human cancer (Figure 2). In quiescent cells, cyclin D level is low as a result of rapid turnover and Rb is hypophosphorylated. Mitogenic signals can jumpstart the cell cycle machinery by induction of cyclin D expression to overcome CKI inhibition. Activated cyclin D-CDK4/6 complexes initiate Rb phosphorylation leading to its subsequent inactivation. Rb represses p16 transcription, thus forming a negative feedback loop to limit duration of cyclin D activation: upon Rb inactivation by cyclin D, p16 expression is derepressed, high p16 level leads to disruption of cyclin D-cdk4/6 complexes and subsequent degradation of cyclin D. Growth inhibitory signals such as glucocorticoids, TGF-β, cyclic AMP and contact inhibition, upregulate expression and/or activity of CKIs or downregulate cyclin D and CDK4/6 to block Rb phosphorylation resulting in cell cycle arrest (Rogatsky et al., 1997; reviewed by Weinberg, 1995).

Rb is also phosphorylated in S and near the G2 to M transition, presumably by cyclin A-CDK2 and cyclin B-cdc2. During mitosis, Rb is rapidly dephosphorylated by an anaphase-specific phosphatase, probably protein phosphatase type 1 (PP-1), and stays hypophosphorylated in

G0/early G1 (reviewed by Mittnacht, 1998). This cell-cycle dependent phosphorylation of Rb suggests that Rb activity must be tightly regulated throughout the cell cycle.

The function of Rb is not limited to G1 regulation and is important in other cellular processes, such as differentiation and apoptosis protection (reviewed by Wang, 1997; Yee et al., 1998). The versatility of Rb is manifested by the fact that Rb has been reported to bind and regulate some forty cellular proteins, many of which are involved in transcription, although the physiological significance of many of these protein interactions remains to be established (reviewed by Taya, 1997).

Phenotypes of Rb-deficient mice

Rb-/- mice die *in utero* between the 14^{th} and 15^{th} day of gestation, with defects in hematopoiesis as well as the central and peripheral nervous systems, including excessive proliferation and excessive cell death. Interestingly, unlike humans carrying a germline mutation in one copy of the retinoblastoma gene, who develop childhood bilateral retinoblastoma, Rb+/- mice did not develop retinoblastoma but were predisposed to malignancy and often developed pituitary and thyroid tumors. In addition to abnormalities in cell cycle regulation, the differentiation of multiple tissues also appeared defective (reviewed by Mulligan and Jacks, 1998).

Rb-/- cells have a G1 phase that is 3 to 4 hours shorter than that of Rb+/+ cells. Interestingly, Rb-/- cells exhibit the same serum-dependence as Rb+/+ cells, but the requirement of protein synthesis for passage through the R point appeared to be largely bypassed in Rb-/- cells (Herrera et al., 1996a). In Rb-/- cells, chromatin structure appeared more relaxed, likely as a result of reduced histone H1 phosphorylation by CDK2 (Herrera et al., 1996b).

Role of Rb in cell cycle regulation

As mentioned above, Rb functions to regulate G1 to S progression mainly by repressing expression of E2F target genes, such as cyclin E and p107, in G0-G1 (reviewed by Dyson, 1998). This is achieved not only by inhibiting transactivation but also by converting E2F from a transactivator to a repressor, which is most convincingly demonstrated by the following

experiments. First, expression of a chimeric protein containing the E2F DNA binding domain and the Rb transcriptional repression domain is sufficient to restore G1 arrest in Rb-deficient cells. Second, the ability of Rb to repress transcription and to form stable complexes with DNA-bound E2F are both necessary for Rb-induced G1 arrest.

It has been suggested that Rb, when targeted by E2F to promoters that contain binding sites for other transcription factors, can bind to adjacent transcription factors and block their interaction with the basal transcription machinery. Another mechanism by which Rb represses transcription of E2F target genes is by recruitment of histone deacetylase HDAC1 to remodel chromatin at target promoters. Deacetylation of histones on nucleosomes is thought to repress transcription by compacting chromatin and thereby limiting access of DNA by the transcription machinery, while nucleosome acetylation by histone acetyltransferases is thought to activate transcription. In support of the idea that Rb can repress transcription by invoking chromatin remodeling at the target promoter, two Rb-binding proteins, RbAp48 and RbAp46, have been found in a number of multi-protein complexes involved in chromatin remodeling and/or transcriptional repression (reviewed by Pazin and Kadonaga, 1997b; Roth and Allis, 1996). One of the RbAp48 and/or RbAp46-containing complexes possesses both histone deacetylase and chromatin remodeling activities, raising the possibility that efficient histone acetylation on nucleosomes may require nucleosome remodeling (Tong et al., 1998; Wade et al., 1998; Zhang et al., 1998).

A Rb-chromatin link is further strengthened by the finding that the BRG-1 and hBrm proteins bind and cooperate with Rb to induce G1 arrest (reviewed by Taya, 1997). BRG-1 and hBrm are the two human homologs of the yeast SWI2/SNF2 protein and contain DNA-dependent ATPase activity. Each can form large multi-protein complexes, which are able to remodel chromatin structure *in vitro* in the presence of ATP and can function as a transcriptional coactivator (reviewed by Pazin and Kadonaga, 1997a; Pollard and Peterson, 1998). Interestingly, it appears that hBrm can cooperate with Rb to either potentiate or inhibit transactivation by different transcription factors. For example, Rb can recruit hBrm to upregulate transcription mediated by glucocorticoid-receptor (Singh et al., 1995), while simultaneous binding of Rb to hBrm and to DNA-bound E2F1 may covert hBrm to a repressor thereby inhibiting transactivation by E2F1 (Trouche et al., 1997).

In addition, Rb has also been shown to repress transcription by RNA polymerase I (Pol I) and RNA polymerase III (Pol III) by binding to thereby inhibiting upstream binding factor (UBF) and TFIIIB required for Pol I and Pol III transcription, respectively (reviewed by White, 1997).

Genetic redundancy of the mammalian Rb/E2F pathway

In mammals, p107 and p130 have been identified to be structurally and functionally related to Rb. p107 and p130 appear more similar to each other than to Rb. Unlike Rb, p107 and p130 are not known to be mutated in human cancer, and thus are not considered tumor suppressor genes. Nonetheless, Rb, p107 and p130 share many biochemical properties *in vivo*, such as the ability to interact with E2F and regulate expression of E2F target genes, inactivation by CDK phosphorylation and binding of DNA tumor virus oncoproteins, which indicates a functional overlap among them. Genetic studies of mice mutant for these genes, either singly or multiply, in conjunction with biochemical analysis of mutant-derived cells, have further revealed distinct and partially overlapping functions of these proteins and their specific ability to functionally compensate for the absence of one another (reviewed by Mulligan and Jacks, 1998; Nevins, 1998).

In striking contrast to the severe phenotypes of Rb-deficient mice described above, p107- and p130-deficient mice develop normally and exhibit no tumor predisposition or any obvious phenotype. However p107-/-; p130-/- animals die shortly after birth due to respiratory failure, with shortened limb and rib bones and excessive proliferation of chondrocytes. p107 appears to be upregulated in quiescent p130-/- T lymphocytes and fully compensates for p130 function in these cells. These results indicate that p107 and p130 can substitute for each other. A functional overlap has also been observed between Rb and p107. While Rb-/- and Rb+/- mice lack retinal phenotypes, Rb+/- p107-/- animals exhibit fully penetrant retinal dysplasia, which is not observed in other double mutant combinations (reviewed by Mulligan and Jacks, 1998).

To elucidate the molecular mechanisms that underlie the differences in mutant phenotypes, much attention has been focused on the regulation of E2F activities by Rb family members (reviewed by Dyson, 1998; Nevins, 1998). Studies of expression of E2F target genes in cells deficient in one or more Rb family members have revealed that p107 and p130 redundantly regulate a set of E2F target genes that is different from those regulated by Rb. This target gene difference is

likely the result of regulated complex formation between E2F and Rb family members by different mechanisms, as illustrated below.

Rb family members have been shown to bind different E2F proteins with different specificities (reviewed by Dyson, 1998; Nevins, 1998). There exist six E2F proteins. Rb bind preferentially to E2F1, 2 and 3, p107 and p130 binds preferentially to E2F4 and 5, respectively. E2F6 lacks the binding site for Rb family members and can repress transcription independent of Rb family members.

Another layer of complexity is imposed by different cell cycle regulation of the Rb family and the E2F family protein levels. While Rb is present through out the cell cycle, p130 and p107 levels are inversely related. p130 only accumulates in quiescent cells and appears to be degraded following CDK phosphorylation at entry into the cell cycle. Conversely, p107 is generally only found in proliferating cells, as a result of transcriptional derepression at late G1. Likewise, E2F family members are also differentially regulated (reviewed by Helin, 1998; Nevins, 1998). First, transcription of E2F1, 2, 3 is derepressed in G1, while E2F4 and 5 appear to be present throughout the cell cycle. Second, in S phase, phosphorylation by cyclin A-CDK2 of DP1 bound to E2F1, E2F2 or E2F3 inactivates their activity. Third, E2F1 and E2F4 are actively degraded by the ubiquitin-proteosome pathway. Lastly, unlike E2F1, which is constitutively nuclear localized, E2F4 is largely nuclear localized during G0 and becomes increasingly cytoplasmic as cells exit G0 and proceed into and through the cell cycle. E2F4 lacks functional nuclear localization signal and their nuclear translocation is mediated through interaction with p107, p130 or DP2, which are predominantly nuclear.

Together, these different regulatory mechanisms result in distinct cell cycle profiles of E2F proteins complexed with Rb family members. p130/E2F complexes are abundant in quiescent or differentiating cells. Conversely, p107/E2F complexes are most readily detected in cycling cells, and especially during S phase. Rb/E2F complexes have been found mainly in G1 phase and also in differentiated, quiescent and S phase cells. The functional significance of these different complexes is not well understood.

Elucidation of the *in vivo* functions of different complexes of E2F and Rb family members and their coordinate action in cell cycle regulation remains a challenging issue for future research.

Genetic interaction between Rb and E2F1

Overexpression of E2F1 can activate transcription of S phase genes and drive quiescent cells into S phase and then induce apoptosis. E2F1-deficient mice exhibit tumor induction, tissue atrophy and reduced apoptosis in a tissue-specific fashion. These results indicate that E2F1 is a unique molecule with characteristics of both an oncogene and a tumor suppressor gene, and that E2F1 perform dual roles, one in cell cycle progression and the other in apoptosis (reviewed by Dyson, 1998). Phenotypic analyses of mice doubly mutant for Rb and E2F1, in heterozygous and/or homozygous combinations, have proven to be an important complement to previous overexpression studies in mammalian cell lines (Tsai et al., 1998; Yamasaki et al., 1998). Inactivation of E2F1 variably suppresses S phase entry and ectopic cell death in Rb-/- mice, resulting in a delay but not rescue of the lethality caused by the Rb-/- mutation. Furthermore, E2F1 inactivation reduced the penetrance of pituitary and thyroid tumors in Rb1+/- mice. By contrast, the phenotypes of E2F1-/- is largely unaffected by Rb+/-. These *in vivo* studies demonstrated that E2F1 acts downstream of and is negatively regulated by Rb both in cell cycle progression and in apoptosis.

Linking Ras and the cell cycle machinery: Rb is downstream of Ras?

Ras proteins act as molecular switches that relay proliferative signals from cell-surface receptors to the nucleus and cytoskeleton. Activation of Ras has frequently been implicated in human cancer. Transformation of cultured primary cells requires in addition to activated Ras a cooperating oncogene or loss of tumor suppressor genes. In fact, activation of Ras in primary cells leads to induction of CKIs such as p21 and p16, resulting in G1 arrest and premature senescence (reviewed by Lloyd, 1998). Expression of cyclin D or inactivation of p16, p19, p21, or p53, which activates p21 expression, can lift the Ras-imposed growth arrest resulting in transformation. Similarly, cooperating oncogenes appear to act by overcoming the inhibitory effects of CKIs on the cell cycle. For example, in growth-factor deprived primary cells, Ras and Myc act cooperatively to upregulate cyclin E level, downregulate p27 level and induce DNA synthesis, while either alone has little effect. Interestingly, Ras and Myc induce S phase without detectable hyperphosphorylation of Rb. Several independent experiments suggest that S phase entry in the presence of hypophosphorylated Rb is likely a result of activation of E2F

transcription and of cyclin E-CDK2 activity independent of Rb phosphorylation (reviewed by Mittnacht, 1998).

Accumulating evidence indicates that the mitogenic response to Ras activation upon growth factor stimulation is mediated by the MAP kinase pathway (reviewed by Lloyd, 1998). Activation of the MAP kinase cascades appears to be required for the induction of cyclin D1, downregulation of p27 level and inactivation of p27 by phosphorylation. Presumably, these events result in the inactivation of Rb. Indeed, it has been demonstrated that Rb-deficient cells largely bypass the requirement for Ras to proliferate, indicating Rb acts downstream of or in parallel to Ras. It seems likely, however, that Rb does not account for all aspects of Ras regulation of the cell cycle, as primary mouse embryo fibroblasts lacking Rb are only partially protected from the effects of inhibiting Ras.

It has been suggested that Ras effector pathways other than the MAP kinase pathway participate in signal transduction from Ras to the cell cycle machinery. First, Ras has been shown to be required at multiple points in early and late G1 (Dobrowolski et al., 1994). Ras activates the MAP kinase pathway only transiently from G0 to G1 in response to mitogen to induce expression of immediate early genes. Interestingly, Ras appears to be maximally activated independent of growth factors in mid-G1 when MAKP activity has already subsided (Taylor and Shalloway, 1996). How this activation is achieved and what effector pathway is activated are still unknown. Recent findings have implicated the PI3 kinase pathway downstream of Ras and in synergy with Raf to mediate induction of DNA synthesis, loss of contact inhibition, anchorage-independent growth and protection against cell death (reviewed by Lloyd, 1998).

Role of Rb in differentiation

The role of Rb in differentiation is evidently revealed by Rb-deficient mice partially rescued either by a Rb minigene or by inactivation of E2F1 (Tsai et al., 1998), and by use of *in vitro* differentiation models (reviewed by Mulligan and Jacks, 1998). Rb appears to promote differentiation independent of its function to repress E2F target genes. It has been proposed that this differentiation promoting activity of Rb is also important for its tumor suppressor function. Differentiation is a precisely coordinated process of irreversible cell cycle withdrawal followed

by tissue-specific gene expression. It has become increasingly clear that Rb impacts both cell cycle withdrawal and expression of differentiation genes. Potentiation of transactivation by Rb binding to transcription factors seems to be a recurring theme in every tissue studied.

Rb as transcriptional coactivator

Accumulating evidence indicates that Rb can positively regulate transcription by binding to and potentiating transactivation of a number of non-E2F transcription factors, including ATF-2, MyoD, the glucocorticoid receptor (GRα), C/EBP and NF-IL6 (reviewed by Sellers and Kaelin, 1996). The mechanism for the transcription coactivator function of Rb is not well understood, but limited evidence suggests that it might involve chromatin remodeling. In one study, hBrm/BRG1 was shown to be recruited by Rb to activate transcription by glucocorticoid receptors (Singh et al., 1995). In another case, Rb has been shown by *in vivo* footprinting to increase promoter occupancy thereby facilitate transcription activation (Osborne et al., 1997).

Rb and neuronal differentiation

Rb-/- neurons often undergo ectopic proliferation and apoptosis. Surviving neurons express lower levels of neuronal differentiation markers and exhibit defective neurite outgrowth and survival in culture. Recent studies suggest that Rb is not required for induction of early neuronal gene expression, but is essential for cell cycle withdrawal and survival of neuronal progenitor cells at the time they would normally become postmitotic neurons. It has been proposed that loss of Rb results in aberrant uncoupling of neuronal differentiation and cell cycle withdrawal, and that the conflicting signals that arise from the inability of determined neurons to exit the cell cycle activates both p53-dependent and independent apoptosis pathways (reviewed by Mulligan and Jacks, 1998).

Surprisingly, differentiated, postmitotic neurons do not appear to require Rb family activity for survival or quiescence (Slack et al., 1998). Complementing this finding, studies of necdin, a nuclear protein expressed exclusively in postmitotic neurons, may act in place of Rb in postmitotic neurons to prevent cell cycle reentry by binding E2F1 and repressing transcription (Taniura et al., 1998).

Rb and muscle differentiation

Muscle cells represent the best-characterized differentiation system. The myogenic family of basic helix-loop-helix proteins, which include MyoD, myogenin, Myf5 and Mrf4, are critical regulators of muscle determination and differentiation. Myf5 and MyoD act preferentially in myoblast specification, whereas myogenin and Mrf4 drive terminal differentiation (Megeney and Rudnicki, 1995).

Rb appears to promote differentiation of muscle cells by binding MyoD family members and activating transcription of muscle differentiation genes (reviewed by Mulligan and Jacks, 1998). Rb gene expression is induced and the protein accumulates in the active hypophosphorylated form during muscle differentiation. Initial muscle development appeared grossly normal in the absence of Rb both *in vivo* and in culture probably as a consequence of functional compensation by p107 (Schneider et al., 1994). However closer examination reveals defective muscle gene expression and an accumulation of S and G2 phase cells due to cell cycle reentry. The cell cycle reentry phenotype in Rb-deficient cells is likely a result of downregulation of p107 expression as constitutive expression of p107 rescued the phenotype (Schneider et al., 1994).

The positive role of Rb in muscle differentiation appears to be counteracted by the HMG box transcription repressor HBP1. HBP1 binds Rb and p130 and its expression is induced during muscle differentiation (Lavender et al., 1997; Tevosian et al., 1997). Contrary to expected role of HBP1 in promoting differentiation, constitutive expression of wild-type HBP1 but not Rb/p130-binding-defective mutants blocks differentiation following cell cycle withdrawal, presumably by acting downstream of Myf5 to inhibit activation of MyoD and myogenin expression. Coexpression of Rb or the MyoD family members can overcome the block and restore differentiation (Yee et al., 1998).

A very similar picture has emerged from studies of p202, a 52-kDa protein that binds and inhibits transactivation by a number of transcription factors, including MyoD and myogenin (Datta et al., 1998). p202 expression is induced during muscle differentiation yet constitutive expression of p202 blocked differentiation following cell cycle withdrawal. Intriguingly, p202 also binds Rb (Choubey and Lengyel, 1995). The effect of this interaction on the function of both proteins in muscle differentiation remains to be determined.

It has been hypothesized that HBP1 and p202 may function as a 'differentiation checkpoint' to suspend tissue-specific gene expression while promoting cell cycle withdrawal to ensure that cell cycle withdrawal is complete prior to activation of differentiation genes (Yee et al., 1998). This model predicts that a checkpoint protein such as HBP1 and p202 must be downregulated as differentiation progresses to allow expression of the terminal phenotype. Analysis of expression pattern and phenotypes of mice deficient for these genes should gain insight into how HBP1 and p202 interact with Rb and p130 to coordinate gene expression in muscle differentiation.

Rb and adipocyte differentiation

Rb-/- primary adipocytes fail to undergo spontaneous differentiation in culture and expression of Rb can restore differentiation (reviewed by Mulligan and Jacks, 1998). Rb is found to be hyperphosphorylated early during adipocyte differentiation and later becomes hypophosphorylated (Shao and Lazar, 1997). Rb, p107 and p130 have been shown to bind to C/EBPs (CCAAT/enhancer-binding proteins) in differentiating cells to potentiate promoter binding and transactivation of a C/EBP responsive reporter, whereas mutations in Rb that disrupt binding block adipocyte differentiation. The role of Rb in adipocyte cell cycle withdrawal is unclear. It appears that a peroxisome proliferator activated receptor (PPARγ) can induce adipocytes to exit the cell cycle by downregulating the phosphatase PP2A leading to phosphorylation of DP1 and inactivation of E2F activity (Altiok et al., 1997).

Rb and keratinocyte differentiation

The AP-1 family of transcription factors, composed of either Jun-Jun homodimers or Jun-Fos, Jun-ATF heterodimers, plays a critical role in the differentiation of keratinocytes (Eckert and Welter, 1996). Binding of Rb to c-Jun in differentiating keratinocytes results in increased AP-1 site binding and transactivation by c-Jun, which can be disrupted by expression of the viral oncoprotein HPV E7 (Nead et al., 1998). Interestingly, the p21 CKI also participates in keratinocyte differentiation (Di Cunto et al., 1998). p21 expression *in vivo* correlates with the onset but not the establishment of the terminally differentiated phenotype. In primary keratinocyte culture, p21 expression is upregulated early during differentiation coincident with CDK inhibition and G1 arrest. However, as keratinocytes become terminally differentiated, p21 protein level is downregulated by ubiquitin-mediated degradation. Interestingly and

paradoxically, differentiation is inhibited both in p21-/- keratinocytes and those that constitutively express p21. This contradiction is reminiscent of the HBP1 and p202 proteins in muscle differentiation discussed above, and resonates with the 'differentiation checkpoint' hypothesis: p21 might be a differentiation checkpoint in keratinocytes to ensure completion of cell cycle withdrawal prior to terminal differentiation. It is of great interest to see if and how p21 interacts with Rb and c-Jun to regulate the expression of keratinocyte differentiation genes.

In summary, Rb appears to regulate differentiation of multiple tissues by coordinating terminal cell cycle withdrawal and activation of tissue-specific gene expression. However, it should be noted that *in vitro* differentiation models may not fully recapitulate *in vivo* differentiation processes. To verify and complement studies carried out in the *in vitro* models, it is important to analyze differentiation *in vivo*, for example, by mosaic analysis using Rb chimera mice, or by conditional targeting of Rb in various tissues. Interestingly, it has been shown that Rb-/- embryonic stem cells readily contribute to most adult tissues in Rb chimera mice, suggesting a cell non-autonomous role of Rb in development (reviewed by Mulligan and Jacks, 1998; McClatchey and Jacks, 1998). Further analysis of the role of Rb later in development should provide more insight into its tumor suppressor function.

Other roles of Rb

Rb and DNA damage checkpoint

Rb-deficient cells but not those deficient in p107 and/or p130 are defective in cell cycle arrest induced by DNA damage, indicating the DNA damage checkpoint exerts its effect through Rb (Harrington et al., 1998). DNA damage-imposed cell cycle arrest is probably mediated by p53. p53 level is upregulated in response to DNA damage leading to activation of p21 expression. p21 inhibits CDK activities resulting in Rb hypophosphorylation and G1 arrest (Figure 3). Consistent with this view, mice lacking p21 develop normally, but are partially defective in G1 arrest in response to ionizing irradiation (Brugarolas et al., 1995; Deng et al., 1995). Furthermore, overexpression of p21 causes both G1 arrest and G2 arrest, with G1 arrest largely dependent on the presence of Rb. Interestingly, Rb-deficient, G2-arrested cells in response to p21 expression

undergo DNA endoreplication, suggesting a role of Rb in preventing DNA replication during G2 (Niculescu et al., 1998).

Rb and cell death

The massive cell deaths by p53-dependent as well as p53-independent mechanisms in Rb-deficient mice indicate a role of Rb in cell death protection (reviewed by Wang, 1997). Apotosis of Rb-/- cells is in part mediated by E2F1, as inactivation of E2F1 in Rb-/- animals rescued or reduced cell deaths in a tissue-specific manner (Tsai et al., 1998). Apoptosis induced by E2F1 is in part p53-dependent (reviewed by Dyson, 1998). Independent lines of evidence indicate that E2F1 acts upstream of p53 to promote cell death (Pan et al., 1998; Tsai et al., 1998), by directly activating expression of p19 (Bates et al., 1998; Palmero et al., 1998). p19 is generated by alternative splicing from the same gene that encodes p16, expression of p19 leads to a p53-dependent G1 arrest (Kamijo et al., 1997). p19 has been shown to bind and promote degradation of MDM2. MDM2 is an oncoprotein found to be amplified in tumors and can bind either Rb or p53 to inhibit their functions (reviewed by Levine, 1997). Thus, p19 acts to trigger growth arrest and cell death by stabilization and activation of p53 (Kamijo et al., 1998; Pomerantz et al., 1998; Stott et al., 1998; Zhang et al., 1998). Taken together, these results reveal that there is a safeguard mechanism against aberrant cell growth: abnormal proliferative signals, such as loss of Rb or activation of Ras, trigger p53-mediated cell death by E2F1 induction of p19 (Figure 3).

Interestingly, recent studies have demonstrated that, when cells are induced to undergo programmed cell death, Rb is cleaved at a C-terminal caspase-consensus site, which is conserved in human, mouse, chick and *Xenopus* Rb but not in p107 and p130 (reviewed by Tan and Wang, 1998). Rb cleavage results in loss of binding to MDM2, another caspase substrate cleaved during programmed cell death. Expression of a non-cleavable form of Rb can block cell death in certain setting. The functional significance of Rb cleavage by caspases awaits further characterization.

Structure/Function studies of Rb

Functional domains important for Rb protein binding, regulation by phosphorylation and growth suppression have been carefully dissected by overexpression studies of various Rb mutants in mammalian cells and in transgenic animals.

Protein binding domains

The minimal growth suppression domain in Rb, from amino acid 379 to 869, contains at least three distinct protein binding sites, for proteins that contain the LXCXE motif (X is any amino acid), for E2F, and for the c-Abl tyrosine kinase and the oncoprotein MDM2, as well as a nuclear localization signal (Figure 4). These protein-binding sites can be occupied simultaneously. The so called 'A pocket' (amino acids 379-572) and 'B pocket' (amino acids 646-772) separated by an intervening spacer, define a domain that mediates transcriptional repression and binding of proteins that contain the LXCXE motif as well as a number of proteins that lack the motif. It has been demonstrated that the repressor and coactivator functions of Rb, which both require the A/B pocket, can be independently mutated, indicating that these functions map to different sequences in the A/B pocket (Sellers et al., 1998). Binding of E2F requires the A/B pocket plus some adjacent C-terminal residues. The region C-terminal to the A/B pocket within the minimal growth suppression domain, the so called C pocket, is involved in binding of c-Abl and MDM2. c-Abl expression can cause G1 arrest that is dependent on Rb and p53 (Sawyers et al., 1994; Wen et al., 1996). However, the physiological role of c-Abl-Rb interaction remains to be established.

Phosphorylation sites

As discussed above, Rb activity is regulated by phosphorylation (reviewed by Mittnacht, 1998). Sixteen potential sites for CDK-mediated phosphorylation (Ser/Thr-Pro motifs) exist in Rb, and 11of these sites have been shown to be phosphorylated *in vivo*. Different CDK-cyclin complexes preferentially phosphorylate Rb at distinct sites *in vitro*, suggesting that different CDK-cyclin complexes may exert distinct effects on Rb function *in vivo*. Furthermore, disruption of the LXCXE, c-Abl and E2F binding activities of Rb requires phosphorylation of distinct sites (Knudsen and Wang, 1996; Knudsen and Wang, 1997). Specifically, Thr821 and Thr826 are

required for inhibition of LXCXE binding, whereas Ser807 and Ser811 are required to inhibit c-Abl binding. A group of seven C-terminal domain sites (Ser780, Ser788, Ser795, Ser807, Ser811, Thr821 and Thr826) and two spacer sites (Ser608, 612) are redundantly involved in the regulation of Rb-E2F interaction, i.e., phosphorylation of either of the two groups is sufficient to block binding. The seven C-terminal sites are located in the E2F binding region therefore phosphorylation of these sites may affect the E2F binding domain. Interestingly, phosphorylation of the two sites in the spacer, which is not involved in E2F binding, appears to inhibit Rb-E2F interaction only in the presence of the N-terminal region of Rb. It is likely that the N-terminal region and the spacer may modulate the conformation of the E2F binding domain. This hypothesis is supported by several observations. First, it has been shown that small internal deletions of the N-terminal region can inhibit Rb-E2F interaction (Qian et al., 1992). By contrast, complete deletion of the Rb N-terminal region results in enhanced growth suppression (Xu et al., 1994). Second, interactions between different domains of Rb have been reported. The A and B pocket domains interact with each other to form the repressor motif (Chow and Dean, 1996); the N and C-terminal regions of Rb also interact with each other at least in yeast (Hensey et al., 1994). It is conceivable that phosphorylation of the spacer sites may affect one or more of these intramolecular interactions to inhibit E2F binding.

Several lines of evidence indicate the functional importance of Rb N-terminal region. First, N-terminal mutations in Rb are associated with low-penetrance retinoblastoma (Dryja et al., 1993; Lohmann et al., 1994). Second, Overexpression of human Rb N-terminal internal deletion mutants in transgenic mice cannot rescue Rb mutant phenotypes in development and tumor suppression (Riley et al., 1997). Third, N-terminal region is evolutionarily conserved among Rb family members. Proteins that interact with the N-terminal domain of Rb include an 84 kDa novel nuclear matrix protein that localizes to sites of RNA processing (Durfee et al., 1994), a 70 kDa heat shock cognate protein (Inoue et al., 1995), and a kinase apparently active in G2 and M phases (Sterner et al., 1996). However, the physiological relevance of these interactions has not been established.

p107 and p130 are also substrates for phosphorylation by G1 cyclins. However, Rb, p107 and p130 appear to be differentially regulated by phosphorylation. For example, the spacer regions of p107 and p130, which mediate binding of p107 and p130 to cyclin A-CDK2 and cyclin E-

CDK2, are conserved with each other but not with that of Rb. Furthermore, only three of the phosphorylation sites in Rb, Ser788, Ser795 and Ser807, are conserved in p107 and p130. How p107 and p130 are regulated by CDK phosphorylation is an important issue for understanding the different functions normally carried out by Rb family members, therefore warrants further analysis.

Chromatin and Cancer

The findings that Rb can recruit histone deacetylase, hBrm and BRG-1 to regulate transcription implicate chromatin remodeling in Rb-mediated growth suppression. The cancer-chromatin link has been substantially extended by recent findings that implicate aberrant chromatin-remodeling enzymatic activities in human malignancies.

It has been demonstrated that chromosomal translocations that fuse DNA binding proteins such as MLL (for myeloid leukemia) and MOZ (for monocytic zinc finger protein) to CBP are associated with acute myeloid leukemia (Borrow et al., 1996; Sobulo et al., 1997). CBP (CREB binding protein) and the closely related p300 are global transcriptional coactivators that modulate the activity of a number of DNA-binding transcription factors, presumably by targeted acetylation of chromatin. CBP has intrinsic histone acetyltransferase activity (Ogryzko et al., 1996), and can also recruit another histone acetyltransferase P/CAF (Yang et al., 1996).

Recruitment of histone deacetylase by the oncogenic, chimeric retinoic acid receptor has been shown to play a crucial role in the pathogenesis of acute promyelocytic leukemia (Grignani et al., 1998; Lin et al., 1998).

Most interestingly, hSNF5/INI1, which encodes a member of the chromatin-remodeling SWI/SNF multi-protein complexes, has recently been identified as a gene frequently mutated in malignant rhabdoid tumors, an extremely aggressive form of pediatric cancer (Versteege et al., 1998). This finding raised the exciting possibility of the SWI/SNF chromatin remodeling proteins acting as tumor suppressors.

Taken together, these findings underscore the importance of a tightly regulated chromatin environment in normal growth control, indicate that deregulation of histone acetylation and chromatin remodeling might be an important molecular event in tumorigenesis.

Developmental control of cell cycle

Normal development of multicellular organisms requires the precise orchestration of proliferation of precursor cells and differentiation. Rb has emerged as an important coordinator of cell cycle withdrawal and onset of differentiation. However the developmental control of Rb and cell cycle progression is not well understood. Genetic systems such as *Drosophila* and *C. elegans* present excellent opportunities to study coordinated control of pattern formation and proliferation by evolutionarily conserved signaling pathways. Such studies are relevant not only from the point of view of developmental biology, but also from that of cancer biology, as a number of patterning genes have been implicated in human cancer (reviewed by Marshall and Nigg, 1998).

Developmental control of cell cycle in *Drosophila*

Drosophila tissues display divergent cell cycle profiles tailored to fit their respective developmental programs (reviewed by Edgar and Lehner, 1996). For example, during late embryogenesis, the cells in the central nervous system (CNS) undergo rounds of rapid proliferation without apparent gap phases. In the endocycling tissues such as the gut, rounds of DNA replication occur without intervening mitoses. The cells of the imaginal discs, the embryonic primordia that produce adult appendages, arrest in G1 during embryogenesis and reinitiate proliferation only after hatching and substantial cell growth.

Drosophila shares many components of the mammalian cell cycle machinery, including the G1 and G2 cyclins and their CDKs, dE2F, dDP, an Rb-like protein (RBF), a p21 CKI (Dacapo), and a CDC25-like phosphatase that activates the mitotic cyclin cdc2 (String). Studies of the developmental coordination of cell cycle in the *Drosophila* embryo and imaginal discs have established Cyclin E as the limiting regulator of entry into S phase, and String as the limiting regulator of entry into M phase (reviewed by Edgar and Lehner, 1996).

Mutant analyses revealed that *cyclin E* is required for S phase, but *dE2F* and *dDP* are not. Unlike *cyclin E* mutants, which arrest in G1 during embryogenesis, the *dDP* and *dE2F* mutants proceed normally through embryogenesis but die as late larvae or early pupae with underdeveloped tissues. A closer look at the cell-cycle defects in these mutants reveal that DNA replication can occur in the absence of dDP and dE2F activities, presumably driven by the activity of Cyclin E, but with a slower kinetics (Royzman et al., 1997). In addition to its role as an activator of S phase *in vivo*, *dE2F* may also have a role in post-mitotic differentiation (Brook et al., 1996). A second E2F, *dE2F2*, has been identified in *Drosophila*. In contrast to the role of dE2F as a transactivator, preliminary results indicate that dE2F2 can repress transcription (Sawado et al., 1998).

Genetic interactions between *dE2F* and *cyclin E* have been examined (Duronio et al., 1998; Duronio et al., 1996; Duronio and O'Farrell, 1995). Interestingly, *cyclin E* expression requires dE2F in the endocycling cells but is independent of dE2F in the proliferating CNS. Furthermore, Cyclin E appears to negatively regulate its own expression in the endocycling cells but positively regulate its own expression in the CNS, although it is not known if either is mediated by dE2F. The tissue-specific interaction between *cyclin E* and *dE2F* suggests that there might exist additional regulators of *cyclin E* expression, likely dE2F2. Nonetheless, in *Drosophila*, Cyclin E and dE2F form a positive feedback loop similar to that in mammalian cells: E2F activates *cyclin E* expression, Cyclin E in turn phosphorylates and inactivates Rb resulting in either transactivation by 'free' E2F or derepression.

RBF was the first invertebrate Rb-related protein identified (Du et al., 1996). Although the *RBF* loss-of-function phenotype has not been reported, overexpression studies suggest that the growth control pathway mediated by Rb might be conserved from invertebrates to mammals. RBF protein associates with and antagonizes the activity of dE2F and dDP *in vivo*, and appears to be phosphorylated and negatively regulated by Cyclin E.

Mutations in *dacapo* cause additional cell divisions when wild-type tissues undergo cell-cycle exit and differentiation but notably they do not result in unrestricted proliferation and permanent cell cycle withdrawal eventually occur with no apparent defects in pattern formation or cell fate determination. Overexpression of *dacapo* can reduce and delay S phase entry and inhibit G1

progression, which is enhanced by reducing Cyclin E level. Expression pattern of Dacapo coincides with decrease in Cyclin E level and correlates precisely with cell cycle withdrawal during development. Therefore, Dacapo appears to promote developmentally programmed cell cycle withdrawal in concert with declining Cyclin E level but is not required for differentiation or the maintenance of postmitotic status (de Nooij et al., 1996; Lane et al., 1996).

Study of cell cycle control in *Drosophila* has moved from the initial stage of phenotype analysis of cell cycle mutants to an exciting new stage: cell cycle regulation by developmental genes. For example, transcription of string, the single limiting factor for entry into mitosis, is directly controlled by patterning information, thus linking cell cycle control to other aspects of pattern formation. This is most elegantly demonstrated by study of the development of wing sensory bristles (Johnston and Edgar, 1998). In the wing imaginal disc, the secreted morphogen Wingless induces at the dorsoventral boundary a zone of non-proliferating cells (ZNC), which gives rise to sensory bristles of the adult wing. Wingless induces G2 arrest in two subdomains of the ZNC by inducing the proneural genes *achaete* and *scute*, which encode transcription factors that repress *string* expression. Notch activity, which creates a third subdomain by inhibiting *achaete* and *scute* expression thus lifting G2 arrest, in conjunction with Wingless activity, which likely inhibit dE2F activity, results in G1 arrest. These findings suggest that differentiation and proliferation in the wing margin is coordinately regulated by the same signaling pathways. The significance of cell-cycle arrest in the ZNC and of G1 arrest versus G2 arrest is unknown. In addition, it has been shown that dE2F activity in the wing promotes cell cycle progression by activating transcription of both *cyclin E* and *string* without much effect on growth, such that both too little and too much dE2F activity trigger cell death as a consequence of uncoupled proliferation and growth (Neufeld et al., 1998).

Another example is compound eye development. The developing eye imaginal disc can be divided into five subdomains by their distinct positions in the cell cycle (Thomas et al., 1994). This exquisite pattern appears to involve a number of cell cycle genes, including *cyclins A* and *B*, *string*, *RBF* (Du et al., 1996), *dE2F* (Brook et al., 1996; Du et al., 1996), and *dacapo* (de Nooij et al., 1996; Lane et al., 1996). Genetic screens have begun to identify genes that regulate these cell cycle components to set up the subdomains. For example, cell cycle arrest in G1 at the onset of cellular differentiation and morphogenesis in the eye is mediated by novel regulators *roughex*

and *rca1*. Roughex inhibits Cyclin A accumulation in early G1 by targeting Cyclin A for destruction and is down-regulated by Cyclin E in late G1 (Thomas et al., 1994; Thomas et al., 1997). Rca1, on the other hand, are required for Cyclin A accumulation and cell cycle progression (Dong et al., 1997). Recent findings have implicated Decapentaplegic (Dpp), a TGF-β family member, in establishing G1 arrest by inhibiting expression of Cyclins A, E and B independent of Roughex and Dacapo (Horsfield et al., 1998). Further analysis of coordination of proliferation and differentiation in the eye mediated by different signaling pathways, such as the hedgehog pathway and the RTK/Ras pathway, will continue to advance the field.

Developmental control of cell cycle in *C. elegans*

C. elegans is well-suited for the study of developmental cell cycle control, with an invariant cell lineage, the possibility to observe in real time and in live animals cell divisions and corresponding gene expression pattern using GFP reporters. Furthermore, with the completion of genome sequencing, cell cycle genes can be easily identified and mutations in them can be isolated by PCR screening of mutagenized animal pools for deletion alleles (Science, Dec. 11 issue, 1998). Loss-of-function phenotypes can also be studied by RNA mediated interference (RNAi) (Fire et al., 1998). This approach can be combined with study of previously identified genetic pathways that regulate developmental timing of postembryonic cell divisions.

Developmental cell cycle control of the vulval precursor cells has been studied in most detail. The vulval equivalence group consists of six cells, termed P(3-8).p, which are multipotent cells capable of expressing any of the 3 fates: the 1° and 2° vulval fates and the 3° non-vulval fates (Figure 5) (reviewed by Sternberg and Horvitz, 1986). Multiple signaling pathways influence the P(3-8).p cell fate determination (Figure 6) (reviewed by Sternberg and Horvitz, 1991; Sundaram and Han, 1996), including the *let-23* RTK/*let-60* Ras inductive signaling pathway, the LIN-12/Notch pathway that mediates lateral inhibition, two functionally redundant inhibitory pathways mediated by the class A and B synthetic multivulva (synMuv) genes, and the *bar-1* β-catenin-mediated Wnt signaling pathway that regulates fusion of P(3-8).p cells with the hypodermal syncytium prior to their divisions (Eisenmann et al., 1998). We have shown that the class B synMuv genes *lin-35* and *lin-53* encode proteins similar to Rb and Rb-binding proteins RbAp48 and RbAp46, respectively, and identified the histone deacetylase gene *hda-1* as a class

B synMuv gene by its antisense phenotype. Based on these findings, we propose that the class B synMuv genes antagonize the Ras pathway by repressing transcription of vulval cell fate genes (Lu and Horvitz, 1998 and Chapter 2 of this thesis).

Recent data suggest that cell cycle status of P(3-8).p cells has a profound influence on their responses to the various signaling pathways described above. Ras signaling acts during G1/S phase of the P(3-8).p cell cycle (M. Huang and P. Sternberg, personal communications), whereas LIN-12 activity is required before S phase to specify the 1° versus 2° fate, and after S phase to specify the 2° versus 3° fate (V. Ambros, personal communications).

The timing of G1 progression and developmental competence in the vulval precursor cells is regulated by the heterochronic gene *lin-14* (Euling and Ambros, 1996). The normal timing of P(3-8).p cell division requires down-regulation of *lin-14* activity before determination of vulval cell fates. Constitutive *lin-14* activity leads to delay and block of P(3-8).p cell division, whereas loss of *lin-14* function causes precocious vulval precursor cell divisions and vulval development. How does *lin-14* regulate the P(3-8).p cell cycle? At least part of the answer lies in the regulation of *cki-1* (Hong et al., 1998). *cki-1* is one of the two p21-like genes identified in *C. elegans* and is required for quiescence. Its expression is under exquisite control by upstream developmental genes. In the P(3-8).p, *cki-1* expression level closely correlate with *lin-14* activity. While constitutive expression of *cki-1* in P6.p results in G1 arrest, loss of *cki-1* function causes P(3-8).p to undergo one round of precocious division resulting in the generation of 12 multipotent vulval precursor cells. In contrast to *lin-14* loss-of-function mutants, timing and pattern of vulval development is essentially normal in *cki-1*(RNAi) animals, despite the precocious divisions and the extra precursor cells. This result indicates that vulval precursor cells in *cki-1*(RNAi) animals are still subject to the normal temporal control of vulval differentiation by *lin-14*, and *cki-1* is only one of the many downstream targets of *lin-14*.

Another gene that regulates the number of cell divisions in diverse cell lineages is the gene *cul-1*, which is similar to the yeast gene CDC53 required for ubiquitin-mediated degradation of G1 cyclins (Kipreos et al., 1996; Mathias et al., 1996). Although *cul-1* mutants display supernumerary cell divisions in the vulval cell lineages, extra vulval precursor cells were not

observed, suggesting that *cki-1* and *cul-1* do not function equivalently in the vulval precursor cells.

Whether any of the signaling pathways regulates the P(3-8).p cell cycle, in particular the *lin-35* Rb-mediated pathway, remains to be answered. Study of P(3-8).p cell cycle in the context of signaling pathways that determine vulval cell fate will continue to be a focus of future research on vulval development.

References

Altiok, S., Xu, M., and Spiegelman, B. M. (1997). PPARgamma induces cell cycle withdrawal: inhibition of E2F/DP DNA- binding activity via down-regulation of PP2A. Genes Dev *11*, 1987-1998.

Bartek, J., Bartkova, J., and Lukas, J. (1996). The retinoblastoma protein pathway and the restriction point. Curr Opin Cell Biol *8*, 805-814.

Bates, S., Phillips, A. C., Clark, P. A., Stott, F., Peters, G., Ludwig, R. L., and Vousden, K. H. (1998). p14ARF links the tumour suppressors RB and p53. Nature *395*, 124-125.

Borrow, J., Stanton, V. P., Jr., Andresen, J. M., Becher, R., Behm, F. G., Chaganti, R. S., Civin, C. I., Disteche, C., Dube, I., Frischauf, A. M., Horsman, D., Mitelman, F., Volinia, S., Watmore, A. E., and Housman, D. E. (1996). The translocation t(8;16)(p11;p13) of acute myeloid leukaemia fuses a putative acetyltransferase to the CREB-binding protein. Nat Genet *14*, 33-41.

Brook, A., Xie, J. E., Du, W., and Dyson, N. (1996). Requirements for dE2F function in proliferating cells and in post- mitotic differentiating cells. EMBO J *15*, 3676-3683.

Brugarolas, J., Chandrasekaran, C., Gordon, J. I., Beach, D., Jacks, T., and Hannon, G. J. (1995). Radiation-induced cell cycle arrest compromised by p21 deficiency. Nature *377*, 552-557.

Choubey, D., and Lengyel, P. (1995). Binding of an interferon-inducible protein (p202) to the retinoblastoma protein. J Biol Chem *270*, 6134-6140.

Chow, K. N., and Dean, D. C. (1996). Domains A and B in the Rb pocket interact to form a transcriptional repressor motif. Mol Cell Biol *16*, 4862-4868.

Datta, B., Min, W., Burma, S., and Lengyel, P. (1998). Increase in p202 expression during skeletal muscle differentiation: inhibition of MyoD protein expression and activity by p202. Mol Cell Biol *18*, 1074-1083.

de Nooij, J. C., Letendre, M. A., and Hariharan, I. K. (1996). A cyclin-dependent kinase inhibitor, Dacapo, is necessary for timely exit from the cell cycle during *Drosophila* embryogenesis. Cell *87*, 1237-1247.

Deng, C., Zhang, P., Harper, J. W., Elledge, S. J., and Leder, P. (1995). Mice lacking p21CIP1/WAF1 undergo normal development, but are defective in G1 checkpoint control. Cell *82*, 675-684.

Di Cunto, F., Topley, G., Calautti, E., Hsiao, J., Ong, L., Seth, P. K., and Dotto, G. P. (1998). Inhibitory function of p21Cip1/WAF1 in differentiation of primary mouse keratinocytes independent of cell cycle control. Science *280*, 1069-1072.

Dobrowolski, S., Harter, M., and Stacey, D. W. (1994). Cellular ras activity is required for passage through multiple points of the G0/G1 phase in BALB/c 3T3 cells. Mol Cell Biol *14*, 5441-5449.

Dong, X., Zavitz, K. H., Thomas, B. J., Lin, M., Campbell, S., and Zipursky, S. L. (1997). Control of G1 in the developing *Drosophila* eye: rca1 regulates Cyclin A. Genes Dev *11*, 94-105.

Dryja, T. P., Rapaport, J., McGee, T. L., Nork, T. M., and Schwartz, T. L. (1993). Molecular etiology of low-penetrance retinoblastoma in two pedigrees. Am J Hum Genet *52*, 1122-1128.

Du, W., Vidal, M., Xie, J. E., and Dyson, N. (1996). RBF, a novel RB-related gene that regulates E2F activity and interacts with cyclin E in *Drosophila*. Genes Dev *10*, 1206-1218.

Du, W., Xie, J. E., and Dyson, N. (1996). Ectopic expression of dE2F and dDP induces cell proliferation and death in the *Drosophila* eye. EMBO J *15*, 3684-3692.

Durfee, T., Mancini, M. A., Jones, D., Elledge, S. J., and Lee, W. H. (1994). The amino-terminal region of the retinoblastoma gene product binds a novel nuclear matrix protein that co-localizes to centers for RNA processing. J Cell Biol *127*, 609-622.

Duronio, R. J., Bonnette, P. C., and O'Farrell, P. H. (1998). Mutations of the *Drosophila* dDP, dE2F, and cyclin E genes reveal distinct roles for the E2F-DP transcription factor and cyclin E during the G1-S transition. Mol Cell Biol *18*, 141-151.

Duronio, R. J., Brook, A., Dyson, N., and O'Farrell, P. H. (1996). E2F-induced S phase requires cyclin E. Genes Dev *10*, 2505-2513.

Duronio, R. J., and O'Farrell, P. H. (1995). Developmental control of the G1 to S transition in *Drosophila*: cyclin E is a limiting downstream target of E2F. Genes Dev *9*, 1456-1468.

Dyson, N. (1998). The regulation of E2F by pRB-family proteins. Genes Dev *12*, 2245-2262.

Eckert, R. L., and Welter, J. F. (1996). Transcription factor regulation of epidermal keratinocyte gene expression. Mol Biol Rep *23*, 59-70.

Edgar, B. A., and Lehner, C. F. (1996). Developmental control of cell cycle regulators: a fly's perspective. Science *274*, 1646-1652.

Eisenmann, D. M., Maloof, J. N., Simske, J. S., Kenyon, C., and Kim, S. K. (1998). The β-catenin homolog BAR-1 and LET-60 ras coordinately regulate the hox gene *lin-39* during *caenorhabditis elegans* vulval development. Development *125*, 3667-3680.

Euling, S., and Ambros, V. (1996). Heterochronic genes control cell cycle progress and developmental competence of *C. elegans* vulva precursor cells. Cell *84*, 667-676.

Fire, A., Xu, S., Montgomery, M. K., Kostas, S. A., Driver, S. E., and Mello, C. C. (1998). Potent and specific genetic interference by double-stranded RNA in *Caenorhabditis elegans*. Nature *391*, 806-811.

Grignani, F., De Matteis, S., Nervi, C., Tomassoni, L., Gelmetti, V., Cioce, M., Fanelli, M., Ruthardt, M., Ferrara, F. F., Zamir, I., Seiser, C., Lazar, M. A., Minucci, S., and Pelicci, P. G. (1998). Fusion proteins of the retinoic acid receptor-alpha recruit histone deacetylase in promyelocytic leukaemia. Nature *391*, 815-818.

Harrington, E. A., Bruce, J. L., Harlow, E., and Dyson, N. (1998). pRB plays an essential role in cell cycle arrest induced by DNA damage. Proc Natl Acad Sci U S A *95*, 11945-11950.

Hatakeyama, M., Brill, J. A., Fink, G. R., and Weinberg, R. A. (1994). Collaboration of G1 cyclins in the functional inactivation of the retinoblastoma protein. Genes Dev *8*, 1759-1771.

Heichman, K. A., and Roberts, J. M. (1994). Rules to replicate by. Cell *79*, 557-562.

Helin, K. (1998). Regulation of cell proliferation by the E2F transcription factors. Curr Opin Genet Dev *8*, 28-35.

Hensey, C. E., Hong, F., Durfee, T., Qian, Y. W., Lee, E. Y., and Lee, W. H. (1994). Identification of discrete structural domains in the retinoblastoma protein. Amino-terminal domain is required for its oligomerization. J Biol Chem *269*, 1380-1387.

Herrera, R. E., Sah, V. P., Williams, B. O., Makela, T. P., Weinberg, R. A., and Jacks, T. (1996a). Altered cell cycle kinetics, gene expression, and G1 restriction point regulation in Rb-deficient fibroblasts. Mol Cell Biol *16*, 2402-2407.

Herrera, R. E., Chen, F., and Weinberg, R. A. (1996b). Increased histone H1 phosphorylation and relaxed chromatin structure in Rb-deficient fibroblasts. Proc Natl Acad Sci U S A *93*, 11510-11515.

Hong, Y., Roy, R., and Ambros, V. (1998). Developmental regulation of a cyclin-dependent kinase inhibitor controls postembryonic cell cycle progression in *Caenorhabditis elegans*. Development *125*, 3585-3597.

Horsfield, J., Penton, A., Secombe, J., Hoffman, F. M., and Richardson, H. (1998). decapentaplegic is required for arrest in G1 phase during *Drosophila* eye development. Development *125*, 5069-5078.

Inoue, A., Torigoe, T., Sogahata, K., Kamiguchi, K., Takahashi, S., Sawada, Y., Saijo, M., Taya, Y., Ishii, S., Sato, N., and et al. (1995). 70-kDa heat shock cognate protein interacts directly with the N- terminal region of the retinoblastoma gene product pRb. Identification of a novel region of pRb-mediating protein interaction. J Biol Chem *270*, 22571-22576.

Johnston, L. A., and Edgar, B. A. (1998). Wingless and Notch regulate cell-cycle arrest in the developing *Drosophila* wing. Nature *394*, 82-84.

Kamijo, T., Weber, J. D., Zambetti, G., Zindy, F., Roussel, M. F., and Sherr, C. J. (1998). Functional and physical interactions of the ARF tumor suppressor with p53 and Mdm2. Proc Natl Acad Sci U S A *95*, 8292-8297.

Kamijo, T., Zindy, F., Roussel, M. F., Quelle, D. E., Downing, J. R., Ashmun, R. A., Grosveld, G., and Sherr, C. J. (1997). Tumor suppression at the mouse INK4a locus mediated by the alternative reading frame product p19ARF. Cell *91*, 649-659.

Kipreos, E. T., Lander, L. E., Wing, J. P., He, W. W., and Hedgecock, E. M. (1996). *cul-1* is required for cell cycle exit in *C. elegans* and identifies a novel gene family. Cell *85*, 829-839.

Knudsen, E. S., and Wang, J. Y. (1996). Differential regulation of retinoblastoma protein function by specific Cdk phosphorylation sites. J Biol Chem *271*, 8313-8320.

Knudsen, E. S., and Wang, J. Y. (1997). Dual mechanisms for the inhibition of E2F binding to RB by cyclin- dependent kinase-mediated RB phosphorylation. Mol Cell Biol *17*, 5771-5783.

Lane, M. E., Sauer, K., Wallace, K., Jan, Y. N., Lehner, C. F., and Vaessin, H. (1996). Dacapo, a cyclin-dependent kinase inhibitor, stops cell proliferation during *Drosophila* development. Cell *87*, 1225-1235.

Lavender, P., Vandel, L., Bannister, A. J., and Kouzarides, T. (1997). The HMG-box transcription factor HBP1 is targeted by the pocket proteins and E1A. Oncogene *14*, 2721-2728.

Lees, E. (1995). Cyclin dependent kinase regulation. Curr Opin Cell Biol *7*, 773-780.

Levine, A. J. (1997). p53, the cellular gatekeeper for growth and division. Cell *88*, 323-331.

Lin, R. J., Nagy, L., Inoue, S., Shao, W., Miller, W. H., Jr., and Evans, R. M. (1998). Role of the histone deacetylase complex in acute promyelocytic leukaemia. Nature *391*, 811-814.

Lloyd, A. C. (1998). Ras versus cyclin-dependent kinase inhibitors. Curr Opin Genet Dev *8*, 43-48.

Lohmann, D. R., Brandt, B., Hopping, W., Passarge, E., and Horsthemke, B. (1994). Distinct RB1 gene mutations with low penetrance in hereditary retinoblastoma. Hum Genet *94*, 349-354.

Lu, X., and Horvitz, H. R. (1998). *lin-35* and *lin-53*, two genes that antagonize a *C. elegans* Ras pathway, encode proteins similar to Rb and its binding protein RbAp48. Cell *95*, 981-991.

Lundberg, A. S., and Weinberg, R. A. (1998). Functional inactivation of the retinoblastoma protein requires sequential modification by at least two distinct cyclin-cdk complexes. Mol Cell Biol *18*, 753-761.

Marshall, C. J., and Nigg, E. A. (1998). Oncogenes and cell proliferation. Cancer genes: lessons from genetics and biochemistry. Curr Opin Genet Dev *8*, 11-13.

Mathias, N., Johnson, S. L., Winey, M., Adams, A. E., Goetsch, L., Pringle, J. R., Byers, B., and Goebl, M. G. (1996). Cdc53p acts in concert with Cdc4p and Cdc34p to control the G1-to-S-phase transition and identifies a conserved family of proteins. Mol Cell Biol *16*, 6634-6643.

McClatchey, A. I., and Jacks, T. (1998). Tumor suppressor mutations in mice: the next generation. Curr Opin Genet Dev *8*, 304-310.

Megeney, L. A., and Rudnicki, M. A. (1995). Determination versus differentiation and the MyoD family of transcription factors. Biochem Cell Biol *73*, 723-732.

Mittnacht, S. (1998). Control of pRB phosphorylation. Curr Opin Genet Dev *8*, 21-27.

Morgan, D. O. (1995). Principles of CDK regulation. Nature *374*, 131-134.

Mulligan, G., and Jacks, T. (1998). The retinoblastoma gene family: cousins with overlapping interests. Trends Genet *14*, 223-229.

Nead, M. A., Baglia, L. A., Antinore, M. J., Ludlow, J. W., and McCance, D. J. (1998). Rb binds c-Jun and activates transcription. EMBO J *17*, 2342-2352.

Neufeld, T. P., de la Cruz, A. F., Johnston, L. A., and Edgar, B. A. (1998). Coordination of growth and cell division in the *Drosophila* wing. Cell *93*, 1183-1193.

Nevins, J. R. (1998). Toward an understanding of the functional complexity of the E2F and retinoblastoma families. Cell Growth Differ *9*, 585-593.

Niculescu, A. B., 3rd, Chen, X., Smeets, M., Hengst, L., Prives, C., and Reed, S. I. (1998). Effects of p21(Cip1/Waf1) at both the G1/S and the G2/M cell cycle transitions: pRb is a critical determinant in blocking DNA replication and in preventing. Mol Cell Biol *18*, 629-643.

Ogryzko, V. V., Schiltz, R. L., Russanova, V., Howard, B. H., and Nakatani, Y. (1996). The transcriptional coactivators p300 and CBP are histone acetyltransferases. Cell *87*, 953-959.

Osborne, A., Tschickardt, M., and Blanck, G. (1997). Retinoblastoma protein expression facilitates chromatin remodeling at the HLA-DRA promoter. Nucleic Acids Res *25*, 5095-5102.

Palmero, I., Pantoja, C., and Serrano, M. (1998). p19ARF links the tumour suppressor p53 to Ras. Nature *395*, 125-126.

Pan, H., Yin, C., Dyson, N. J., Harlow, E., Yamasaki, L., and Dyke, T. V. (1998). Key roles for E2F1 in signaling p53-dependent apoptosis and in cell division within developing tumors. Mol Cell *2*, 283-292.

Pardee, A. B. (1989). G1 events and regulation of cell proliferation. Science *246*, 603-608.

Pazin, M. J., and Kadonaga, J. T. (1997a). SWI2/SNF2 and related proteins: ATP-driven motors that disrupt protein- DNA interactions? Cell *88*, 737-740.

Pazin, M. J., and Kadonaga, J. T. (1997b). What's up and down with histone deacetylation and transcription? Cell *89*, 325-328.

Pollard, K. J., and Peterson, C. L. (1998). Chromatin remodeling: a marriage between two families? Bioessays *20*, 771-780.

Pomerantz, J., Schreiber-Agus, N., Liegeois, N. J., Silverman, A., Alland, L., Chin, L., Potes, J., Chen, K., Orlow, I., Lee, H. W., Cordon-Cardo, C., and DePinho, R. A. (1998). The Ink4a tumor suppressor gene product, p19Arf, interacts with MDM2 and neutralizes MDM2's inhibition of p53. Cell *92*, 713-723.

Qian, Y., Luckey, C., Horton, L., Esser, M., and Templeton, D. J. (1992). Biological function of the retinoblastoma protein requires distinct domains for hyperphosphorylation and transcription factor binding. Mol Cell Biol *12*, 5363-5372.

Riley, D. J., Liu, C. Y., and Lee, W. H. (1997). Mutations of N-terminal regions render the retinoblastoma protein insufficient for functions in development and tumor suppression. Mol Cell Biol *17*, 7342-7352.

Rogatsky, I., Trowbridge, J. M., and Garabedian, M. J. (1997). Glucocorticoid receptor-mediated cell cycle arrest is achieved through distinct cell-specific transcriptional regulatory mechanisms. Mol Cell Biol *17*, 3181-3193.

Roth, S. Y., and Allis, C. D. (1996). Histone acetylation and chromatin assembly: a single escort, multiple dances? Cell *87*, 5-8.

Royzman, I., Whittaker, A. J., and Orr-Weaver, T. L. (1997). Mutations in *Drosophila* DP and E2F distinguish G1-S progression from an associated transcriptional program. Genes Dev *11*, 1999-2011.

Sawado, T., Yamaguchi, M., Nishimoto, Y., Ohno, K., Sakaguchi, K., and Matsukage, A. (1998). dE2F2, a novel E2F-family transcription factor in drosophila *melanogaster*. Biochem Biophys Res Commun *251*, 409-415.

Sawyers, C. L., McLaughlin, J., Goga, A., Havlik, M., and Witte, O. (1994). The nuclear tyrosine kinase c-Abl negatively regulates cell growth. Cell *77*, 121-131.

Schneider, J. W., Gu, W., Zhu, L., Mahdavi, V., and Nadal-Ginard, B. (1994). Reversal of terminal differentiation mediated by p107 in Rb-/- muscle cells. Science *264*, 1467-1471.

Sellers, W. R., and Kaelin, W. G. (1996). RB as a modulator of transcription. Biochim Biophys Acta *1288*, M1-5.

Sellers, W. R., Novitch, B. G., Miyake, S., Heith, A., Otterson, G. A., Kaye, F. J., Lassar, A. B., and Kaelin, W. G., Jr. (1998). Stable binding to E2F is not required for the retinoblastoma protein to activate transcription, promote differentiation, and suppress tumor cell growth. Genes Dev *12*, 95-106.

Shao, D., and Lazar, M. A. (1997). Peroxisome proliferator activated receptor gamma, CCAAT/enhancer- binding protein alpha, and cell cycle status regulate the commitment to adipocyte differentiation. J Biol Chem *272*, 21473-21478.

Sherr, C. J. (1996). Cancer cell cycles. Science *274*, 1672-1677.

Sherr, C. J., and Roberts, J. M. (1995). Inhibitors of mammalian G1 cyclin-dependent kinases. Genes Dev *9*, 1149-1163.

Singh, P., Coe, J., and Hong, W. (1995). A role for retinoblastoma protein in potentiating transcriptional activation by the glucocorticoid receptor. Nature *374*, 562-565.

Slack, R. S., El-Bizri, H., Wong, J., Belliveau, D. J., and Miller, F. D. (1998). A critical temporal requirement for the retinoblastoma protein family during neuronal determination. J Cell Biol *140*, 1497-1509.

Sobulo, O. M., Borrow, J., Tomek, R., Reshmi, S., Harden, A., Schlegelberger, B., Housman, D., Doggett, N. A., Rowley, J. D., and Zeleznik-Le, N. J. (1997). MLL is fused to CBP, a histone acetyltransferase, in therapy-related acute myeloid leukemia with a t(11;16)(q23;p13.3). Proc Natl Acad Sci U S A *94*, 8732-8737.

Sternberg, P. W., and Horvitz, H. R. (1986). Pattern formation during vulval development in *C. elegans*. Cell *44*, 761-772.

Sternberg, P. W., and Horvitz, H. R. (1991). Signal transduction during *C. elegans* vulval induction. Trends Genet *7*, 366-371.

Sterner, J. M., Tao, Y., Kennett, S. B., Kim, H. G., and Horowitz, J. M. (1996). The amino terminus of the retinoblastoma (Rb) protein associates with a cyclin-dependent kinase-like kinase via Rb amino acids required for growth suppression. Cell Growth Differ *7*, 53-64.

Stott, F. J., Bates, S., James, M. C., McConnell, B. B., Starborg, M., Brookes, S., Palmero, I., Ryan, K., Hara, E., Vousden, K. H., and Peters, G. (1998). The alternative product from the human CDKN2A locus, p14(ARF), participates in a regulatory feedback loop with p53 and MDM2. EMBO J *17*, 5001-5014.

Sundaram, M., and Han, M. (1996). Control and integration of cell signaling pathways *during C. elegans* vulval development. Bioessays *18*, 473-480.

Tan, X., and Wang, J. Y. (1998). The caspase-RB connection in cell death. Trends Cell Biol *8*, 116-120.

Taniura, H., Taniguchi, N., Hara, M., and Yoshikawa, K. (1998). Necdin, a postmitotic neuron-specific growth suppressor, interacts with viral transforming proteins and cellular transcription factor E2F1. J Biol Chem *273*, 720-728.

Taya, Y. (1997). RB kinases and RB-binding proteins: new points of view. Trends Biochem Sci *22*, 14-17.

Taylor, S. J., and Shalloway, D. (1996). Cell cycle-dependent activation of Ras. Curr Biol *6*, 1621-1627.

Tevosian, S. G., Shih, H. H., Mendelson, K. G., Sheppard, K. A., Paulson, K. E., and Yee, A. S. (1997). HBP1: a HMG box transcriptional repressor that is targeted by the retinoblastoma family. Genes Dev *11*, 383-396.

Thomas, B. J., Gunning, D. A., Cho, J., and Zipursky, L. (1994). Cell cycle progression in the developing *Drosophila* eye: roughex encodes a novel protein required for the establishment of G1. Cell *77*, 1003-1014.

Thomas, B. J., Zavitz, K. H., Dong, X., Lane, M. E., Weigmann, K., Finley, R. L., Jr., Brent, R., Lehner, C. F., and Zipursky, S. L. (1997). roughex down-regulates G2 cyclins in G1. Genes Dev *11*, 1289-1298.

Thomas, J. H. (1997). Genetic and Molecular Analysis of Synthetic Multivulva Genes in *Caenorhabditis elegans*. Ph.D. Thesis. Massachusetts Institute of Technology, Cambridge, MA.

Tong, J. K., Hassig, C. A., Schnitzler, G. R., Kingston, R. E., and Schreiber, S. L. (1998). Chromatin deacetylation by an ATP-dependent nucleosome remodelling complex. Nature *395*, 917-921.

Trouche, D., Le Chalony, C., Muchardt, C., Yaniv, M., and Kouzarides, T. (1997). RB and hbrm cooperate to repress the activation functions of E2F1. Proc Natl Acad Sci U S A *94*, 11268-11273.

Tsai, K. Y., Hu, Y., Macleod, K. F., Crowley, D., Yamasaki, L., and Jacks, T. (1998). Mutation of E2f-1 suppresses apoptosis and inappropriate S phase entry and extends survival of Rb-deficient mouse embryos. Mol Cell *2*, 293-304.

Versteege, I., Sevenet, N., Lange, J., Rousseau-Merck, M. F., Ambros, P., Handgretinger, R., Aurias, A., and Delattre, O. (1998). Truncating mutations of hSNF5/INI1 in aggressive paediatric cancer. Nature *394*, 203-206.

Wade, P. A., Jones, P. L., Vermaak, D., and Wolffe, A. P. (1998). A multiple subunit Mi-2 histone deacetylase from Xenopus laevis cofractionates with an associated Snf2 superfamily ATPase. Curr Biol *8*, 843-846.

Wang, J. Y. (1997). Retinoblastoma protein in growth suppression and death protection. Curr Opin Genet Dev *7*, 39-45.

Weinberg, R. A. (1995). The retinoblastoma protein and cell cycle control. Cell *81*, 323-330.

Wen, S. T., Jackson, P. K., and Van Etten, R. A. (1996). The cytostatic function of c-Abl is controlled by multiple nuclear localization signals and requires the p53 and Rb tumor suppressor gene products. EMBO J *15*, 1583-1595.

White, R. J. (1997). Regulation of RNA polymerases I and III by the retinoblastoma protein: a mechanism for growth control? Trends Biochem Sci *22*, 77-80.

Xu, H. J., Xu, K., Zhou, Y., Li, J., Benedict, W. F., and Hu, S. X. (1994). Enhanced tumor cell growth suppression by an N-terminal truncated retinoblastoma protein. Proc Natl Acad Sci U S A *91*, 9837-9841.

Yamasaki, L., Bronson, R., Williams, B. O., Dyson, N. J., Harlow, E., and Jacks, T. (1998). Loss of E2F-1 reduces tumorigenesis and extends the lifespan of Rb1(+/-)mice. Nat Genet *18*, 360-364.

Yang, X. J., Ogryzko, V. V., Nishikawa, J., Howard, B. H., and Nakatani, Y. (1996). A p300/CBP-associated factor that competes with the adenoviral oncoprotein E1A. Nature *382*, 319-324.

Yee, A. S., Shih, H. H., and Tevosian, S. G. (1998). New perspectives on retinoblastoma family functions in differentiation. Front Biosci *3*, d532-547.

Zhang, Y., LeRoy, G., Seelig, H. P., Lane, W. S., and Reinberg, D. (1998). The dermatomyositis-specific autoantigen Mi2 is a component of a complex containing histone deacetylase and nucleosome remodeling activities. Cell *95*, 279-289.

Zhang, Y., Xiong, Y., and Yarbrough, W. G. (1998). ARF promotes MDM2 degradation and stabilizes p53: ARF-INK4a locus deletion impairs both the Rb and p53 tumor suppression pathways. Cell *92*, 725-734.

Figure 1. Schematic of a typical ell cycle composed of G1, S, G2 and M phases. The cell cycle is driven by the sequential activities of different cyclin-CDK complexes, as indicated above the schematic. Cell cycle profile of Rb phosphorylation is indicated below the schematic.

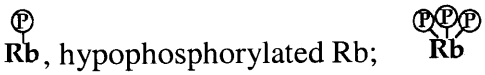

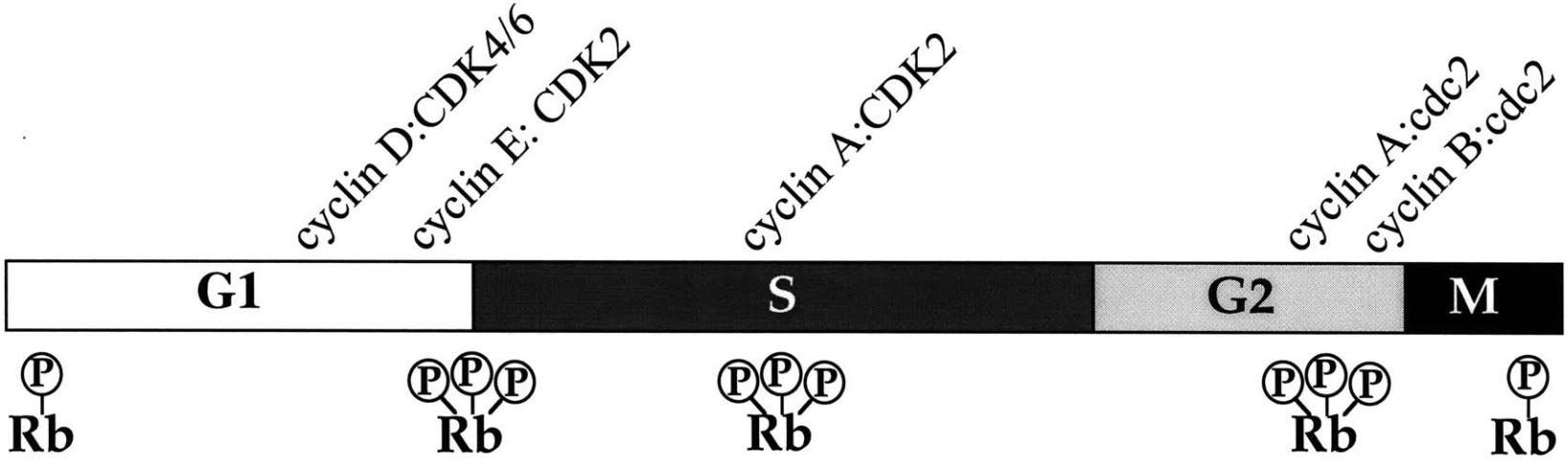
cyclin D:CDK4/6
cyclin E: CDK2
cyclin A:CDK2
cyclin A:cdc2
cyclin B:cdc2
G1
S
G2
M
P
Rb

Figure 2. The Rb tumor suppressor pathway (adapted from Mulligan and Jacks, 1998). Downstream targets of Rb are indicated as E2F and '?'. The components of this pathway are frequently targeted in human cancer, as indicated on the right.

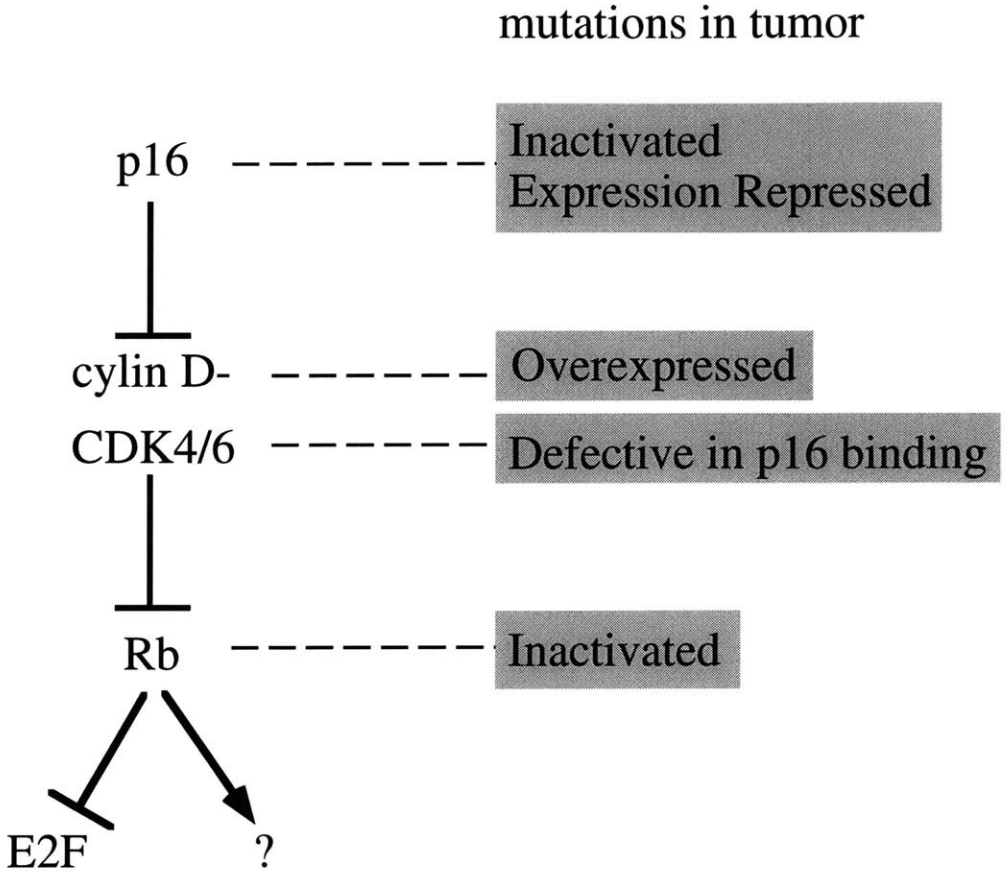
mutations in tumor
p16
Inactivated
Expression Repressed
cylin D-
CDK4/6
Overexpressed
Defective in p16 binding
Rb
Inactivated
E2F
?

Figure 3. The Rb-p53 tumor suppressor network. The p16-Rb and p19-p53 growth control pathways interact to trigger cell cycle arrest and apoptosis in response to aberrant growth signals and stress. Loss of Rb results in apoptosis, which is in part mediated by p53 activation following E2F-1 induction of p19. Cell cycle arrest upon DNA damage requires Rb activity and is likely mediated by p53 induction of p21.

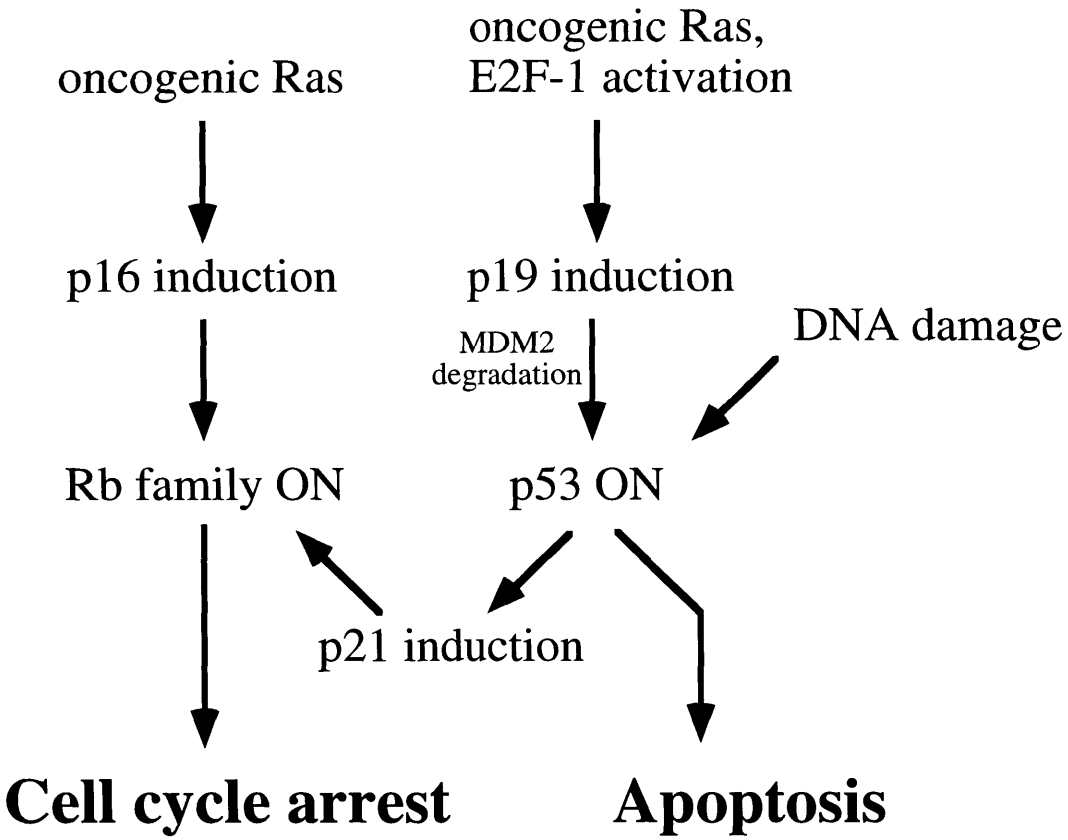
oncogenic Ras
oncogenic Ras,
E2F-1 activation
p16 induction
p19 induction
MDM2
degradation
DNA damage
Rb family ON
p53 ON
p21 induction
Cell cycle arrest
Apoptosis

Figure 4. Structure domains of Rb. The boundaries of the A, B pocket domains are indicated by the positions of amino acid residues above the schematic. The 16 phosphorylation sites are indicated by arrowheads. Filled arrowheads, sites shown to be phosphorylated; open arrowheads, sites not shown to be phosphorylated. T, threonine residue; S, serine residue. NLS, nuclear localization signal. The minimal growth suppression domain of Rb is indicated by the bracket.

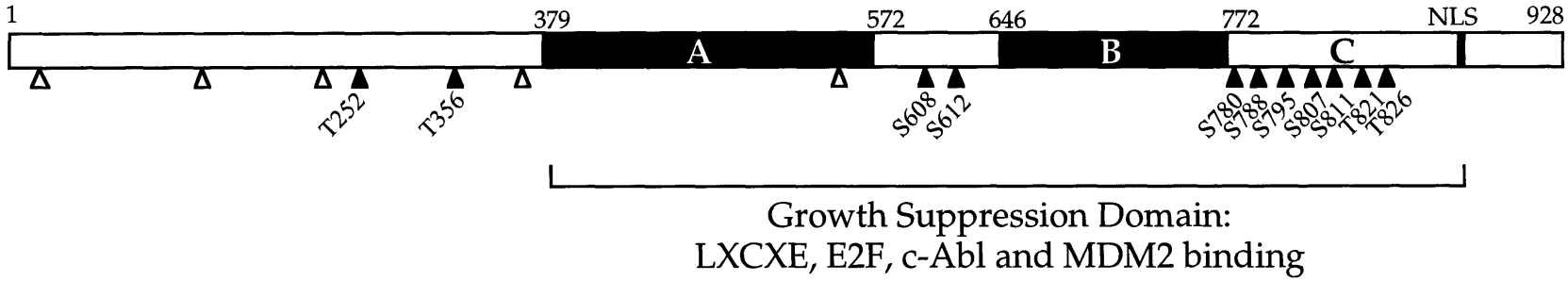
1
379
572
646
772
NLS
928
A
B
C
T252
T356
S608
S612
S780
S788
S795
S807
S811
T821
T826
Growth Suppression Domain:
LXCXE, E2F, c-Abl and MDM2 binding

Figure 5. Overview of vulval development. The vulval equivalence group is composed of six multipotent cells, named P(3-8).p, each capable of expressing any of three fates: the 1° and 2° vulval cell fates, or the 3° non-vulval cell fate. In wild type, P5.p, P6.p and P7.p are induced by a signal from the anchor cell (AC) and express the 2°, 1° and 2° fate, respectively, to form the vulva. The P3.p, P4.p and P8.p, on the other hand, express the non-vulval fate to fuse with the hypodermal syncytium. The positions of the P(3-8).p cells and the anchor cell are shown on top in the schematic of a hermaphrodite (left lateral view, cell sizes not drawn to scale). The division patterns that define the 1°, 2° and 3° fates are shown in the middle, where horizontal lines represent cell divisions. The tissues developed from the P(3-8).p cells are indicated below the brackets.

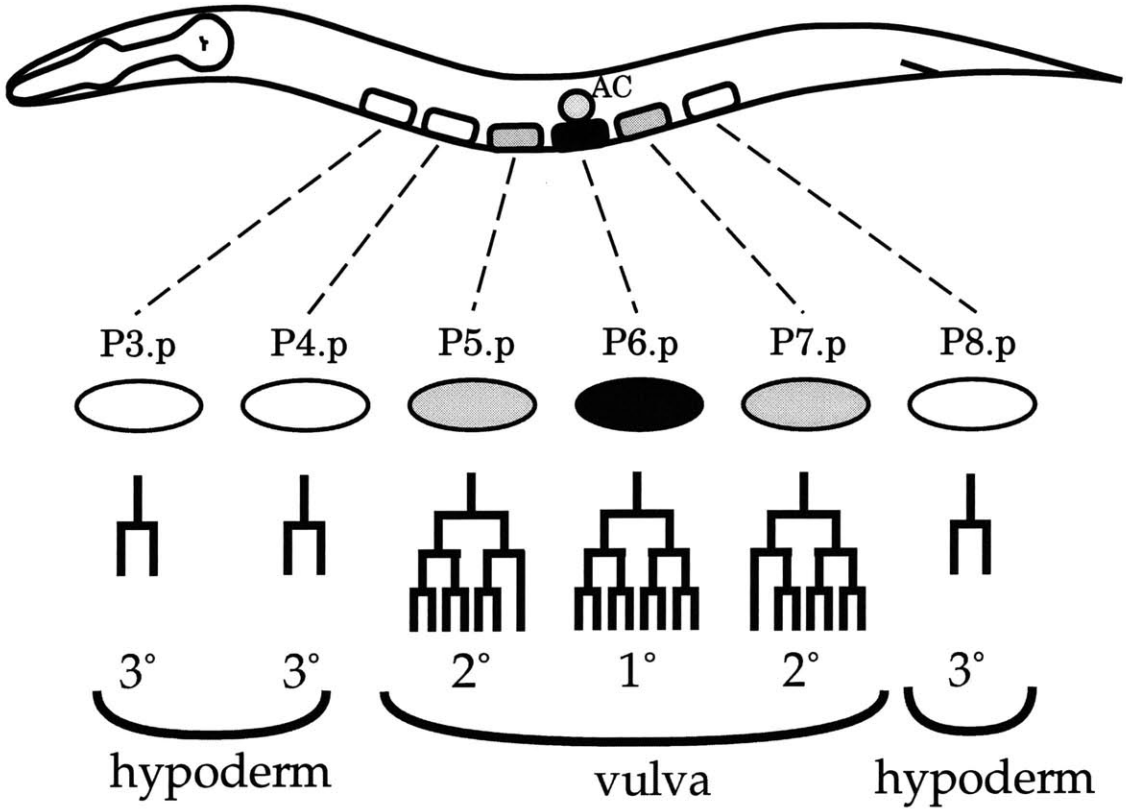
AC
P3.p
P4.p
P5.p
P6.p
P7.p
P8.p
3°
3°
2°
1°
2°
3°
hypoderm
vulva
hypoderm

Figure 6. Multiple signaling systems control vulval development. The inductive signal from the anchor cell is mediated by a conserved RTK/Ras signaling pathway. Lateral signaling mediated by the *lin-12*/Notch pathway is involved in the specification of 2° fate. Hypothetical inhibitory signals from the hypodermis inhibit expression of vulval cell fates through two functionally redundant pathways, the synMuv A and B pathways. The synMuv B genes likely act by *lin-35* Rb-mediated transcription repression. A wnt signal from an unknown source has been suggested to prevent fusion of the P(3-8).p cells with the hypodermis prior to their divisions mediated by the *bar-1* β-catenin gene, as indicated by the dashed arrow.

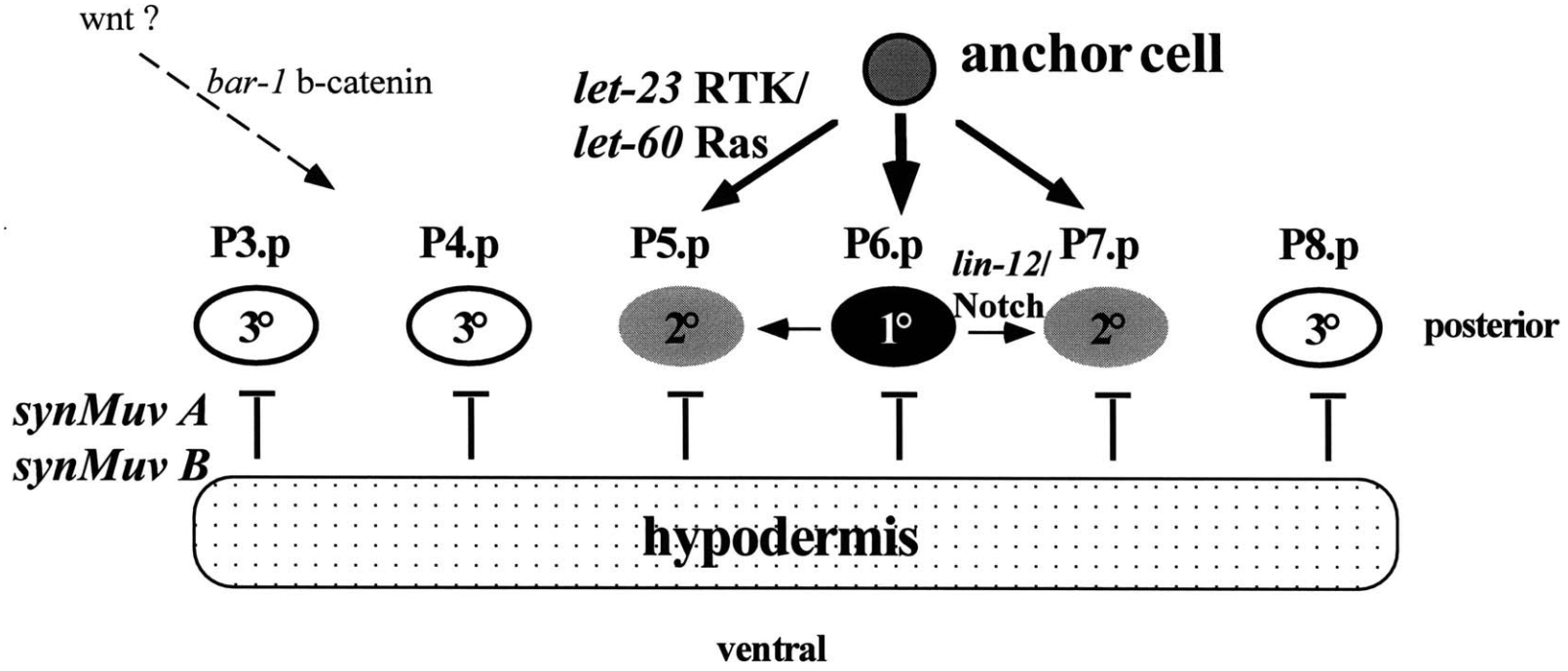
wnt ?
bar-1 b-catenin
let-23 RTK/
let-60 Ras
anchor cell
P3.p
P4.p
P5.p
P6.p
lin-12/
Notch
P7.p
P8.p
3°
3°
2°
1°
2°
3°
posterior
synMuv A
synMuv B
hypodermis
ventral

Chapter 2

lin-35 and *lin-53,* two genes that antagonize a *C. elegans* Ras pathway, encode proteins similar to Rb and its binding protein RbAp48

published in Cell *95*, 981-991 (1998)

Xiaowei Lu and H. Robert Horvitz

Howard Hughes Medical Institute, Massachusetts Institute of Technology, Cambridge, MA 02139

Summary

The Ras signaling pathway for vulval induction in *Caenorhabditis elegans* is antagonized by the activity of the synthetic multivulva (synMuv) genes, which define two functionally redundant pathways. We have characterized two genes in one of these pathways. *lin-35* encodes a protein similar to the tumor suppressor Rb and the closely related proteins p107 and p130. *lin-53* encodes a protein similar to RbAp48, a mammalian protein that binds Rb. In mammals, Rb and related proteins act as regulators of E2F transcription factors, and RbAp48 may act with such proteins as a transcriptional co-repressor. We propose that LIN-35 and LIN-53 antagonize the Ras signaling pathway in *C. elegans* by repressing transcription in the vulval precursor cells of genes required for the expression of vulval cell fates.

Introduction

Extracellular signals can promote or inhibit cell growth and differentiation via distinct signaling systems. The proper integration of multiple signals allows a cell to respond appropriately to its environment and is vital for homeostasis. Inappropriate activity of one or more signaling pathways can lead to tumorigenesis. RTK (receptor tyrosine kinase)/Ras pathways define one class of oncogene signaling pathways (reviewed by Cantley et al., 1991; Hunter, 1997). RTK/Ras pathways function during the normal development of many organisms, including the nematode *C. elegans* (reviewed by Dickson and Hafen, 1994).

In *C. elegans*, the formation of the hermaphrodite vulva is induced by an RTK/Ras signaling pathway. The vulva is generated from six multipotent ventral ectodermal blast cells, P3.p - P8.p (Sulston and Horvitz, 1977; Sulston and White, 1980). Each of these six P(3-8).p cells can potentially adopt either the 1° vulval cell fate, the 2° vulval cell fate or the 3° non-vulval cell fate (Sulston and White, 1980; Kimble, 1981; Sternberg and Horvitz, 1986). During wild-type development, a signal from the gonadal anchor cell induces the nearest P(3-8).p cell, P6.p, to adopt the 1° fate and the adjacent P5.p and P7.p cells to adopt the 2° fate. The cells furthest from the anchor cell, P3.p, P4.p and P8.p, adopt the uninduced 3° fate. Vulval induction acts through a signaling pathway, which includes the *lin-3* EGF-like ligand, the *let-23* RTK, the *sem-5* adaptor, *let-60* Ras, the *ksr-1* kinase, *lin-45* Raf, *mek-2* MEK and *mpk-1* MAP kinase, and regulates the activities of the ETS transcription factor LIN-1 and the winged-helix transcription factor LIN-31 (reviewed by Horvitz and Sternberg, 1991; Sundaram and Han, 1996, Tan et al., 1998).

Vulval induction is negatively regulated by the synthetic multivulva (synMuv) genes (Horvitz and Sulston, 1980; Ferguson and Horvitz, 1989). Loss-of-function mutations in these genes result in a multivulva (Muv) phenotype as a consequence of the expression of vulval cell fates by the P3.p, P4.p and P8.p cells. The Muv phenotype of these mutants requires mutations in two genes. Specifically, these synMuv mutations fall into two classes, referred to as A and B. Animals carrying a class A and a class B mutation have a Muv phenotype, while animals carrying one or more mutations of the same class have a wild-type vulval phenotype. These

mutations appear to define two functionally redundant pathways that negatively regulate the expression of vulval cell fates.

Four class A genes (*lin-8, lin-15*A, *lin-38*, and *lin-56*) and ten class B genes (*lin-9, lin-15*B, *lin-35*, *lin-36*, *lin-37*, *lin-51*, *lin-52*, *lin-53, lin-54*, and *lin-55*) have been identified (Horvitz and Sulston, 1980; Ferguson and Horvitz, 1989; Thomas, 1997). *lin-15* encodes both A and B activities in two non-overlapping transcripts (Ferguson and Horvitz, 1989; Clark et al., 1994; Huang et al., 1994). *lin-15*A, *lin-15*B, *lin-9* and *lin-36* encode novel proteins (Clark et al., 1994; Huang et al., 1994; Beitel, 1994; Thomas, 1997).

To elucidate the molecular mechanism by which the synMuv genes inhibit vulval induction, we have characterized two class B synMuv genes, *lin-35* and *lin-53*. Our findings indicate that in *C. elegans* vulval development an Rb-mediated pathway antagonizes the RTK/Ras pathway of vulval induction.

Results

Molecular identification of *lin-35*

We mapped *lin-35* between *unc-40* and the Tc1 polymorphism *stP124* (Williams et al., 1992) on LGI. We identified two overlapping cosmids from this interval, C03E6 and C32F10, each of which rescued the Muv phenotype of a *lin-35; lin-15*A strain in germline transformation experiments (Figure 1A). The smallest subclone that retained rescuing activity was a 9.3 kb Xho I-EcoR V fragment from the region of overlap between C03E6 and C32F10. The *C. elegans* genome consortium (Wilson et al., 1994) had determined the DNA sequence of this fragment. Using the 9.3 kb minimal rescuing fragment as a probe, we detected a single 3.2 kb transcript in both embryonic and mix-staged poly(A)+ RNA on a northern blot (Figure 1C), and we isolated cDNA clones from an embryonic cDNA library and determined the complete sequence of the longest cDNA (3.2 kb). We deduced the gene structure by comparing the genomic and the cDNA sequences (Figure 1B). The cDNA contains a single open reading frame (ORF) of 961 amino acids and appears to be full-length by three criteria: its size matches that of the transcript detected on the northern blot, it contains the last 11 nucleotides of the SL1 *trans*-spliced leader sequence (Krause and Hirsh,1987) at its 5' end and a poly(A) tail at its 3' end, and expression of this cDNA under control of the *C. elegans* heat-shock promoters (Stringham et al., 1992) rescued the *lin-35* mutant phenotype (data not shown). To confirm that the rescuing activity observed was indeed *lin-35* activity, we identified the molecular lesions associated with the eight existing *lin-35* alleles (Figure 1D). Six alleles are nonsense mutations, and two alleles have an identical splice-acceptor mutation in the fourth intron despite their independent isolation. The allele *n745* contains an early nonsense mutation predicted to eliminate the C-terminal 84% of LIN-35. This allele may completely eliminate *lin-35* function.

lin-35 encodes a protein similar to the tumor suppressor Rb

The predicted LIN-35 protein shares significant sequence similarity with the mammalian pocket proteins, which include the tumor suppressor Rb (Friend et al., 1986), p107 (Ewen et al., 1991) and p130 (Hannon et al., 1993; Li et al., 1993) (Figure 2). The similarity extends across the entire lengths of the proteins, including the "A/B pocket" domains, which mediate interactions

with proteins important for cell-cycle regulation, such as viral oncoproteins and E2F (reviewed by Taya, 1997). Overall, LIN-35 is 20% identical to p130, 19% to p107, 15% to Rb and 16% to RBF, an Rb-related protein in *Drosophila* (Du et al., 1996). Regions important for pocket protein function are more conserved. For example, the N-terminal region of the B pocket domain of LIN-35 (amino acid residues 744-839) is 34% identical to p130, 34% to p107, 29% to Rb and 30% to RBF. The spacer region that separates the A and B pockets of LIN-35 is not related in sequence to those of the pocket proteins. This spacer is short in length, like that of Rb. By contrast, p130 and p107 have much longer spacer regions, which are conserved between them and mediate their stable association with cyclin/cyclin-dependent kinase (CDK) complexes (reviewed by Zhu et al., 1994). Because LIN-35 is not particularly similar in sequence to any one of the three mammalian pocket proteins, *lin-35* may have diverged from an ancestor of the three mammalian genes before these three genes diverged from each other.

LIN-35 protein is present in vulval cells

We raised polyclonal antibodies against a peptide from the N-terminal region of LIN-35. Affinity-purified antisera recognized a single protein of about 110 kDa present in wild-type protein extracts but absent in *lin-35(n745)* extracts on western blots (Figure 3A). Thus, the antisera appeared to recognize specifically the LIN-35 protein product.

We stained wild-type and *lin-35* mutant worms with the purified anti-LIN-35 peptide antisera. In wild-type animals, the nuclei of most if not all cells in embryos and newly hatched L1 larvae stained (Figure 3B, 3C). In older larvae and adults, staining appreared diminished and became restricted to the nuclei of certain cells in the head and tail regions (data not shown) and of the P(3-8).p cells and their descendants (Figure 3D, 3E). We did not observe any staining during these stages in hyp7, the hypodermal syncytium that surrounds the P(3-8).p cells; hpy7 is the proposed site of action of *lin-15* and *lin-37* (Herman and Hedgecock, 1990; Hedgecock and Herman, 1995). The presence of LIN-35 protein in the P(3-8).p cell descendants is consistent with the hypothesis that *lin-35* acts cell-autonomously to regulate vulval development. The distribution of LIN-35 protein suggests that *lin-35* may have other functions. However, mutations in *lin-35* do not have any obvious pleiotropic effects (data not shown). It is possible that other functions of *lin-35,* like those involved in vulval development, are redundant.

lin-53 encodes a protein similar to RbAp48

Based on the finding that *lin-35* encodes a protein similar to Rb, we reasoned that other genes in the class B synMuv pathway might also be evolutionarily conserved. We identified from the *C. elegans* sequence database genomic sequences and expressed sequence tags (ESTs) (Wilson et al., 1994) predicted to encode proteins similar to proteins known to interact with Rb, and we compared their map positions with those of known class B synMuv genes. The cosmid K07A1 contained two predicted genes, named K07A1.12 and K07A1.11, both similar to RbAp48 (p48) and RbAp46 (p46), two closely related proteins that bind to Rb *in vivo* (Huang et al., 1991; Qian et al., 1993; Qian and Lee, 1995). This cosmid mapped near the class B synMuv gene *lin-53* (Ferguson and Horvitz, 1989; Thomas, 1997) between *unc-29* and *lin-11* on LGI. K07A1.11 lies about 100 bp 3' to K07A1.12 in the same orientation. To investigate whether *lin-53* corresponded to either of these genes, we tested to see if cosmid K07A1 would rescue the Muv phenotype of a *lin-53(n833); lin-15A* strain. Since the two existing alleles of *lin-53* are semi-dominant (see below), we looked for a partial rescue. Transgenic animals carrying K07A1 exhibited a Muv phenotype of reduced expressivity and penetrance compared to non-transgenic animals, indicating partial rescue (data not shown).

To confirm that K07A1 indeed contained *lin-53* activity, we determined the sequence of K07A1.12 and K07A1.11 from the two independently isolated *lin-53* alleles, *n833* and *n2978*, and found they carried an identical mutation in K07A1.12 (see below) and had no mutation in K07A1.11. We therefore conclude that K07A1.12 is *lin-53*. We used EST clones (Kohara et al., unpublished results) that correspond to each gene as probes to screen for additional cDNAs. The longest *lin-53* cDNA contained at its 5' end the last seven nucleotides from the *C. elegans trans*-spliced leader SL1 followed by three nucleotides upstream of the first ATG and at its 3' end a poly(A) tail. The longest K07A1.11 cDNA contained at its 5' end the last ten nucleotides from the *C. elegans trans*-spliced leader SL2 (Huang and Hirsh, 1989) followed by six nucleotides upstream of the first ATG and at its 3' end a poly(A) tail (Figure 4A). The tandem arrangement of these two genes in close proximity, with the message of the 3' gene SL2 *trans*-spliced, suggests that they form a complex locus and are co-transcribed (Spieth et al., 1993).

The LIN-53 protein is 72% identical to p48 and 70% to p46, while K07A1.11 is 53% identical to p48 and 52% to p46. p48 and p46 are 7 WD-repeat proteins, which are regulatory proteins that

mediate protein-protein interactions (Neer et al., 1994; Neer and Smith, 1996). Several p48-related proteins have been identified in different organisms, including the p55 subunit of the *Drosophila melanogaster* chromatin assembly factor-1 (Tyler et al., 1996) and the Saccharomyces cerevesiae proteins Msi1p (Ruggieri et al., 1989) and Hat2p (Parthun et al., 1996). LIN-53 is 72%, 27% and 25% identical to these proteins, respectively. The mutation in *lin-53(n833)* and *lin-53(n2978)* animals causes an leucine-to-phenylalanine change at a conserved leucine in the fifth WD domain (Figure 4B).

Since K07A1.11 is 54% identical to LIN-53, we tested whether expression of K07A1.11 could rescue the *lin-53* mutant phenotype. Driven by the *col-10* gene promoter, which is strongly expressed in hypodermal and hypodermal blast cells including the P(3-8).p cells during larval development (Olsen, P. and Ambros, V., personal communication), expression of the *lin-53* cDNA but not of the K07A1.11 cDNA partially rescued the Muv phenotype. This result suggests that K07A1.11 cannot substitute for wild-type *lin-53* function.

Wild-type *lin-53* activity is required for the class B synMuv pathway

To investigate further the role of *lin-53* in the class B synMuv pathway, we used RNA-mediated interference (RNAi), which has been shown to produce a specific phenocopy of the loss-of-function phenotype of a targeted gene by an unknown mechanism (Fire et al., 1998). We assayed the phenotypes of the progeny of wild-type, *lin-15*A or *lin-15*B mothers injected with antisense RNA derived from a *lin-53* cDNA clone. In all cases, antisense RNA injection caused embryonic lethality, suggesting that *lin-53* is required during embryogenesis. Similar observations have been reported by Shi and Mello (1998), who studied the role of the gene we have now identified as *lin-53* in embryonic development.

Because of this lethality, we were unable to use the RNAi technique to address the role of *lin-53* during vulval induction. Instead, we used the *col-10* promoter to drive expression of the antisense strand of a *lin-53* cDNA in hypodermal and hypodermal blast cells. About 18% of *lin-15*A animals carrying the P_{col-10} antisense *lin-53* construct were Muv, and this Muv phenotype was dependent on the presence of the *lin-15*A mutation (Table 2). Neither antisense expression of the K07A1.11 cDNA nor sense expression of the *lin-53* or K07A1.11 cDNAs had any effect in

similar experiments. These experiments suggest that wild-type *lin-53* activity is required for the class B synMuv pathway.

lin-53(n833) is likely to have a dominant-negative effect

Unlike other synMuv mutations, *lin-53(n833)* and *lin-53(n2978)* cause a semi-dominant class B synMuv phenotype, e.g., *lin-53(n833)/+; lin-15*A animals have an incompletely penetrant Muv phenotype (Table 1). Since loss of *lin-53* function causes a class B synMuv phenotype, as indicated by our antisense experiments, *lin-53* might be a haplo-insufficient locus; alternatively, *lin-53(n833)* might be a dominant-negative mutation. To distinguish between these two possibilities, we examined the phenotypes of animals of genotype *+/Df; lin-15*A (the *Df* chromosome was deleted for the *lin-53* locus, see Table 1 for detail). Five of 413 *+/Df; lin-15*A animals examined were Muv (Table 1). This penetrance of the Muv phenotype is much lower than in a *lin-53(n833)/+ ; lin-15*A strain, indicating that a two-fold reduction in wild-type *lin-53* activity only occasionally causes a synMuv phenotype and that *lin-53(n833)* is unlikely to simply reduce or eliminate *lin-53* function. Rather, *lin-53(n833)* is probably a dominant-negative mutation. Consistent with this hypothesis, expression of a *lin-53* cDNA carrying the *n833* mutation (L292F) driven by the *col-10* promoter caused a partially penetrant Muv phenotype in *lin-53(+); lin-15*A animals (Table 1). The *lin-53(n833)* mutation appears to affect only vulval development, while the *lin-53* null phenotype may be embryonic lethality. One explanation for the tissue-specific effect of the *lin-53(n833)* allele could be that vulval development is particularly sensitive to a decreased dosage of wild-type *lin-53*. Alternatively, the dominant-negative mutant LIN-53 protein may be titrating a factor that becomes limiting specifically in vulval tissue.

A GFP::LIN-53 transgene is expressed in the vulval cell nuclei

A transgene containing the *lin-53* cDNA tagged with GFP (Chalfie et al., 1994) at its N-terminus and under the control of the endogenous *lin-53* promoter was capable of partially rescuing the Muv phenotype of *lin-53(n833); lin-15*A animals. We examined the GFP expression pattern in animals carrying an integrated array of this transgene and observed GFP expression in most if not all nuclei during embryogenesis and in newly hatched L1s (Figure 5A, 5B). During larval development, we observed fluorescence in many nuclei in the head and tail regions, similar to the

LIN-35 staining pattern seen with the anti-LIN-35 peptide antibody. GFP was also present in hypodermal cells throughout development (data not shown). At the time of vulval induction, GFP was visible in all P(3-8).p cells and persisted until after the P(3-8).p cell divisions and vulval morphogenesis were complete (Figure 5C, 5D).

A *C. elegans* homolog of histone deacetylase may act in the *lin-35* Rb-mediated synMuv pathway

Based on recent findings that Rb can recruit a histone deacetylase, HDAC1, to repress transcription from target promoters (Brehm et al., 1998; Luo et al., 1998; Magnaghi-Jaulin et al., 1998) and the fact that p48 has been identified as a subunit of histone deacetylase (Taunton, 1996), we investigated whether several *C. elegans* histone deacetylase homologs, *hda-1*, *hda-2* and *hda-3* (Shi and Mello, 1998), might be involved in the synMuv pathway. RNAi of *hda-1* caused embryonic lethality, while RNAi of *hda-2* and *hda-3* produced no obvious phenotypic abnormality in either a *lin-15*A or *lin-15*B background (data not shown). We then tested whether tissue-specific antisense expression of *hda-1* driven by the *col-10* promoter can cause a synMuv phenotype. Similar to *lin-53* antisense expression, *hda-1* antisense expression caused a Muv phenotype in a *lin-15*A background but not in a wild-type background, i.e., a Class B synMuv phenotype. Antisense expression of the closely related *hda-3* gene had no effect (Table 3). This result suggests that the histone deacetylase gene *hda-1* activity is required for the *lin-35* Rb-mediated synMuv pathway.

LIN-35 Rb, LIN-53 p48 and HDA-1 interact *in vitro*

To determine whether LIN-35 Rb can directly bind LIN-53 p48 or HDA-1, as predicted by their sequences, we performed GST pull-down experiments. Bacterially-produced glutothione S-transferase (GST) or GST::LIN-53 or GST::HDA-1 fusion proteins immobilized on beads were incubated with different *in vitro* translated ^{35}S-methionine-labeled proteins. GST::LIN-53 interacted with a fragment of LIN-35 Rb that contains the entire A/B pocket (LIN-35BX) but not with LIN-35 fragments that lack the intact A/B pocket or with control proteins (Figure 6B). Interestingly, GST::LIN-53(L292F) and GST::HDA-1 fusion proteins also interacted with the LIN-35BX fragment (data not shown). It is worth noting that the HDA-1 sequence lacks a recognizable LXCXE motif, which is involved in the interaction between human Rb and HDAC1 (Brehm et al., 1998; Magnaghi-Jaulin et al., 1998). Therefore, HDA-1 does not appear to interact

with LIN-35 Rb via an LXCXE motif. GST::LIN-53 and GST::LIN-53(L292F) fusion proteins also interacted with HDA-1 (Figure 6B and data not shown). None of the proteins tested was retained by GST beads (data not shown). These results indicate that direct physical interactions can occur between any two of the three proteins LIN-35 Rb, LIN-53 p48 and HDA-1. We have not determined whether a ternary complex containing these three proteins can exist.

The *lin-35* and *lin-53* synMuv phenotypes require a functional RTK/Ras signaling pathway

To determine how the *lin-35* and *lin-53* synMuv genes interact with the Ras signaling pathway during vulval development, we analyzed the vulval phenotype of triple mutants carrying either a *lin-35* or a *lin-53* mutation, a mutation in a class A synMuv gene and a vulvaless (Vul) mutation in a Ras signaling gene (Table 4). The synMuv phenotype was epistatic to the Vul phenotype caused by a mutation in the *lin-3* gene, which encodes the inductive signal (Table 4). This observation suggests that the *lin-35* and *lin-53* genes act downstream of or in parallel to *lin-3* and that the synMuv phenotype does not require the *lin-3* inductive signal.

By contrast, the Vul phenotypes of mutations in *let-23* RTK, *sem-5*, *let-60* Ras, *lin-45* Raf and *mpk-1* genes were epistatic to the synMuv phenotype (Table 4). These observations suggest that the *lin-35* and *lin-53* genes act upstream of or in parallel to the RTK/Ras signaling genes. In other words, the expression of vulval cell fates by the P3.p, P4.p and P8.p cells in synMuv mutants requires a functional RTK/Ras signal transduction pathway. These observations concerning *lin-35* and *lin-53* are equivalent to previous observations concerning other synMuv genes (Ferguson et al., 1987; Huang et al., 1994; Thomas, 1997).

Since in synMuv mutants P5.p, P6.p and P7.p generally express normal vulval cell fates, synMuv gene activities are not required in these three cells. To determine whether the synMuv genes can act in the P5.p, P6.p and P7.p cells, we analyzed the phenotype of triple mutants carrying either a *lin-35* or a *lin-53* mutation, a mutation in a class A synMuv gene and a Vul mutation in *lin-2*, *lin-7* or *lin-10* . These three genes act as positive regulators of the LET-23 RTK activity by localizing LET-23 to the basolateral membrane of the P(3-8).p cells, thus allowing better access to the LIN-3 inductive signal from the anchor cell (Kaech et al., 1998). Mutations in *lin-2*, *lin-7* and *lin-10* in general cause P5.p, P6.p and P7.p to adopt the uninduced 3° fate and result in a Vul phenotype. By contrast, in the triple mutants, P5.p, P6.p and P7.p in general adopt a vulval fate

(Table 5). Thus, in these three cells in the absence of receptor localization the activity of RTK/Ras pathway is insufficient to induce vulval cell fates unless synMuv gene activity is eliminated. This observation reveals that synMuv gene activity can function in P5.p, P6.p and P7.p. We conclude that synMuv gene activity acts in all six P(3-8).p cells to antagonize the activity of the RTK/Ras signaling pathway.

Discussion

lin-35 encodes a protein related to Rb, and *lin-53* encodes a protein with striking similarity to an Rb-binding protein, p48 (72% identity). *lin-35*, *lin-53* and a *C. elegans* histone deacetylase gene act in the same genetic pathway to antagonize a Ras signal transduction pathway in *C. elegans*. We propose that in mammals Rb, p48 and histone deacetylase genes act in a tumor suppressor pathway that involves mechanisms and molecules similar to those of the synMuv pathway in *C. elegans* and that may well antagonize a mammalian Ras pathway.

lin-35 Rb, *lin-53* p48 and *hda-1* may act to repress transcription in the P(3-8).p cells

Rb, a key regulator of the mammalian cell cycle (reviewed by Weinberg, 1995; Wang, 1997), acts mainly through E2F transcription factors (composed of E2F and DP heterodimers), which regulate the expression of genes required for entry into S phase (reviewed by Dyson, 1998; Nevins, 1998). Rb, p107 and p130 can interact with DNA-bound E2F either to abolish transactivation or to exert active repression of transcription from target promoters. One mechanism by which Rb represses transcription is to bind and recruit the histone deacetylase HDAC1, presumably to remodel chromatin structure on a target promoter and thereby limit access of the transcriptional machinery to the DNA (Brehm et al., 1998; Luo et al., 1998; Magnaghi-Jaulin et al., 1998). p48 has been found together with HDAC1 in a large co-repressor complex required for Mad-Max-mediated transcriptional repression (Hassig et al., 1997; Laherty et al., 1997).

We propose that the class B synMuv genes inhibit vulval induction by a conserved mechanism: LIN-35 Rb forms a complex with a sequence-specific transcription factor (indicated as "TF" in Figure 7), presumably an E2F-like protein, and recruits a co-repressor complex containing HDA-1, LIN-53 p48 and other proteins (indicated as "X" in Figure 7) to turn off the transcription of vulval-specification genes via E2F-binding sites (Figure 7). In the wild type, in the P3.p, P4.p and P8.p cells, synMuv gene activity antagonizes the basal activity of the RTK/Ras pathway by repressing transcription of vulval genes. As a result, those cells adopt the non-vulval 3° fate. In P5.p, P6.p and P7.p, on the other hand, the antagonistic effect of synMuv gene activity is inactivated or can be overcome by the activated RTK/Ras pathway, thereby releasing

transcriptional repression and permitting the expression of vulval fates. In the P(3-8).p cells of a synMuv mutant, repression cannot occur and all six P(3-8).p cells express vulval fates, resulting in a Muv phenotype. The synMuv genes do not appear to exert their effects by regulating cell cycle progression of the P(3-8).p cells, since all six of these cells have very similar cell cycle profiles (Sulston and Horvitz, 1977; Euling and Ambros, 1996).

Class B synMuv genes act in an intercellular signaling pathway to regulate transcription

Both *lin-35* and *lin-53* appear to be expressed in the P(3-8).p cells and their descendants, consistent with the hypothesis that these class B synMuv genes act in P(3-8).p. Some class B synMuv genes, specifically *lin-15* and *lin-37*, appear to act in the hypodermal cell hyp7 to regulate an intercellular signal (Herman and Hedgecock, 1990; Hedgecock and Herman, 1995), while others, specifically *lin-36* (Thomas, 1997), *lin-35* and *lin-53,* seem to act in the P(3-8).p cells to control the response to that signal. We suggest that a LIN-35 Rb/LIN-53 p48/HDA-1 nuclear complex responds to the intercellular signaling pathway encoded by other class B synMuv genes to regulate transcription during vulval development in *C. elegans*.

Many questions remain to be answered. For example, what are the ligand, receptor and signal transducers in the class B synMuv pathway? So far, none of the cloned class B genes appears to encode a secreted or transmembrane protein. Also, what are the other components of the proposed repressor complex, and what functions might they serve? It is possible that components of the class B synMuv signal transduction pathway are used in biological processes in addition to vulval development, so that mutations in such components would cause pleiotropic effects and would not be isolated as synMuv mutants. Indeed, the null phenotypes of *lin-53* and *hda-1* appear to be embryonic lethality, as indicated by RNAi experiments (this study, Shi and Mello, 1998), and strong mutations in *lin-9* cause sterility (Ferguson and Horvitz, 1989). The characterization of the remaining class B genes and the identification of genes that interact with the known class B genes should provide more insight into this signaling pathway.

How might the synMuv pathway interface with the Ras pathway?

Gene interaction experiments both by us and by others indicate that in synMuv mutants anchor cell-independent activity of the Ras pathway is necessary for the expression of vulval cell fates (Ferguson et al., 1987; Huang et al., 1994; Thomas, 1997). Thus, the synMuv genes must act

genetically upstream of or in parallel to the Ras pathway. Action in parallel would be consistent with recent findings from studies of mammalian cells: dominant-negative Ras and Ras neutralizing antibodies induced an Rb-dependent block in DNA synthesis and G1 arrest (Mittnacht et al., 1997; Peeper et al., 1997), suggesting that Rb functions to inhibit mitogenesis downstream of or in parallel to Ras.

Although we cannot yet assign the precise point of interface between the synMuv and Ras pathways in vulval development, our molecular analyses of the class B synMuv pathway take us one step closer to understanding the nature of the anatagonism between the synMuv genes and the Ras pathway. As we discussed above, we propose that the class B synMuv pathway acts by repressing transcription in the P(3-8).p cells.

What might be the target genes for LIN-35 Rb-mediated transcriptional repression? Candidate genes include those in the *let-23* RTK/*let-60* Ras pathway. However, given the findings of Peeper et al. (1997) cited above, it seems more likely that the class B synMuv genes act to repress genes involved in vulval differentiation. Since the LIN-1 ETS protein also seems likely to act by repressing vulval differentiation genes (Beitel et al., 1995; Tan et al., 1998), LIN-35 Rb and LIN-1 may have at least partially overlapping targets. The identification of target genes for the LIN-35 Rb repressor complex and for the LIN-1 ETS protein may well help establish the nature of the antagonism between the Rb pathway and the Ras pathway both in *C. elegans* and in other organisms.

Experimental Procedures

Strains and Genetics

C. elegans strains were cultured as described by Brenner (1974) and were grown at 20°C unless otherwise noted. Mutations used (Riddle et al., 1997) were as follows: LGI, *unc-40(e271), bli-6(e937), dpy-5(e61), unc-29(e1072), lin-11(n566), lin-10(n299)* and *qDf9* (Ellis and Kimble, 1995); LGII, *lin-7(e1413)* and *let-23(sy97)*; LGIII, *mpk-1(oz140);* LGIV, *lin-3(n378), let-60(n1876)* and *lin-45(sy96),* LGX, *lin-15(n767)* (a class A mutation), *lin-15(n744)* (a class B mutation), *lin-2(n397)* and *sem-5(n2030).* To map *lin-35* with respect to *unc-40* and *stP124*, we isolated Bli non-Unc recombinants from the progeny of *unc-40 stP124 bli-4/lin-35(n2977); lin-15(n433)* hermaphrodites and scored the progeny of these recombinants for *lin-35* and *stP124.* Of 63 recombinants, 19 had *stP124* and were non-Muv, 9 had *stP124* and were Muv, and 35 did not have *stP124* and were Muv.

Transgenic Animals

Germline transformation was performed as described by Mello et al. (1991). DNA (30-100 ng/μl) was coinjected with a *unc-76* rescuing plasmid (100 ng/μl) (Bloom and Horvitz, 1997), and lines of non-Unc-76 transgenic animals were established. Chromosomal integration of extrachromosomal arrays of transgene was accomplished by γ-ray irradiation of transgenic animals.

Identification of cDNAs and Sequence Analysis of cDNAs and Mutant Alleles

To identify *lin-35* and *lin-53* cDNAs, we screened a cDNA library made from *C. elegans* embryonic RNA (Okkema and Fire, 1994). The sequences of the ends of inserts of positive clones were first determined using vector primers, and the complete sequence of the longest cDNA was then determined using primers positioned within the coding sequences. The sequence of at least one additional cDNA clone for each gene was determined to confirm splicing patterns. The sequences of both strands of the coding regions and splice junctions were determined from PCR fragments amplified from the *lin-35* and *lin-53* mutant alleles and purified by gel

electrophoresis. DNA sequences were determined using an automated ABI 373A DNA sequencer (Applied Biosystems).

In vitro Interaction Assays

Wild-type and mutant *lin-53* cDNAs were cloned into vector pGEX4T-3 (Pharmacia), expressed in *E. coli* strain BL21(DE3) and purified with glutothione sepharose beads as recommended by the manufacturer (Pharmacia).

lin-35, *lin-53* and *hda-1* cDNA fragments were cloned into the vector pCITE4a(+) (Novagen) or pRK5. The resulting constructs were used as templates to synthesize ^{35}S-methionine-labeled proteins in the TNT Coupled Reticulocyte Lysate System (Promega). Labeled proteins were incubated with equal amounts of GST fusion proteins for 2 hr at 4°C. Bound proteins were eluted with 2x SDS sample buffer and analyzed by SDS-PAGE (10%) and autoradiography.

Antibodies

A peptide from the N-terminal region of LIN-35, HSRKIRRYQEYIRR, with a cysteine added to its N-terminus was coupled to keyhole limpet hemacyanin (KLH) and used to immunize rabbits and obtain antisera (Zymed). Antibodies were purified over a peptide affinity column (Pierce). For western blots, the LIN-35 protein was visualized using horse-radish peroxidase-conjugated secondary antibodies (Bio-Rad) and chemiluminescent detection reagents (Pierce). Immunocytochemistry was as described by Finney and Ruvkun (1990).

RNA and RNAi Analyses

For northern blot analysis, poly(A)+ RNA was isolated using the FAST TRACK system (Invitrogen). RNA was subjected to electrophoresis and transferred to Nytran. The filter was probed with ^{32}P-radiolabeled *lin-35* genomic DNA. PCR fragments containing cDNA flanked by the T7 and the T3 promoters amplified from the cDNA phage lysates were used for *in vitro* RNA synthesis as described (Fire et al., 1998). The unmodified RNA was resuspended in H_2O and injected at 1-5 μg/μl. Injected animals were moved to a new plate 12 hrs after injection to enrich for progeny that had been subjected to antisense injection.

Acknowledgments

We thank Sander van den Heuvel, Tyler Jacks, Yang Shi and members of the Horvitz laboratory for critically reading this manuscript, Beth James for help with determining DNA sequences, Yuji Kohara for the EST cDNA clones and the *C. elegans* Genetics Center for the deficiency strains used in the *lin-53* gene dosage studies. H. R. H. is an Investigator of the Howard Hughes Medical Institute.

References

Beitel, G. J., Tuck, S., Greenwald, I. and Horvitz, H. R. (1995). The *Caenorhabditis elegans* gene *lin-1* encodes an ETS-domain protein and defines a branch of the vulval induction pathway. Genes Dev. *9*, 3149-3162.

Beitel, G. J. (1994). Genetic and molecular analyses of *let-60 ras*, *lin-1* and *lin-9*: genes that function in *C. elegans* vulval induction. Ph.D. Thesis, Massachusetts Institute of Technology, Cambridge, MA.

Bloom, L. and Horvitz, H. R. (1997). The *Caenorhabditis elegans* gene *unc-76* and its human homologs define a new gene family involved in axonal outgrowth and fasciculation. Proc. Natl. Acad. Sci. U. S. A. *94*, 3414-3419.

Brehm, A., Miska, E. A., McCance, D. J., Reid, J. L., Bannister, A. J. and Kouzarides, T. (1998). Retinoblastoma protein recruits histone deacetylase to repress transcription. Nature *391*, 601-605.

Brenner, S. (1974). The genetics of *Caenorhabditis elegans*. Genetics *77*, 71-94.

Cantley, L. C., Auger, K. R., Carpenter, C., Duckworth, B., Graziani, A., Kapeller, R. and Soltoff, S. (1991). Oncogenes and signal transduction. Cell *64*, 281-302.

Chalfie, M., Tu, Y., Euskirchen, G., Ward, W. W. and Prasher, D. C. (1994). Green fluorescent protein as a marker for gene expression. Science *263*, 802-805.

Clark, S. G., Lu, X. and Horvitz, H. R. (1994). The *Caenorhabditis elegans* locus *lin-15*, a negative regulator of a tyrosine kinase signaling pathway, encodes two different proteins. Genetics *137*, 987-997.

Dickson, B. and E. Hafen. (1994). Genetics of signal transduction in invertebrates. Curr Opin Genet Dev *4,* 64-70.

Du, W., Vidal, M., Xie, J. E. and Dyson, N. (1996). RBF, a novel RB-related gene that regulates E2F activity and interacts with cyclin E in *Drosophila*. Genes Dev. *10*, 1206-1218.

Dyson, N. (1998). The regulation of E2F by pRB-family proteins. Genes Dev *12*, 2245-2262.

Ellis, R. E. and Kimble, J. (1995). The *fog-3* gene and regulation of cell fate in the germ line of *Caenorhabditis elegans*. Genetics *139*, 561-577.

Euling, S. and V. Ambros. (1996). Heterochronic genes control cell cycle progress and developmental competence of *C. elegans* vulva precursor cells. Cell *84,* 667-676.

Ewen, M. E., Xing, Y. G., Lawrence, J. B. and Livingston, D. M. (1991). Molecular cloning, chromosomal mapping, and expression of the cDNA for p107, a retinoblastoma gene product-related protein. Cell *66*, 1155-1164.

Ferguson, E. L. and Horvitz, H. R. (1989). The multivulva phenotype of certain *Caenorhabditis elegans* mutants results from defects in two functionally redundant pathways. Genetics *123*, 109-121.

Ferguson, E. L., Sternberg, P. W. and Horvitz, H. R. (1987). A genetic pathway for the specification of the vulval cell lineages of *Caenorhabditis elegans*. Nature *326*, 259-267.

Finney, M. and Ruvkun, G. (1990). The *unc-86* gene product couples cell lineage and cell identity in *C. elegans*. Cell *63*, 895-905.

Fire, A., Xu, S., Montgomery, M. K., Kostas, S. A., Driver, S. E. and Mello, C. C. (1998). Potent and specific genetic interference by double-stranded RNA in *Caenorhabditis elegans* . Nature *391*, 806-811.

Friend, S. H., Bernards, R., Rogelj, S., Weinberg, R. A., Rapaport, J. M., Albert, D. M. and Dryja, T. P. (1986). A human DNA segment with properties of the gene that predisposes to retinoblastoma and osteosarcoma. Nature *323*, 643-646.

Hannon, G. J., Demetrick, D., and Beach, D. (1993). Isolation of the Rb-related p130 through its interaction with CDK2 and cyclins. Genes Dev. *7*, 2378-2391.

Hassig, C. A., Fleischer, T. C., Billin, A. N., Schreiber, S. L., and Ayer, D. E. (1997). Histone deacetylase activity is required for full transcriptional repression by mSin3A. Cell *89*, 341-347.

Hedgecock, E. M. and Herman, R. K. (1995). The *ncl-1* gene and genetic mosaics of *Caenorhabditis elegans*. Genetics *141*, 989-1006.

Herman, R. K. and Hedgecock, E. M. (1990). Limitation of the size of the vulval primordium of *Caenorhabditis elegans* by *lin-15* expression in surrounding hypodermis. Nature *348*, 169-171.

Horvitz, H. R., and Sternberg, P. W. (1991). Multiple intercellular signalling systems control the development of the *Caenorhabditis elegans* vulva. Nature. *351*, 535-41.

Horvitz, H. R. and Sulston, J. E. (1980). Isolation and genetic characterization of cell-lineage mutants of the nematode *Caenorhabditis elegans*. Genetics *96*, 435-454.

Huang, L. S., Tzou, P. and Sternberg, P. W. (1994). The *lin-15* locus encodes two negative regulators of *Caenorhabditis elegans* vulval development. Mol. Biol. Cell *5*, 395-411.

Huang, S., Lee, W. H. and Lee, E. Y. (1991). A cellular protein that competes with SV40 T antigen for binding to the retinoblastoma gene product. Nature *350*, 160-162.

Huang, X. Y. and Hirsh, D. (1989). A second trans-spliced RNA leader sequence in the nematode *Caenorhabditis elegans*. Proc. Natl. Acad. Sci. U. S. A. *86*, 8640-8644.

Hunter, T. (1997). Oncoprotein networks. Cell *88*, 333-346.

Kaech, S.M., C.W. Whitfield, and S.K. Kim. (1998). The LIN-2/LIN-7/LIN-10 complex mediates basolateral membrane localization of the *C. elegans* EGF receptor LET-23 in vulval epithelial cells. *Cell 94*, 761-771.

Kimble, J. (1981). Alterations in cell lineage following laser ablation of cells in the somatic gonad of *Caenorhabditis elegans*. Dev. Biol. *87*, 286-300.

Krause, M. and Hirsh, D. (1987). A trans-spliced leader sequence on actin mRNA in *C. elegans*. Cell *49*, 753-761.

Laherty, C. D., Yang, W. M., Sun, J. M., Davie, J. R., Seto, E. and Eisenman, R. N. (1997). Histone deacetylases associated with the mSin3 corepressor mediate mad transcriptional repression. Cell *89*, 349-356.

Li, Y., Graham, C., Lacy, S., Duncan, A. M., and Whyte, P. (1993). The adenovirus E1A-associated 130-kD protein is encoded by a member of the retinoblastoma gene family and physically interacts with cyclins A and E. Genes Dev. *7*, 2366-2377.

Luo, R. X., Postigo, A. A. and Dean, D. C. (1998). Rb interacts with histone deacetylase to repress transcription. Cell *92*, 463-473.

Magnaghi-Jaulin, L., Groisman, R., Naguibneva, I., Robin, P., Lorain, S., Le Villain, J. P., Troalen, F., Trouche, D. and Harel-Bellan, A. (1998). Retinoblastoma protein represses transcription by recruiting a histone deacetylase. Nature *391*, 601-605.

Mello, C. C., Kramer, J. M., Stinchcomb, D. and Ambros, V. (1991). Efficient gene transfer in *C. elegans*: extrachromosomal maintenance and integration of transforming sequences. EMBO J. *10*, 3959-3970.

Mittnacht, S., Paterson, H., Olson, M.F. and Marshall, C.J. (1997). Ras signalling is required for inactivation of the tumour suppressor pRb cell-cycle control protein. Curr Biol *7*, 219-221.

Neer, E. J., Schmidt, C. J., Nambudripad, R. and Smith, T. F. (1994). The ancient regulatory-protein family of WD-repeat proteins. Nature *371*, 297-300.

Neer, E. J. and Smith, T. F. (1996). G protein heterodimers: new structures propel new questions. Cell *84*, 175-178.

Nevins, J. R. (1998). Toward an understanding of the functional complexity of the E2F and retinoblastoma families. Cell Growth Differ *9*, 585-593.

Okkema, P. G. and Fire, A. (1994). The *Caenorhabditis elegans* NK-2 class homeoprotein CEH-22 is involved in combinatorial activation of gene expression in pharyngeal muscle. Development *120*, 2175-2186.

Parthun, M. R., Widom, J. and Gottschling, D. E. (1996). The major cytoplasmic histone acetyltransferase in yeast: links to chromatin replication and histone metabolism. Cell *87*, 85-94.

Peeper, D. S., Upton, T. M., Ladha, M. H., Neuman, E., Zalvide, J., Bernards. R., DeCaprio, J. A. and Ewen, M. E. (1997). Ras signalling linked to the cell-cycle machinery by the retinoblastoma protein. Nature *386*, 177-181.

Riddle, D. L., Blumenthal, T., Meyer, B. J. and Priess, J. R. (1997). *C. elegans* II

Ruggieri, R., Tanaka, K., Nakafuku, M., Kaziro, Y., Toh-e, A. and Matsumoto, K. (1989). MSI1, a negative regulator of the RAS-cAMP pathway in *Saccharomyces cerevisiae*. Proc. Natl. Acad. Sci. U. S. A. *86*, 8778-8782.

Qian, Y. W. and Lee, E. Y. (1995). Dual retinoblastoma-binding proteins with properties related to a negative regulator of ras in yeast. J. Biol. Chem. *270*, 25507-25513.

Qian, Y. W., Wang, Y. C., Hollingsworth, R., Jr., Jones, D., Ling, N. and Lee, E. Y. (1993). A retinoblastoma-binding protein related to a negative regulator of Ras in yeast. Nature *364*, 648-652.

Shi, Y. and Mello, C. (1998). A CBP/p300 homolog specifies multiple differentiation pathways in *Caenorhabditis elegans*. Genes Dev. *12*, 943-955.

Spieth, J., Brooke, G., Kuersten, S., Lea, K. and Blumenthal, T. (1993). Operons in *C. elegans*: polycistronic mRNA precursors are processed by trans-splicing of SL2 to downstream coding regions. Cell *73*, 521-532.

Sternberg, P. W. and Horvitz, H. R. (1986). Pattern formation during vulval development in *C. elegans*. Cell *44*, 761-772.

Stringham, E. G., Dixon, D. K., Jones, D. and Candido, E. P. (1992). Temporal and spatial expression patterns of the small heat shock (hsp16) genes in transgenic *Caenorhabditis elegans*. Mol. Biol. Cell *3*, 221-233.

Sulston, J. E. and Horvitz, H. R. (1977). Post-embryonic cell lineages of the nematode, *Caenorhabditis elegans*. Dev. Biol. *56*, 110-156.

Sulston, J. E. and White, J. G. (1980). Regulation and cell autonomy during postembryonic development of *Caenorhabditis elegans*. Dev. Biol. *78*, 577-597.

Sundaram, M. and Han, M. (1996). Control and integration of cell signaling pathways during *C. elegans* vulval development. Bioessays *18*, 473-480.

Tan, P. B., Lackner, M. R., and Kim, S. K. (1998). MAP kinase signaling specificity mediated by the LIN-1 Ets/LIN-31 WH transcription factor complex during *C. elegans* vulval induction. Cell *93*, 569-580.

Taunton, J., Hassig, C. A. and Schreiber, S. L. (1996). A mammalian histone deacetylase related to the yeast transcriptional regulator Rpd3p . Science *272*, 408-411.

Taya, Y. (1997). RB kinases and RB-binding proteins: new points of view. Trends Biochem. Sci. *22(1)*: 14-17.

Thomas, J. H. (1997). Genetic and Molecular Analysis of Synthetic Multivulva Genes in *Caenorhabditis elegans*. Ph.D. Thesis. Massachusetts Institute of Technology, Cambridge, MA.

Tyler, J. K., Bulger, M., Kamakaka, R. T., Kobayashi, R. and Kadonaga, J. T. (1996). The p55 subunit of *Drosophila* chromatin assembly factor 1 is homologous to a histone deacetylase-associated protein. Mol. Cell. Biol. *16*, 6149-6159.

Wang, J. Y. (1997). Retinoblastoma protein in growth suppression and death protection. Curr. Opin. Genet. Dev. *7*, 39-45.

Weinberg, R. A. (1995). The retinoblastoma protein and cell cycle control. Cell *81*, 323-330.

Williams, B. D., Schrank, B., Huynh, C., Shownkeen, R. and Waterston, R. H. (1992). A genetic mapping system in *Caenorhabditis elegans* based on polymorphic sequence-tagged sites. Genetics *131*, 609-624.

Wilson, R., Ainscough, R., Anderson, K., Baynes, C., Berks, M., Bonfield, J., Burton, J., Connell, M., Copsey, T., Cooper, J. et al. (1994). 2.2 Mb of contiguous nucleotide sequence from chromosome III of *C. elegans*. Nature *368*, 32-38.

Zhu, L., Enders, G. H., Wu, C. L., Starz, M. A., Moberg, K. H., Lees, J. A., Dyson, N. and Harlow E. G. (1994) Growth suppression by members of the retinoblastoma protein family. Cold Spring Harb. Symp. Quant. Biol. *59*, 75-84.

Figure 1. Cloning of *lin-35*

A. Genetic and physical maps of the *lin-35* region (from the ACEDB database; *e.g.* Wilson et al., 1994). Dashed lines indicate alignments between the genetic and physical maps. Short horizontal lines represent cosmid clones assayed in germline transformation experiments. Cosmids that rescued the *lin-35* mutant phenotype are shown in bold (see text).

B. Deletions and subclones derived from cosmids C32F10 and C03E6 were tested for *lin-35* rescuing activity. The penetrance of rescued lines was less than 20% Muv on average, as compared to more than 90% Muv in non-rescued lines and the starting mutant strain. +, rescue. -, no rescue. At the bottom is the structure of the *lin-35* gene deduced from the genomic and cDNA sequences. The *trans*-spliced leader SL1, the initiation and stop codons and the poly(A) tail are indicated. Solid boxes indicate coding sequences, and open boxes indicate non-coding sequences. The positions of the eight *lin-35* mutations are indicated by the vertical lines above the boxes.

C. Northern blot analysis of *lin-35*. *lin-35* message is present in both embryonic (E) and mixed-staged (M) poly(A)+ RNA (3 μg in each lane) from wild-type *C. elegans* as detected using the 9.3 kb Xho I-EcoR V minimal rescuing fragment as a probe.

D. *lin-35* mutations. Each predicted mutant protein is represented schematically by a box labeled with its length in amino acids. Wild-type LIN-35 is shown on top. The A/B pockets are indicated by solid boxes. The region required for E2F binding includes the A and B pockets and the hatched box.

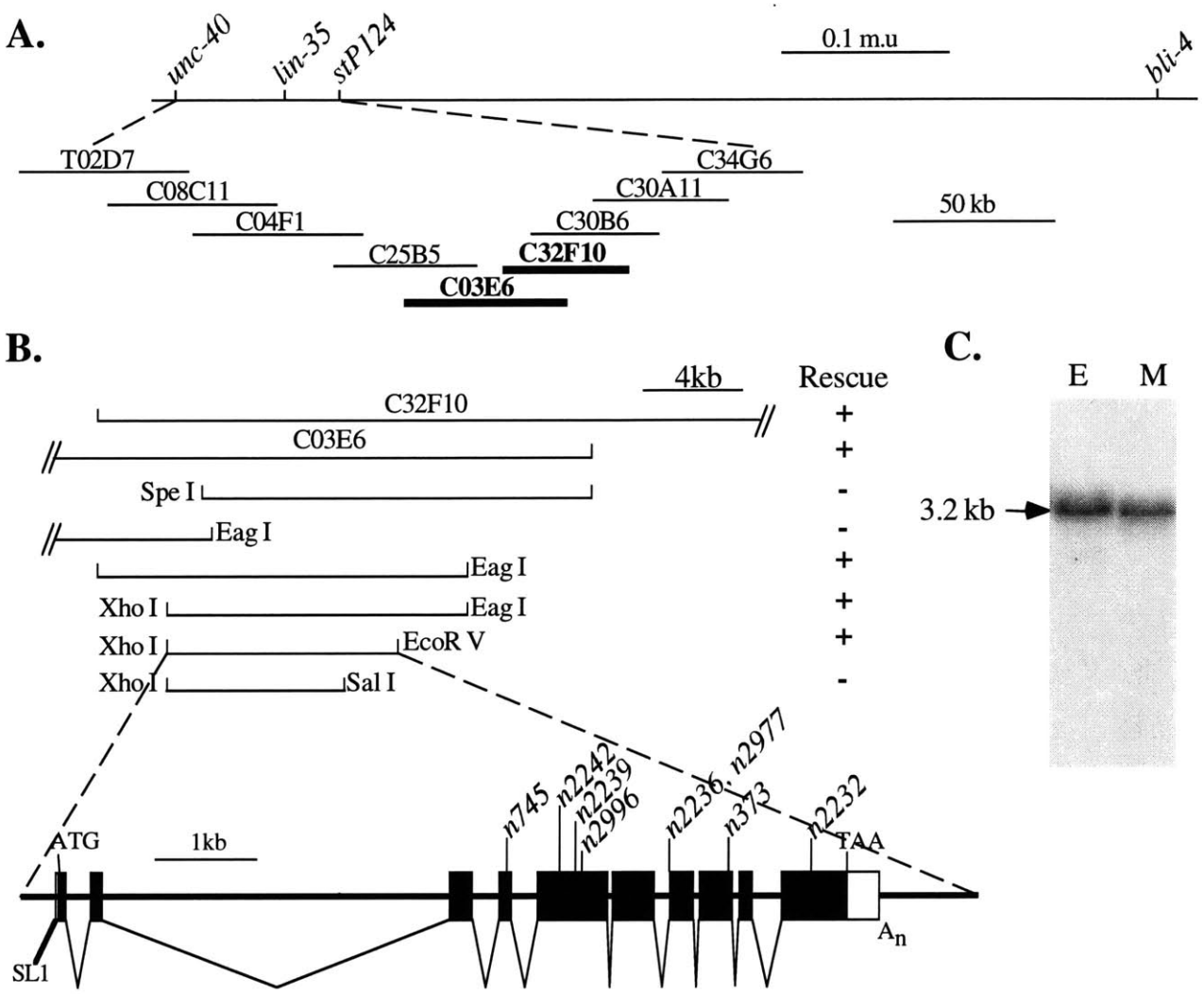

D.

Allele	Change in Nucleotide Sequence and Predicted Consequence	Predicted Protein Product
wild-type	———	1 A B 961
n745	TGG to TGA, W151stop	1 150
n2242	CAA to TAA, Q236stop	1 235
n2239	TGG to TGA, W285stop	1 284
n2996	CAA to TAA, Q305stop	1 304
n2236	tttcagAG to tttcaaAG, splice acceptor	1 525
n2977	tttcagAG to tttcaaAG, splice acceptor	1 525
n373	CAA to TAA, Q700stop	1 699
n2232	CGA to TGA, R837stop	1 836

Figure 2. Sequence alignment of LIN-35 and other pocket proteins

The numbers on the right indicate amino-acid positions. Identities with LIN-35 are shaded in black, and identities among other pocket proteins are shaded in grey. Two amino-acid residues known to be mutated in Rb in human cancers are labeled with asterisks. The A and B pockets are underlined, and the region at the C-terminus also required for E2F binding is indicated by the dashed line.

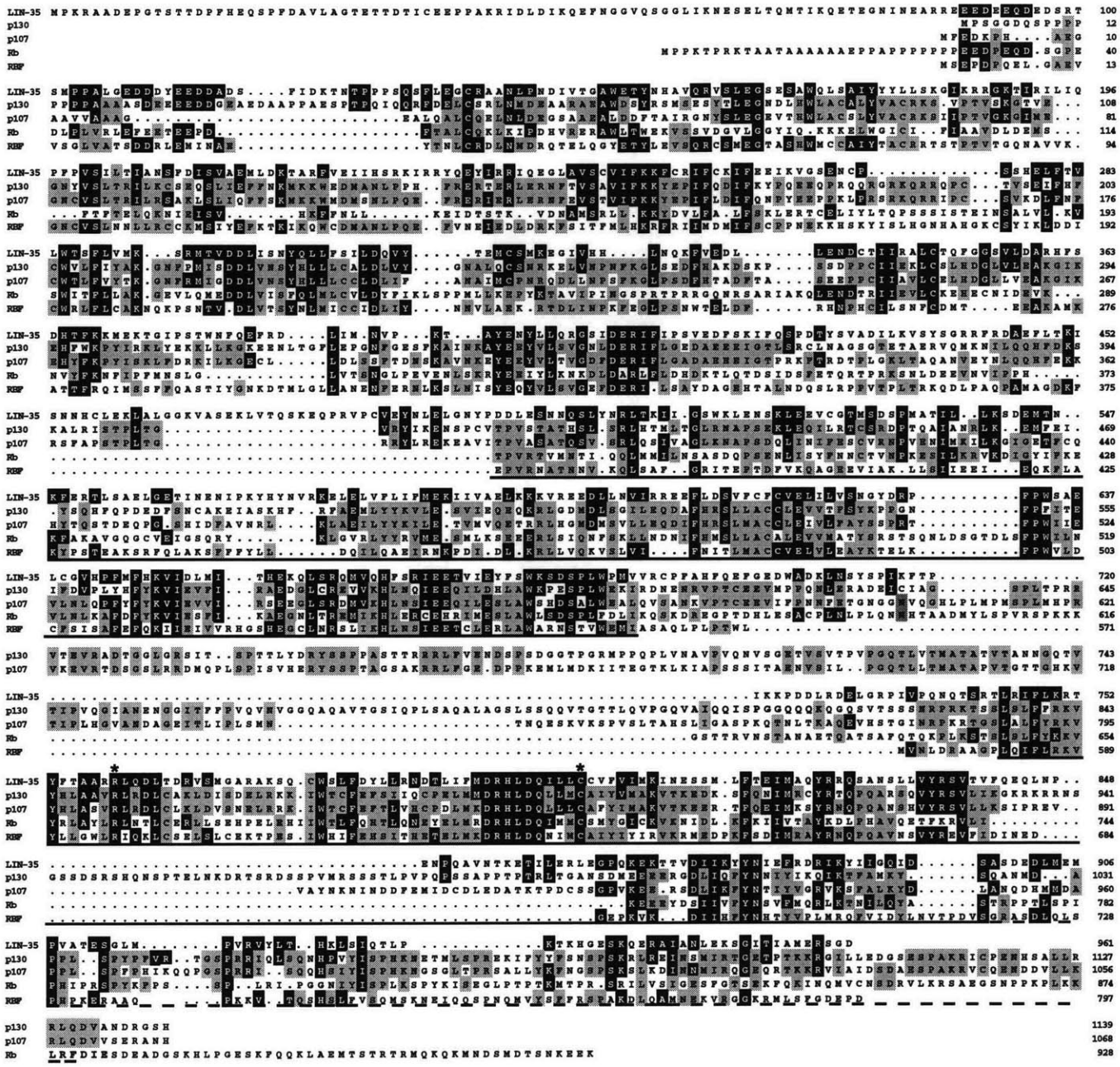

Figure 3. LIN-35 protein expression

A. Anti-LIN-35 peptide antibodies detected a protein of expected size (110 kDa) in wild-type (lane 1) but not in *lin-35(n745)* mutant (lane 2) extracts. The molecular weights of marker proteins are indicated.

B-D. Whole-mount staining of wild-type embryos and larvae using anti-LIN-35 peptide antibodies. Scale bar, 10 μm.

B, C. LIN-35 is broadly expressed in embryos and in newly hatched L1s.

D. LIN-35 staining in nuclei of P(3-8).p cells (arrows) in an L3 animal.

E. LIN-35 staining in nuclei of the developing L4 vulva. Ventral is down, anterior is to the left. Arrow points to the invagination located at the center of the developing vulva.

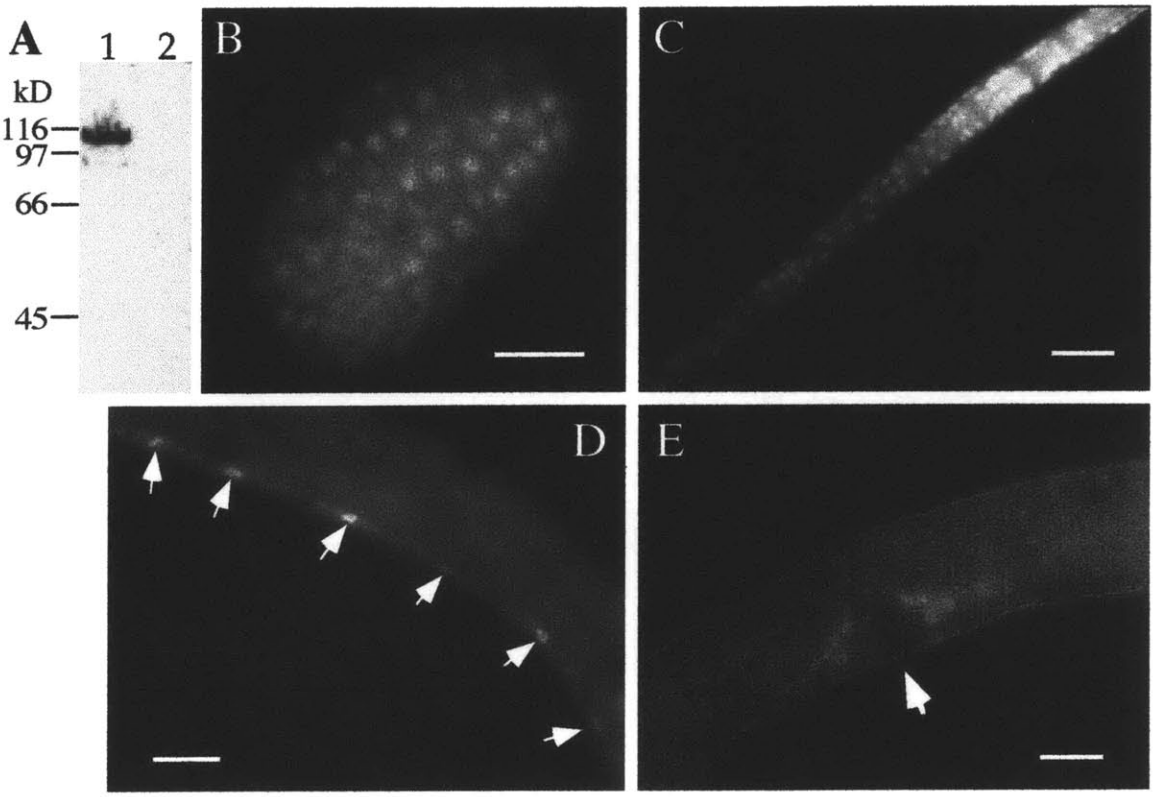
A
1
2
kD
116
97
66
45
B
C
D
E

Figure 4. *lin-53* structure and similarity to human p48

A. Genomic organization of the *lin-53*/K07A1.11 locus. The top horizontal line indicates cosmid K07A1, which is missing the presumptive 5' regulatory region and part of the first exon of *lin-53*. Solid boxes indicate coding sequences, and open boxes indicate non-coding sequences. SL1 and SL2 *trans*-spliced leaders, initiation and stop codons, and poly(A) tails are indicated.

B. Sequence alignment of LIN-53, K07A1.11, human p48 and p46, *Drosophila* p55, and *S. cerevisiae* Hat2p and Msi1p. Identities with LIN-53 are shaded in black, and identities among other proteins are shaded in grey. The signature residues of each WD repeat are indicated by asterisks. The two identical *lin-53* L292F mutations (*n833*, *n2978*) are indicated by the arrow.

A.

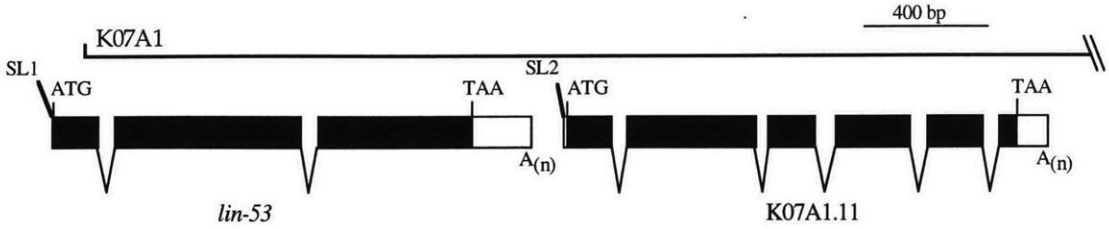
400 bp
K07A1
SL1
ATG
TAA
A(n)
SL2
ATG
TAA
A(n)
lin-53
K07A1.11

B.

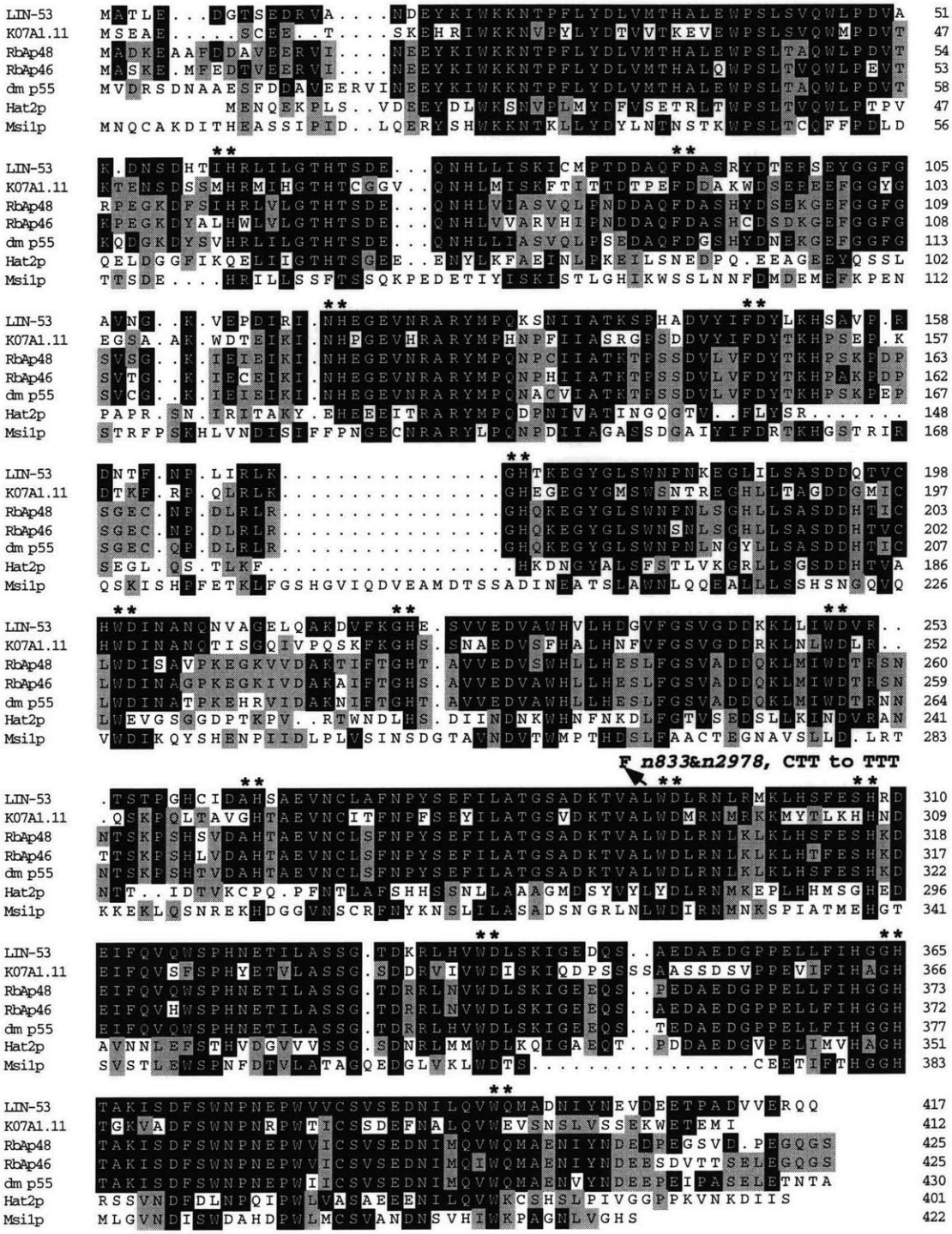
LIN-53
K07A1.11
RbAp48
RbAp46
dm p55
Hat2p
Msi1p
F n833&n2978, CTT to TTT

Figure 5. A GFP::LIN-53 transgene is expressed in many nuclei

A, B. GFP is expressed in most nuclei in embryos and newly hatched L1s.

C. GFP is expressed in the nuclei of P(3-8).p cells (arrows) in an L3 animal.

D. GFP is expressed in the nuclei of the developing L4 vulva. Ventral is down, anterior is to the left. Arrowhead points to the invagination located at the center of the developing vulva. Scale bar, 10 μm.

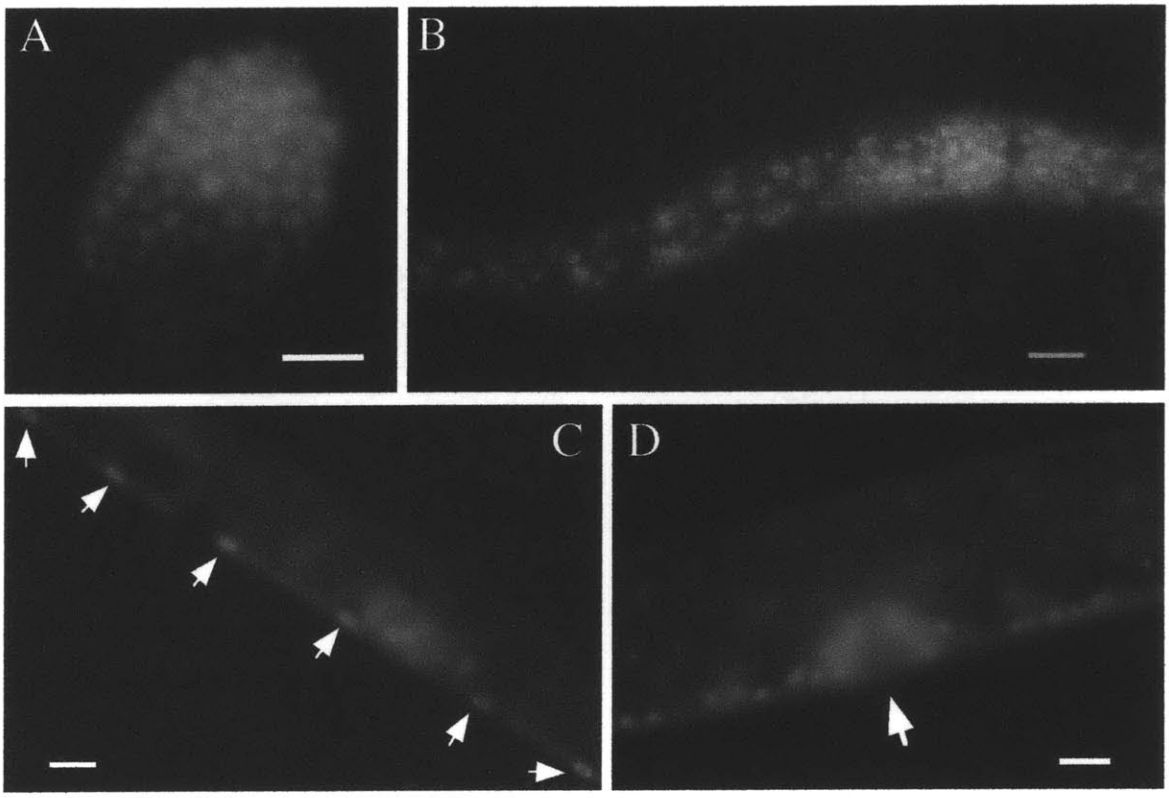
A
B
C
D

Figure 6. LIN-35 Rb, LIN-53 p48 and HDA-1 *in vitro* interactions

A. Schematic of LIN-35 Rb fragments used.

B. GST::LIN-53 interaction with LIN-35 Rb and HDA-1. Left panel, GST::LIN-53 beads were incubated with *in vitro* translated ^{35}S-methionine-labeled LIN-35 fragments, luciferase, CED-4, EGL-1 or HDA-1. Right panel, 20% of the input radiolabeled proteins used in the experiments shown in the left panel. The molecular weights of marker proteins are indicated.

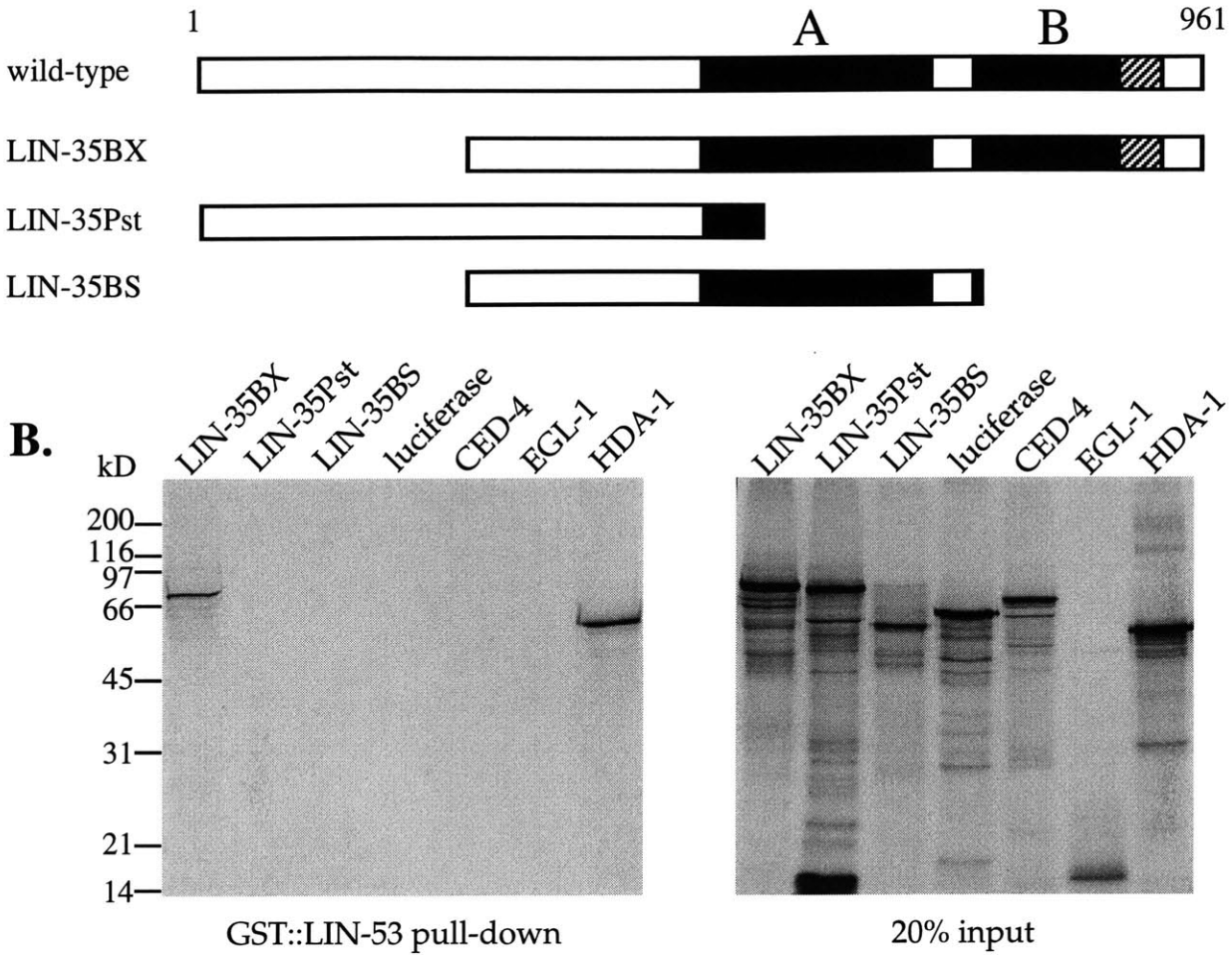
A.
1
A
B
961
wild-type
LIN-35BX
LIN-35Pst
LIN-35BS
B.
kD
LIN-35BX
LIN-35Pst
LIN-35BS
luciferase
CED-4
EGL-1
HDA-1
200
116
97
66
45
31
21
14
GST::LIN-53 pull-down
20% input

Figure 7. Models for how LIN-35 and LIN-53 may cooperate to repress transcription
"TF" indicates a sequence-specific transcription factor, presumably, an E2F-like protein; the closed box indicates a DNA-binding site for "TF" in the promoter. In the P3.p, P4.p and P8.p cells of wild-type animals, the synMuv genes are active, a repressor complex "X" that contains LIN-53 and HDA-1 is recruited by the DNA-bound LIN-35/TF complex to turn OFF transcription, and the 3° fate is expressed. In the P5.p, P6.p and P7.p cells of wild-type animals, synMuv genes are inactive or their effect is overcome by the signal-dependent activation of the Ras pathway. As a result, the transcription of vulval cell-fate genes is ON, leading to the expression of 1° or 2° fates. By contrast, in the P3-8.p cells of synMuv mutants, repression is relieved, transcription is ON, and the 1° or 2° fates are expressed.

A.

	Transcription	Cell Fate in *synMuv A* background
wild type, P3.p, P4.p and P8.p	OFF	3°
wild type, P5.p, P6.p and P7.p	ON	1°/2°
synMuv mutants, P(3-8).p	ON	1°/2°

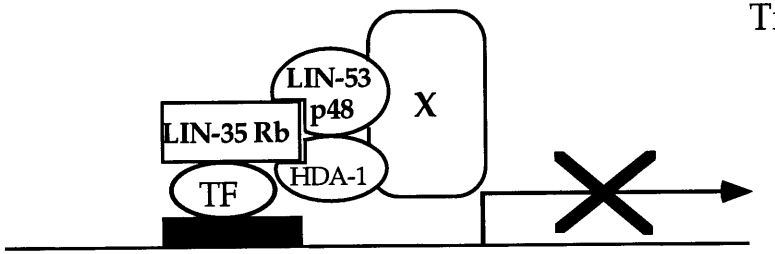

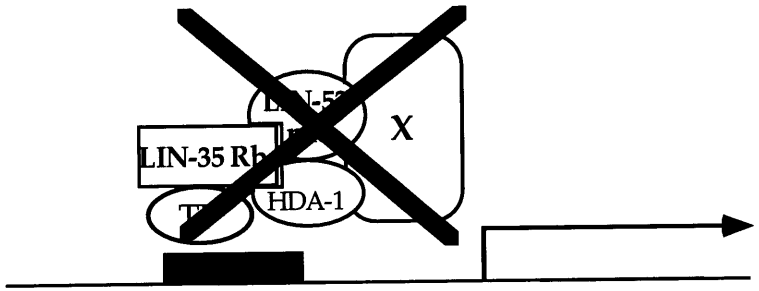

Table 1. *lin-53* tissue-specific antisense expression causes a synMuv phenotype

Construct	Percent Muv (n)	
	unc-76; lin-15A	*unc-76*
P_{col-10} — *lin-53* antisense	18±5% (672)[a]	0 (many)
P_{col-10} — *lin-53*	0 (many)	ND
P_{col-10} — K07A1.11	0 (many)	ND
P_{col-10} — K07A1.11 antisense	0 (many)	ND

ND, not determined. a, number obtained from three transgenic lines.

Table 2. *lin-53(n833)* may act as a dominant-negative allele

lin-53 Genotype[a]	percent Muv (n)
n833/n833	100 (many)
n833/+	12 (500)[b]
+/qDf9	1 (413)[c]
n833/qDf9	100 (many)
+/+; Ex[n833]	17±6 (504)[d]

All strains tested were homozygous for *lin-15*A.
Muv, animals with at least one pseudovulva on their ventral sides. n, number of animals scored.
a, in heterozygous strains, *lin-53(n833)* chromosomes were marked with *dpy-5*, and *lin-53(+)* chormosomes with *unc-29* and *lin-11*.
b, number indicates penetrance of Muv phenotype among *n833/+* progeny from *n833/+* hermaphrodites.
c, number indicates penetrance of Muv phenotype among *+/qDf9* progeny from *+/qDf9* hermaphrodites. *qDf9* deletes *lin-53* as confirmed by PCR of homozygous deficiency embryos.
d, number obtained from three transgenic lines.

Table 3. *hda-1* tissue-specific antisense expression causes a synMuv phenotype

Construct	Percent Muvs (n)	
	unc-76; lin-15A	*unc-76*
P_{col-10} — *hda-1* antisense	21±9% (462)[a]	0 (many)
P_{col-10} — *hda-3* antisense	0 (many)	ND

ND, not determined. a, number obtained from three transgenic lines.

Table 4. Epistasis analysis between synMuv and Vul mutations

Genotype[a]	Vulval Phenotype
synMuv[a]	Muv
lin-3(n378)	Vul
lin-3(n378); synMuv	Muv
let-23(lf)	Vul
let-23(lf); synMuv	Vul
sem-5(lf)	Vul
sem-5(lf); synMuv	Vul
let-60(lf)[b]	Vul
let-60(lf); synMuv	Vul
lin-45(lf)	Vul
lin-45(lf); synMuv	Vul
mpk-1(lf)[c]	Vul
mpk-1(lf); synMuv	Vul

a, two synMuv genotypes were studied: *lin-35(n745); lin-15*A and *lin-53(n833); lin-15*A .
b, *let-60(lf)* animals were derived from *let-60(lf)*/+ heterozygotes in order to rescue the maternal-effect L1 larval lethality.
c, vulval phenotype was assayed at 25°C, since *mpk-1(oz140)* is temperature-sensitive.

Table 5. Gene interactions with *lin-2*, *lin-7* and *lin-10*

Genotype[a]	Vulval Phenotype	Percent Induced						
		P3.p	P4.p	P5.p	P6.p	P7.p	P8.p	n
wild type	wild-type	0	0	100	100	100	0	many
synMuv[a]	Muv	100	100	100	100	100	100	24
lin-2(lf)	Vul	0	5	48	62	38	0	21
lin-2(lf); synMuv	Muv, Muv/Vul[b]	64	79	100	100	96	71	28
lin-7(lf)	Vul	0	0	22	30	11	0	27
lin-7(lf); synMuv	Muv, Muv/Vul	49	73	92	100	89	57	37
lin-10(lf)	Vul	0	0	14	33	19	0	21
lin-10(lf); synMuv	Muv, Muv/Vul	58	79	96	100	96	50	24

a, two synMuv genotypes were studied: *lin-35(n745); lin-15*A (shown) and *lin-53(n833); lin-15*A (not shown, but similar).
b, Muv/Vul, animals with both ectopic vulval tissues and non-functional vulvae.

Chapter 3

lin-37, a gene that acts in the *lin-35* Rb pathway in *C. elegans*, encodes a novel protein

Xiaowei Lu

Howard Hughes Medical Institute, Massachusetts Institute of Technology
Cambridge, MA 02139

Summary

lin-37 has been previously shown to act cell non-autonomously in the *lin-35* Rb pathway, which functions redundantly with another pathway to antagonize Ras signaling during vulval development in *C. elegans* . To investigate the role of *lin-37* in the proposed *lin-35* Rb-mediated transcriptional repression of vulval cell fate genes, we have characterized this gene molecularly. The predicted LIN-37 protein is a novel hydrophilic protein of 275 amino acids. Furthermore, a *lin-37*::GFP transgene carrying a nuclear localization signal is expressed in both the vulval precursor cells and surrounding hypodermal cells at the time of vulval induction.

Introduction

Intercellular signaling pathways play important roles in development and homeostasis of multicellular organisms. Genetic and molecular analyses of pattern formation and cell fate determination in *C. elegans* and in *Drosophila* have identified components of multiple evolutionarily conserved signaling pathways, a number of which have been implicated in human cancer.

One of the best-studied pathways is the Ras signaling pathway. Ras proteins act as molecular switches that relay proliferative signals from cell-surface receptors to the nucleus by sequential activation of Raf, MAP kinase kinase (MEK) and MAP kinase. Since Ras activity has profound effect on cell proliferation, it is of importance to elucidate the mechanisms that modify Ras signaling activity. To this end, we have begun to characterize a group of genes that antagonize Ras signaling during vulval development in *C. elegans*.

The development of *C. elegans* hermaphrodite vulva is developed from six vulval precursor cells, termed P(3-8).p, each of which is capable of expressing either a vulval cell lineage (1°, 2°) or a non-vulval cell lineage (3°) (Kimble, 1981). In wild-type, P(5-7).p cells express vulval fates and their 22 descendants form the adult vulva. P3.p, P4.p and P8.p cells, on the other hand, express the non-vulval fate.

Cell fate determination of these cells is regulated by multiple signaling systems (reviewed by Sternberg and Horvitz, 1991; Sundaram and Han, 1996). A conserved receptor tyrosine kinase (RTK)/Ras pathway acts to induce P(5-7).p cells to express vulval fates (reviewed by Sternberg and Han, 1998). Inactivation of this pathway causes all six vulval precursor cells to express the non-vulval fate resulting in a vulvaless (Vul) phenotype. By contrast, two functionally redundant pathways act to prevent P3.p, P4.p and P8.p cells from expressing the vulval fates (Ferguson and Horvitz, 1989; Thomas, 1997). While inactivation of either pathway alone has no effect on vulval development, inactivation of both pathways causes all six vulval precursor cells to express vulval fates resulting in a synthetic multivulva (synMuv) phenotype. Thus, it appears that the synMuv genes normally act to antagonize the Ras signaling activity to inhibit expression

of vulval fates by P3.p, P4.p and P8.p cells. Genetic epistasis analysis has indicated that synMuv genes act through or in parallel to the Ras signaling pathway, as the Vul phenotype caused by mutations that inactivate the Ras pathway is epistatic to the synMuv phenotype (Ferguson et al., 1987; Thomas, 1997; Lu and Horvitz, 1998 and Chapter 2 of this thesis).

A total of 14 genes have been identified by genetic screens (Ferguson and Horvitz, 1989; Thomas, 1997). Four genes (*lin-8*, *lin-15*A, *lin-38* and *lin-56*) act in one of the inhibitory pathways and are called the class A genes. Ten genes (*lin-9, lin-15*B, *lin-35, lin-36, lin-37, lin-51, lin-52, lin-53, lin-54* and *lin-55*) act in the other inhibitory pathway and are called the class B genes. *lin-15*A and *lin-15*B are two co-transcribed, non-overlapping genes in a complex locus. Both encode novel proteins and act cell non-autonomously (Clark et al., 1994; Huang et al., 1994; Herman and Hedgecock, 1990). Since *lin-15*A is the only cloned class A gene, little is known about the nature of the class A pathway. By contrast, recent cloning of several class B genes has shed light on the nature of the class B pathway. *lin-35* encodes a protein similar to the tumor suppressor Rb and closely related p107 and p130. *lin-53* encodes a protein similar to the mammalian Rb-binding proteins RbAp48 and RbAp46 (Lu and Horvitz, 1998). *lin-55* encodes a DP-like protein (C. Ceol and H. R. Horvitz, personal communications). Furthermore, *hda-1*, a histone deacetylase gene (Shi and Mello, 1998; Lu and Horvitz, 1998), and *C. elegans E2F-1* may act as class B synMuv genes (C. Ceol and H. R. Horvitz, personal communications). Based on these findings, we have proposed that in P3.p, P4.p and P8.p cells, LIN-35 Rb/E2F-1/LIN-55 DP may recruit LIN-53 p48 and HDA-1 to promoters of vulval cell fate genes containing E2F sites to repress transcription, resulting in expression of the non-vulval fate. Since *lin-9, lin-15*B and *lin-36* encode novel proteins, their function in *lin-35* Rb-mediated transcriptional repression is unclear (Beitel, 1994; Clark et al., 1994; Huang et al., 1994; Thomas, 1997). *lin-36* has been shown act in the P(3-8).p cells and is expressed in the P(3-8).p nuclei (Thomas, 1997), therefore it might encode a regulator or a component of the LIN-35 Rb repressor complex.

In contrast to *lin-36*, *lin-37* has been shown to be required in cells other than the P(3-8).p cells for its function, similar to *lin-15*A and *lin-15*B (Hedgecock and Herman, 1995). Thus, the class B synMuv genes may be components of an intercellular signaling pathway that act to repress transcription of vulval cell fate genes. To further understand the role of *lin-37* in *lin-35* Rb-mediated synMuv pathway, we have molecularly characterized *lin-37*. Our results show that *lin-*

37 encodes a novel hydrophilic protein of 275 amino acids. Furthermore, using a *lin-37*::GFP reporter with a nuclear localization signal, we show that the *lin-37* promoter is expressed both in P(3-8).p cells and in hypodermal cells at the time of vulval induction.

Results

Positional cloning of *lin-37*

lin-37 was previously mapped between *sma-3* and *unc-36* on linkage group III. We further mapped *lin-37* between *sma-3* and *mec-14*, both of which had been cloned and positioned on the physical map (Wilson et al., 1994). Cosmid clones from the region were injected as pools together with the *rol-6* marker DNA into *synMuv A; lin-37(n758)* animals in germline transformation experiments (Mello et al., 1991). Two overlapping cosmid clones, F31H1 and C49B6, each rescued the synMuv phenotype of *lin-37(n758)* (Figure 1). Subclones of C49B6 narrowed down the rescuing activity to a 13.8 kb fragment from the region of overlap. The sequence of this region was determined by the *C. elegans* genome project (Wilson et al., 1994). Based on Genefinder prediction, the minimal rescuing fragment contains five genes, three of which are confirmed by matching cDNA clones, namely ZK418.4, ZK418.5 and R01H2.6. Curiously, attempts to further narrow the *lin-37* rescuing activity have failed. To determine which predicted gene is required for the rescuing activity, we introduced frameshift mutations into the minimal rescuing fragment to disrupt each of the five open reading frames (ORFs) individually and tested for rescue by the resulting fragment. Disruption of none but one predicted gene, ZK418.4, eliminated the rescuing activity, indicating ZK418.4 is likely to encode *lin-37* activity (Figure 2).

Identification of molecular lesions of *lin-37* alleles

To confirm that ZK418.4 is indeed *lin-37,* genomic DNA in ZK418.4 region was amplified from wild-type and *lin-37* animals using polymerase chain reaction (PCR) and their sequences were determined. Mutations were identified in both *lin-37* alleles, *n758* and *n2234* (Ferguson and Horvitz, 1989; Thomas, 1997). *n758* contains a G to A transition at the splice donor site after the first exon, truncating most of the predicted LIN-37 protein therefore is likely to be a null allele.

n2234 contains a A to T transversion resulting in an amber mutation that deletes more than half of the protein (Figure 3A). Given that the *lin-37* minimal rescuing fragment contains substantial sequences outside the ZK418.4 region, we also analyzed genomic DNA from wild-type, *lin-37(n758)* and *lin-37(n2234)* animals by Southern blotting. Using the minimal rescuing fragment as a probe, we did not detect any gross rearrangement in either *lin-37* mutants (data not shown). Taken together, these results indicate that ZK418.4 is *lin-37*.

Isolation of *lin-37* cDNAs

We screened half a million plaques from a mixed-stage cDNA library using a 5 kb Bgl II fragment that spans the predicted *lin-37* ORF as a probe (Figure 2), and isolated 20 independent cDNA clones. Analysis of the end sequences of these clones revealed that they map to two adjacent, non-overlapping genomic regions, one corresponding to *lin-37*, the other corresponding to ZK418.5, a predicted ORF 5' to *lin-37*. The two genes are transcribed in the same direction and are separated by about 170 basepairs. The ZK418.5 cDNAs were not analyzed further. The complete sequences of the longest *lin-37* cDNA clones were determined and used to deduce intron-exon structure of the *lin-37* locus (Figure 3A). Genefinder correctly predicted the first four exons but missed the last exon. Multiple cDNAs have the last four nucleotides of the *C. elegans trans*-spliced leader SL2 (Huang and Hirsh, 1989) immediately proceeding the first ATG, indicating that *lin-37* message is probably SL2 *trans*-spliced. The tandem arrangement of ZK418.5 and *lin-37* in close proximity, together with the fact that *lin-37* is SL2 trans-spliced, indicates that these two genes form a complex locus and are co-transcribed (Spieth et al., 1993). Importantly, expression of a *lin-37* cDNA driven by the *dpy-30* gene promoter, which is constitutively and universally expressed (Hsu and Meyer, 1994), rescued the *lin-37* synMuv phenotype, further demonstrating that the activity encoded by the cDNA is both necessary and sufficient for *lin-37* function (data not shown). The sequences 3' to the *lin-37* locus on the minimal rescuing fragment may contain critical regulatory sequences required for proper expression.

lin-37 message is present in both embryonic and mixed-staged RNA

Using a *lin-37* cDNA as a probe, we detected a single transcript in both embryonic and mixed-stage RNAs on a northern blot (Figure 3B). The size of the transcript is about 1 kb, which

corresponds to the size of the longest cDNA. Using the entire minimal rescuing fragment as a probe, we detected two major bands in both embryonic and mixed-stage RNAs, one about 1kb in size, the other about 0.8 kb in size (data not shown). The 1 kb band likely corresponds to *lin-37* messages, and the 0.8 kb band likely corresponds to both ZK418.5 and R01H2.6 messages, guessing from the size of their respective cDNA clones. Thus, a large portion of the minimal rescuing fragment is probably not transcribed.

lin-37 encodes a novel protein

Conceptual translation of the *lin-37* cDNA produces a protein of 275 amino acids (Figure 4A). Blast searches revealed no significant similarity to known proteins or EST clones in the current data base. Search of potential protein domains or motifs in LIN-37 using various programs available on the Internet did not identify any obvious candidate. The LIN-37 protein is hydrophilic and does not seem to have a signal sequence or transmembrane domain, as indicated by the Kyte-Doolittle hydropathy plot (Figure 4B). It is also unlikely to form a coiled-coil secondary structure as predicted by the COILS program.

Expression of a transgene of *lin-37*::GFP with a nuclear localization signal

To begin to characterize the expression pattern of *lin-37,* we constructed a green fluorescence protein (GFP) reporter construct (Chalfie et al., 1994). We replaced about 11 kb sequences 3' to codon 93 of *lin-37* in the minimal rescuing fragment with the coding sequences of GFP carrying a nuclear localization signal (GFP^{NLS}) followed by the 3' untranslated region (UTR) of the *unc-54* gene (Figure 5). This resulted in the in-frame fusion of GFP after condon 93 of LIN-37. We characterized in transgenic animals the expression of this fusion protein, driven by the remaining genomic sequences present on the minimal rescuing fragment (Figure 6). During embryogenesis, LIN-37::GFP is expressed in the nuclei of most if not all cells. At the time of vulval induction, LIN-37::GFP is expressed in the nuclei of P(3-8).p and their descendants as well as the hypodermal cells, which persists until after vulval morphogenesis is complete. GFP fluorescence also persists in a number of unidentified cells in the head and tail regions. This expression pattern is reminiscent to that of a *lin-53*::GFP gene (Lu and Horvitz, 1998). However, it should be noted that expression pattern of the *lin-37*::GFP transgene almost certainly does not fully reflect the spatial and temporal pattern of the endogenous gene, since the transgene

lacks the sequences required for rescue by the minimal rescuing fragment. Nonetheless, *lin-37* is likely to be broadly expressed. Characterization of LIN-37 endogenous expression pattern by immunocytochemistry is underway. A GFP 'tag' construct sufficient to rescue the *lin-37* phenotype will be used for identifying regulatory elements important for directing proper expression of *lin-37*.

Discussion

We undertook molecular characterization the class B synMuv gene *lin-37* in hope of gaining insight into how this gene might act in the *lin-35* Rb-mediated pathway to inhibit vulval cell fate.

Our results indicate that *lin-37* encodes a novel protein and it is likely to be broadly expressed. We found that regulation of *lin-37* expression may be quite complex. First, *lin-37* and another gene, ZK418.5, form a complex locus and their transcription is probably co-regulated. Since no mutations in ZK418.5 have been identified, and the biochemical activities carried out by either gene product are unknown, it is not clear what the significance of this coregulation is. Second, proper expression of *lin-37* requires distant regulatory sequences downstream of the transcription unit, an enhancer by definition. This is revealed by the requirement of the distal 2.8 kb sequences (from Pvu II to Kpn I, Figure 2), almost 8 kb 3' to *lin-37*, for rescuing activity. It is tempting to speculate that transcriptional regulation of *lin-37* might be one way to control the class B synMuv activity.

As alluded to above, the biochemical function carried out by *lin-37* remains a mystery. Interestingly, a *lin-37*::GFP transgene is expressed in vulval precursor cells and their descendants as well as surrounding hypodermal cells. Could *lin-37* serve some function in the P(3-8).p cells? A cell non-autonomous site of action is proposed for *lin-37* (Hedgecock and Herman, 1995). The first cell division of the zygote give rise to two blast cells, called AB and P1. *lin-37* function does not appear to be required in either AB or P1: loss of *lin-37* function in AB only occasionally resulted in a Muv phenotype, and loss of *lin-37* function in P1 or ABp (the posterior daughter of AB) never conferred a Muv phenotype. The difference between AB mosaics and AB.p mosaics is not a result of maternal rescue, neither is it likely a result of zygotic expression since there is little zygotic expression in early embryos (Riddle et al., 1997). Therefore, hpy7, the

multinucleated hypodermal syncytium that surrounds the P(3-8).p cells, is postulated to be the anatomical focus of *lin-37* activity, since hpy7 is derived from both AB and P1. It is proposed that, since AB-derived hpy7 nuclei outnumber those derived from P1, only in AB mosaics does *lin-37* activity become limiting in hyp7, resulting in a Muv phenotype at a low frequency. Wherever it may act, *lin-37* is not solely required in P(3-8).p, since the P(3-8).p cells are exclusively derived from ABp and *lin-37* ABp mosaics were non-Muv. *lin-15* was also postulated to act in hyp7 (Herman and Hedgecock, 1990). Because loss of *lin-15* activity in either AB or P1 can cause a Muv phenotype, *lin-15* activity may be more dosage-sensitive than *lin-37*. By contrast, *lin-36* has been shown to be required only in ABp but not P1, indicating that *lin-36* functions within the P(3-8).p cells. *lin-37* and *lin-15* might act in the hypodermis to regulate an inhibitory signal that controls the activity of the *lin-35* Rb repressor complex in the P(3-8).p nuclei to antagonize the Ras signaling activity (Figure 7).

To elucidate in what cells *lin-37* acts to inhibit vulval induction, it may be informative to misexpress *lin-37* driven by tissue-specific promoters. We have tested the *lin-31* gene promoter, which is exclusively expressed in the P(3-8).p cells (Tan et al., 1998), and the *col-10* gene promoter, which is expressed both in hypodermal cells and the P(3-8).p cells (P. Olsen and V. Ambros, personal communications). To test the potency of the *lin-31* promoter, we used it to drive expression of *lin-36*, which has been shown to act in the P(3-8).p cells, in *lin-36; lin-15A* Muv animals. Curiously, the Muv phenotype of transgenic animals is not rescued. Assuming the transgene was expressed, this result suggests that the *lin-31* promoter is not sufficient to drive proper expression of *lin-36* in the P(3-8).p cells. By contrast, expression of *lin-36*, *lin-35* or *lin-53* driven by the *col-10* promoter is sufficient to rescue their respective mutant phenotypes (data not shown). However whether these genes are required in the hypodermis or in the P(3-8).p cells can not be distinguished using the *col-10* promoter. It may be possible to dissect a vulva-specific minimal promoter from the *lin-36* promoter, which has been shown to drive reporter gene expression in a number of cells including the P(3-8).p cells.

Where might *lin-37* act in the class B pathway? Ordering the action of the class B genes is difficult, since different loss of function mutants have essentially identical phenotypes, and no gain-of-function mutations have been identified to date. In addition, synMuv mutants tested so far exhibit similar interactions with Ras signaling mutants. These include *lin-15*, which likely

acts more upstream in the synMuv pathway, and *lin-36*, *lin-35* and *lin-53*, which likely regulate more downstream events. Studies have been initiated to characterize suppressor mutations that differentially suppress different synMuv mutants (S. G. Clark and H. R. Horvitz, unpublished results; C. Ceol and H. R. Horvitz, personal communications). Although subject to a number of caveats, these analyses may be instrumental in ordering the pathway. Furthermore, as the molecular identities of a number of synMuv genes are now known, gain-of-function mutations can be created drawing on analogy to mammalian pathways. For example, constitutive gain-of-function effects have been achieved by eliminating or mutating various negative regulatory sequence in mammalian Rb (Chow and Dean, 1996; Knudsen and Wang, 1997; Xu et al., 1994). If a *lin-35* Rb gain-of-function mutation can be similarly engineered, it can be very useful to distinguish where other class B synMuv genes act with respect to *lin-35* Rb. Lastly, in collaboration with other researchers, we have begun to study potential protein-protein interactions with the cloned synMuv genes, including *lin-37,* using a yeast two-hybrid approach (M. Vidal, personal communications).

Experimental Procedures

Strains and Genetics

C. elegans strains were maintained at 20°C as described by Brenner (1974). Mutations were as follows: LGII, *lin-8(n111)*; LGIII, *lon-1(e185), sma-3(e491), mec-14(u55), unc-36(e251), lin-37(n758), lin-37(n2234)*; LGV, *unc-76(e911);* LGX, *lin-15(n767)* (a class A mutation). To map *lin-37* with respect to *sma-3* and *mec-14*, we isolated Sma non-Mec non-Unc recombinants from the progeny of *sma-3 mec-14 unc-36/lon-1 lin-37(n758); lin-15(n767)* animals and scored the progeny of these recombinants for *lin-37*. Of 21 recombinants, 19 were Lin and 2 were non-Lin.

Transgenic Animals

Germline transformation was performed as described by Mello et al. (1991). DNA (20-100 ng/μl) was coninjected with a dominant *rol-6* plasmid pRF4 or an *unc-76* rescuing plasmid (100 ng/μl) (Bloom and Horvitz, 1997), and lines of Rol or non-Unc-76 transgenic animals were established, respectively.

Sequence Analysis of cDNAs and Mutant Alleles

Inserts of cDNA clones isolated from the Okkema mixed-staged cDNA library (Okkema and Fire, 1994) were PCR amplified using either a pair of vector primers or a vector primer and a gene-specific primer. DNA sequences of the PCR fragments were determined using an automated ABI 373A DNA sequencer (Applied Biosystems). In the case of genomic fragments, the sequences of both strands of the coding regions and splice junctions were determined.

Plasmid construction

Cosmid fragments were subcloned into the BlueScript SK(+) (Strategene). cDNA inserts were PCR amplified with primer containing appropriate restriction sites and cloned into the BlueScript SK(+). Regions subject to PCR were confirmed to be mutation-free by DNA sequence determination. The *lin-37*::GFP construct was made as follows: the minimal rescuing fragment was cut with Sma I and Eag I to remove all sequences 3' to codon 93 of *lin-37*. The Sma I-Eag I fragment from the vector pPD95.70 (A. Fire, personal communications), which contains the coding sequences of GFP with the SV40 large T nuclear localization signal, followed by the *unc-54* 3' UTR, was then cloned into the Sma I-Eag I digested minimal rescuing fragment.

Reference

Beitel, G. J. (1994). Genetic and Molecular Analyses of *let-60 ras*, *lin-1* and *lin-9*: Genes that Function in *C. elegans* Vulval Induction. Ph. D. Thesis. Massachusetts Institute of Technology, Cambridge.

Chalfie, M., Tu, Y., Euskirchen, G., Ward, W. W., and Prasher, D. C. (1994). Green fluorescent protein as a marker for gene expression. Science *263*, 802-805.

Chow, K. N., and Dean, D. C. (1996). Domains A and B in the Rb pocket interact to form a transcriptional repressor motif. Mol Cell Biol *16*, 4862-4868.

Clark, S. G., Lu, X., and Horvitz, H. R. (1994). The *Caenorhabditis elegans* locus *lin-15*, a negative regulator of a tyrosine kinase signaling pathway, encodes two different proteins. Genetics *137*, 987-997.

Ferguson, E. L., and Horvitz, H. R. (1989). The multivulva phenotype of certain *Caenorhabditis elegans* mutants results from defects in two functionally redundant pathways. Genetics *123*, 109-121.

Ferguson, E. L., Sternberg, P. W., and Horvitz, H. R. (1987). A genetic pathway for the specification of the vulval cell lineages of *Caenorhabditis elegans*. Nature *326*, 259-267.

Hedgecock, E. M., and Herman, R. K. (1995). The *ncl-1* gene and genetic mosaics of *Caenorhabditis elegans*. Genetics *141*, 989-1006.

Herman, R. K., and Hedgecock, E. M. (1990). Limitation of the size of the vulval primordium of *Caenorhabditis elegans* by *lin-15* expression in surrounding hypodermis. Nature *348*, 169-171.

Hsu, D. R., and Meyer, B. J. (1994). The *dpy-30* gene encodes an essential component of the *Caenorhabditis elegans* dosage compensation machinery. Genetics *137*, 999-1018.

Huang, L. S., Tzou, P., and Sternberg, P. W. (1994). The *lin-15* locus encodes two negative regulators of *Caenorhabditis elegans* vulval development. Mol Biol Cell *5*, 395-411.

Huang, X. Y., and Hirsh, D. (1989). A second trans-spliced RNA leader sequence in the nematode *Caenorhabditis elegans*. Proc Natl Acad Sci U S A *86*, 8640-8644.

Kimble, J. (1981). Alterations in cell lineage following laser ablation of cells in the somatic gonad of *Caenorhabditis elegans*. Dev Biol *87*, 286-300.

Knudsen, E. S., and Wang, J. Y. (1997). Dual mechanisms for the inhibition of E2F binding to RB by cyclin- dependent kinase-mediated RB phosphorylation. Mol Cell Biol *17*, 5771-5783.

Lu, X., and Horvitz, H. R. (1998). *lin-35* and *lin-53*, two genes that antagonize a *C. elegans* Ras pathway, encode proteins similar to Rb and its binding protein RbAp48. Cell *95*, 981-991.

Mello, C. C., Kramer, J. M., Stinchcomb, D., and Ambros, V. (1991). Efficient gene transfer in *C. elegans*: extrachromosomal maintenance and integration of transforming sequences. EMBO J *10*, 3959-3970.

Okkema, P. G., and Fire, A. (1994). The *Caenorhabditis elegans* NK-2 class homeoprotein CEH-22 is involved in combinatorial activation of gene expression in pharyngeal muscle. Development *120*, 2175-2186.

Riddle, D. L., Blumenthal, T., Meyer, B. J., and Priess, J. R. (1997). *C. elegans* II (Cold Spring Harbor, New York: Cold Spring Harbor Press).

Shi, Y., and Mello, C. (1998). A CBP/p300 homolog specifies multiple differentiation pathways in *Caenorhabditis elegans*. Genes Dev *12*, 943-955.

Spieth, J., Brooke, G., Kuersten, S., Lea, K., and Blumenthal, T. (1993). Operons in *C. elegans*: polycistronic mRNA precursors are processed by trans-splicing of SL2 to downstream coding regions. Cell *73*, 521-532.

Sternberg, P. W., and Han, M. (1998). Genetics of RAS signaling in *C. elegans*. Trends Genet *14*, 466-472.

Sternberg, P. W., and Horvitz, H. R. (1991). Signal transduction during *C. elegans* vulval induction. Trends Genet *7*, 366-371.

Sundaram, M., and Han, M. (1996). Control and integration of cell signaling pathways during *C. elegans* vulval development. Bioessays *18*, 473-480.

Tan, P. B., Lackner, M. R., and Kim, S. K. (1998). MAP kinase signaling specificity mediated by the LIN-1 Ets/LIN-31 WH transcription factor complex during *C. elegans* vulval induction. Cell *93*, 569-580.

Thomas, J. H. (1997). Genetic and Molecular Analysis of Synthetic Multivulva Genes in *Caenorhabditis elegans*. Ph.D. Thesis. Massachusetts Institute of Technology, Cambridge, MA.

Wilson, R., Ainscough, R., Anderson, K., Baynes, C., Berks, M., Bonfield, J., Burton, J., Connell, M., Copsey, T., Cooper, J., and et al. (1994). 2.2 Mb of contiguous nucleotide sequence from chromosome III of *C. elegans*. Nature *368*, 32-38.

Xu, H. J., Xu, K., Zhou, Y., Li, J., Benedict, W. F., and Hu, S. X. (1994). Enhanced tumor cell growth suppression by an N-terminal truncated retinoblastoma protein. Proc Natl Acad Sci U S A *91*, 9837-9841.

Figure 1. Genetic and physical maps of the *lin-37* region. Cosmid and YAC clones in the physical map are indicated by horizontal lines. Dashes lines indicate corresponding positions of *sma-3* and *mec-14* on both maps. The two cosmid clones that each rescued the *lin-37* phenotype are shown in bold.

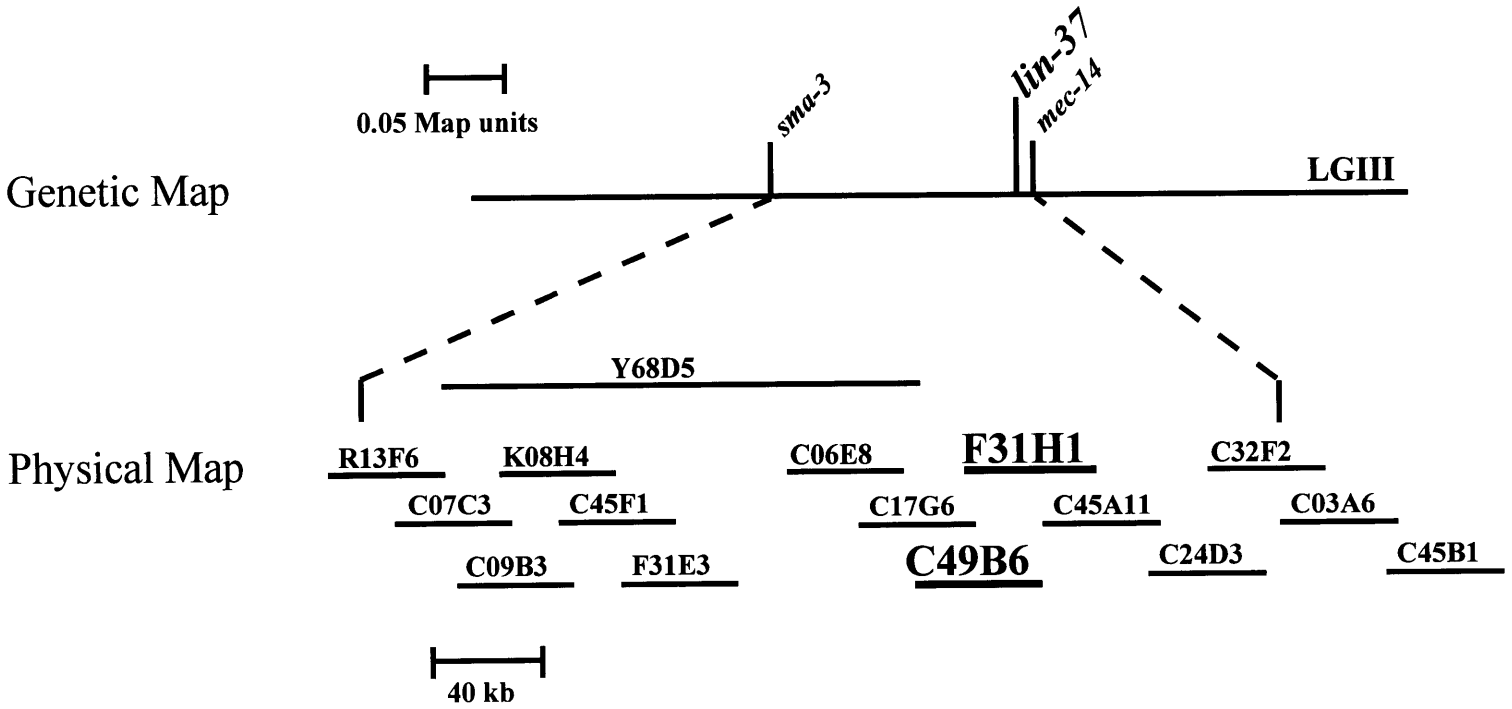
Genetic Map
0.05 Map units
sma-3
lin-37
mec-14
LGIII
Physical Map
Y68D5
R13F6
K08H4
C06E8
F31H1
C32F2
C07C3
C45F1
C17G6
C45A11
C03A6
C09B3
F31E3
C49B6
C24D3
C45B1
40 kb

Figure 2. The 13.8 kb *lin-37* minimal rescuing fragment contains five predicted genes, as indicated on the bottom. Arrows indicate direction of transcription. Disruption of ZK418.4 (by AcccIII fill-in) but not the other ORFs abolished the rescuing activity, indicating that ZK418.4 encodes *lin-37* activity. Rescuing constructs are indicated by thick lines, non-rescuing constructs are shown in thin lines. +, rescue; -, no rescue. Numbers on the right indicate number of rescuing lines among established transgenic lines.

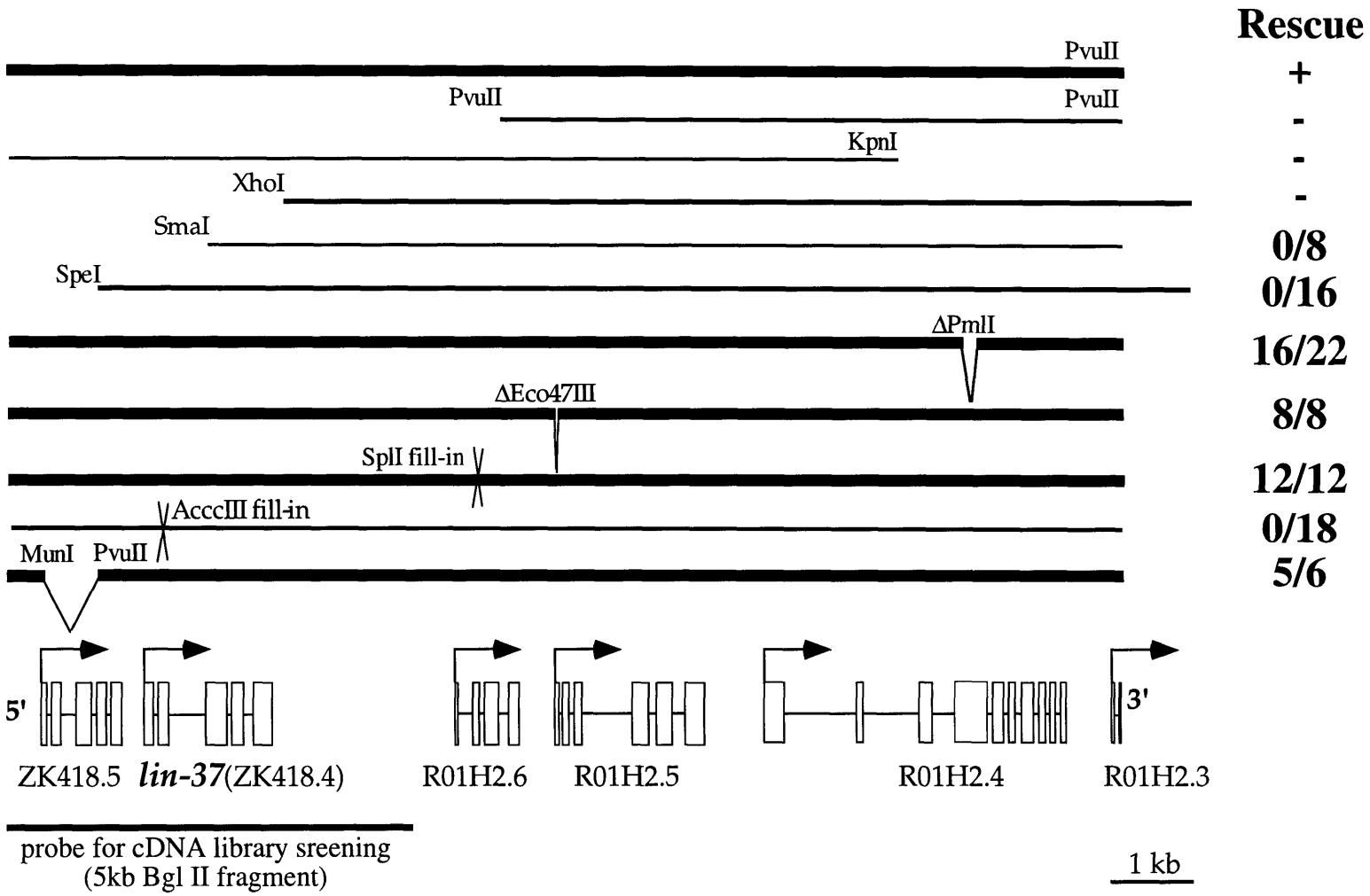
Rescue
PvuII
+
PvuII
PvuII
-
KpnI
-
XhoI
-
SmaI
0/8
SpeI
0/16
ΔPmlI
16/22
ΔEco47III
8/8
SplI fill-in
12/12
AcccIII fill-in
0/18
MunI
PvuII
5/6
5'
3'
ZK418.5
lin-37(ZK418.4)
R01H2.6
R01H2.5
R01H2.4
R01H2.3
probe for cDNA library sreening
(5kb Bgl II fragment)
1 kb

Figure 3. A, molecular lesions in *lin-37* alleles. The positions of the mutations are indicated by arrows above the schematic of a *lin-37* cDNA. The nucleotide changes and predicted effects are indicated below the cDNA. B, *lin-37* message is present in both embryonic and mixed-stage RNAs. A *lin-37* cDNA was used as a probe. The approximate size of the transcripts is indicated on the left. E, embryonic; M, mixed-stage.

A

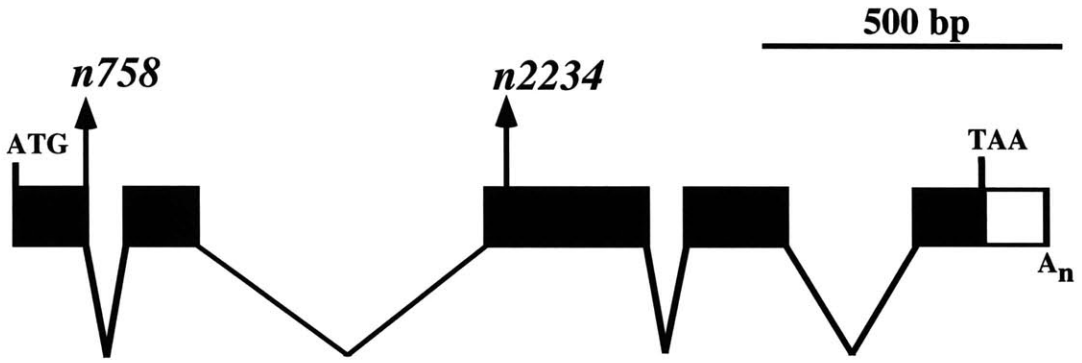

n758, ACgt to ACat, splice donor

n2234, AAG to TAG, K105amber

B

Figure 4. A, *lin-37* cDNA sequence and conceptual translation of the cDNA. B, the Kyte-Doolittle hydrophathy plot indicates that LIN-37 is a hydrophilic protein. Positive values indicate positive hydrophobicity.

A

```
ATGTCAGAAATAGATCCACTTGCCGAGTTCTTGCTTCCAGAAGACGGAGATCGAAATGCT   60
M  S  E  I  D  P  L  A  E  F  L  L  P  E  D  G  D  R  N  A     20

CGTCAAAATGATCCATTGATAAGCGGAGGTCCACTTCCATTGGAATCGCCAAGCAGAAAA  120
R  Q  N  D  P  L  I  S  G  G  P  L  P  L  E  S  P  S  R  K     40

CTCACATCCCTGTTATCCTATGATCCGACAGTTCCGGAGTCACCGGATATGAAATTCGCC  180
L  T  S  L  L  S  Y  D  P  T  V  P  E  S  P  D  M  K  F  A     60

AGAAAACGTCTGGGAAATCTGCTGACAACCATAAAACATCACCCATCGGAAATAATTGGA  240
R  K  R  L  G  N  L  L  T  T  I  K  H  H  P  S  E  I  I  G     80

GTACTCCCAGAAGATTATACTCGTGCTGATGAAGAGCCCGGGCGCCAAGGACGTCCACCA  300
V  L  P  E  D  Y  T  R  A  D  E  E  P  G  R  Q  G  R  P  P    100

GGTCGCCCTCGTAAGATGCCGCGTCACGAATCTTCAACTTCACTTATGGAATCACCACGC  360
G  R  P  R  K  M  P  R  H  E  S  S  T  S  L  M  E  S  P  R    120

AAGACTATGACTCGTGATTCTAAAATTATGTTTGAATTGCGTGGAAAACCATTCGAAATG  420
K  T  M  T  R  D  S  K  I  M  F  E  L  R  G  K  P  F  E  M    140

ATAGCTGGACGTTTTGAAGAAGAATATTCACTTGGTAGAGCATGGGTTAAAGGACACATG  480
I  A  G  R  F  E  E  E  Y  S  L  G  R  A  W  V  K  G  H  M    160

AATAATGAATATGAACCAATAAAAGCTCAAAGGACAGACTATGCACCGAATCTGGCTGTT  540
N  N  E  Y  E  P  I  K  A  Q  R  T  D  Y  A  P  N  L  A  V    180

GATTATCTTGCATGTCGCGAGATTCATCGAATGCCACGTCCAGATAAATCAATTCCTGAG  600
D  Y  L  A  C  R  E  I  H  R  M  P  R  P  D  K  S  I  P  E    200

CTGCCAATTGTTCCATCTAGAATCGATGAATTCGACGCTACAGTCGATCCAAGATATGAA  660
L  P  I  V  P  S  R  I  D  E  F  D  A  T  V  D  P  R  Y  E    220

ACAGATTTGAAAAATGAATACATTCGTCATTGGAAACAAGTCAAAAAAGGTTGGTGTGCT  720
T  D  L  K  N  E  Y  I  R  H  W  K  Q  V  K  K  G  W  C  A    240

CATCAACGTCGTCGGACTGCTCCCCATGCAAGAAGCATAGCATTAATCAACAAAATCTAC  780
H  Q  R  R  R  T  A  P  H  A  R  S  I  A  L  I  N  K  I  Y    260

CAGCCTGGAGAGTCGAAAACTGTCGAGCAAGCACTTGGTCTTATTTAAATATTCTAACAT  840
Q  P  G  E  S  K  T  V  E  Q  A  L  G  L  I  *               275

GTAATTTCAATTTATCTCTTACTTTCTGATCTTGCTATCACATGTCTCTTATTTCAAAAA  900

TCTCACTTTAAAATTCATATAAATAATGGGTTTATTCAAATACATCATCTTGAC
```

B

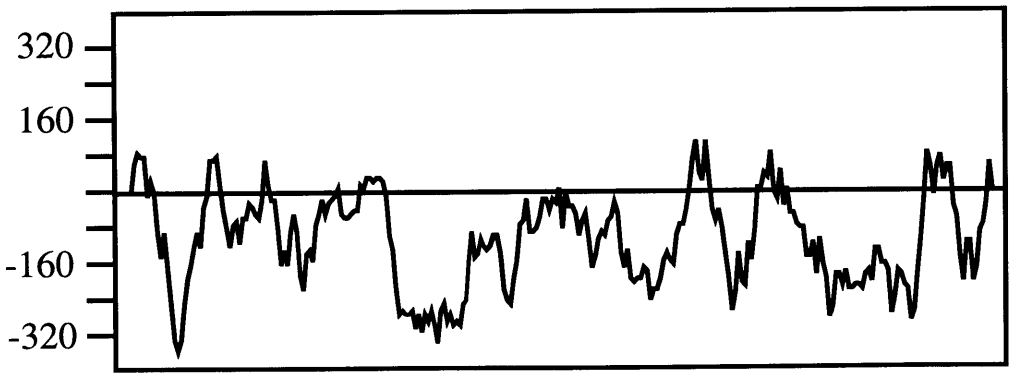

K-D plot

Figure 5. The structure of the *lin-37*::GFP fusion construct. The *lin-37* minimal rescuing fragment is shown on the bottom for comparison. ZK418.5 coding exons are shaded in grey, *lin-37* coding exons are indicated in black. GFP coding sequences are indicated by the hatched box, the *unc-54* 3' UTR is indicated by the open box. NLS, the nuclear localization signal of the SV40 large T antigen.

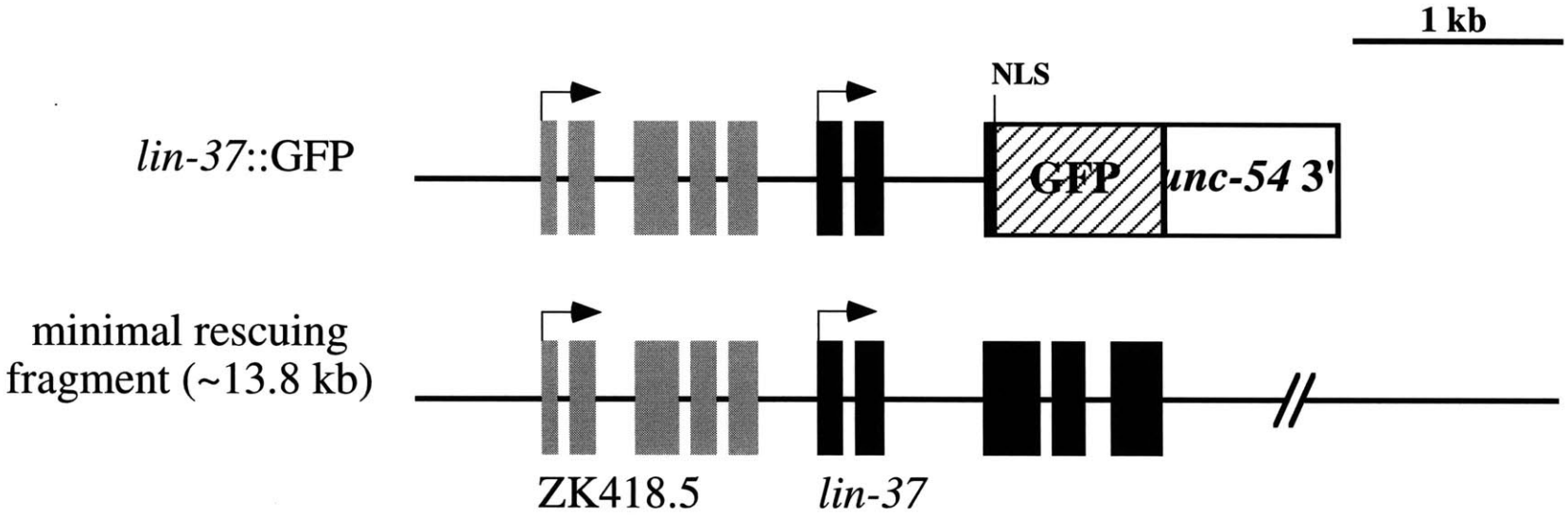
1 kb
NLS
lin-37::GFP
GFP
unc-54 3'
minimal rescuing
fragment (~13.8 kb)
ZK418.5
lin-37

Figure 6. Expression pattern of a *lin-37*::GFP transgene. A, GFP is broadly expressed during embryogenesis. B-D, GFP is expressed in the P(3-8).p cells and their descendants during vulval development. B, GFP expression in the P(3-8).p cells (arrowheads). C, GFP expression in the P(3-8).p daughter cells. P5.p, P6.p, P7.p and P8.p daughters, indicated by the brackets, are visible in this micrograph. D, GFP expression in P(3-8).p granddaughter cells (bracket) as cell divisions are just complete and invagination begins. E, F, GFP is expressed in the hypodermal cells throughout development. E, a lower magnification micrograph showing hypodermal GFP expression in the entire animal (focus on the older larva). F, hypodermal GFP expression in the region of the developing vulva. The bright area is the developing vulva outside the focal plane.

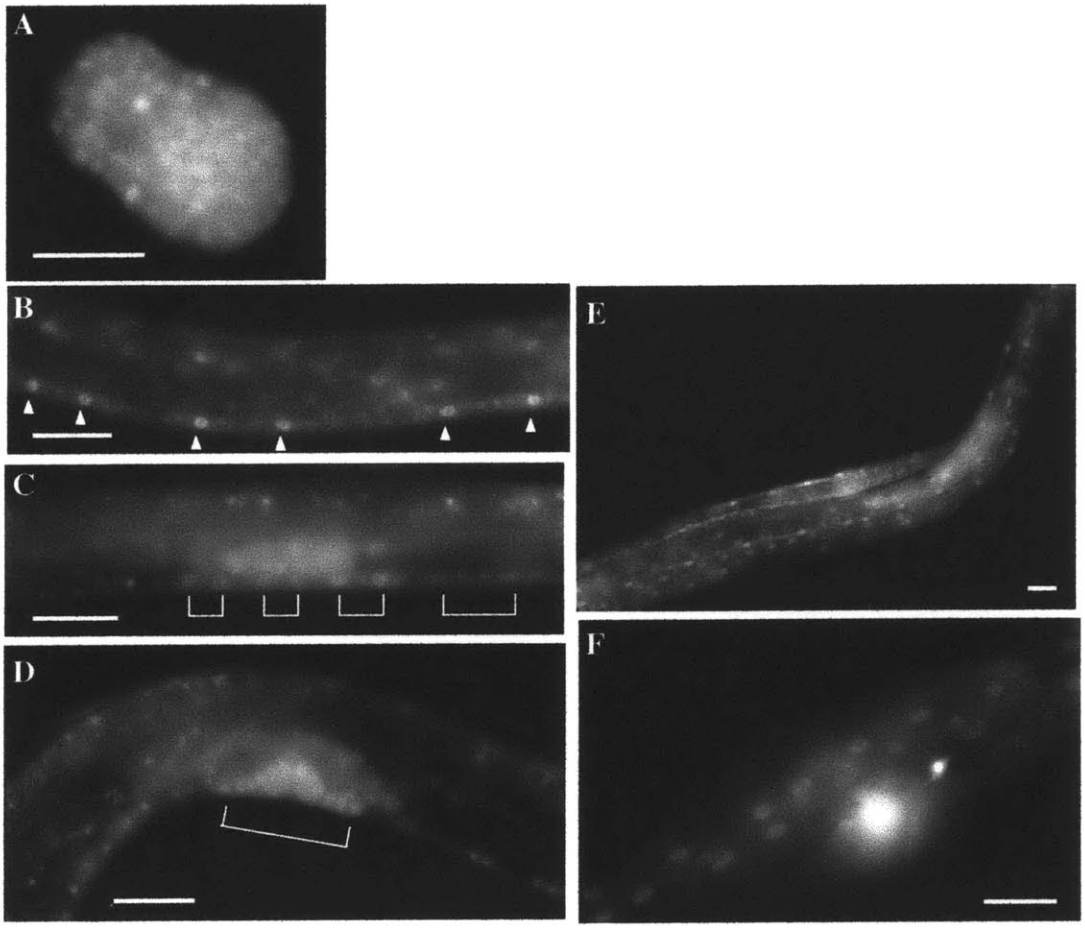
A
B
C
D
E
F

Figure 7. A model for the *lin-35* Rb-mediated inhibitory pathway in vulval development. *lin-37* might act in the hypodermis to regulate an inhibitory signal that controls the activity of the *lin-35* Rb repressor complex in the P(3-8).p nuclei to antagonize the Ras signaling activity.

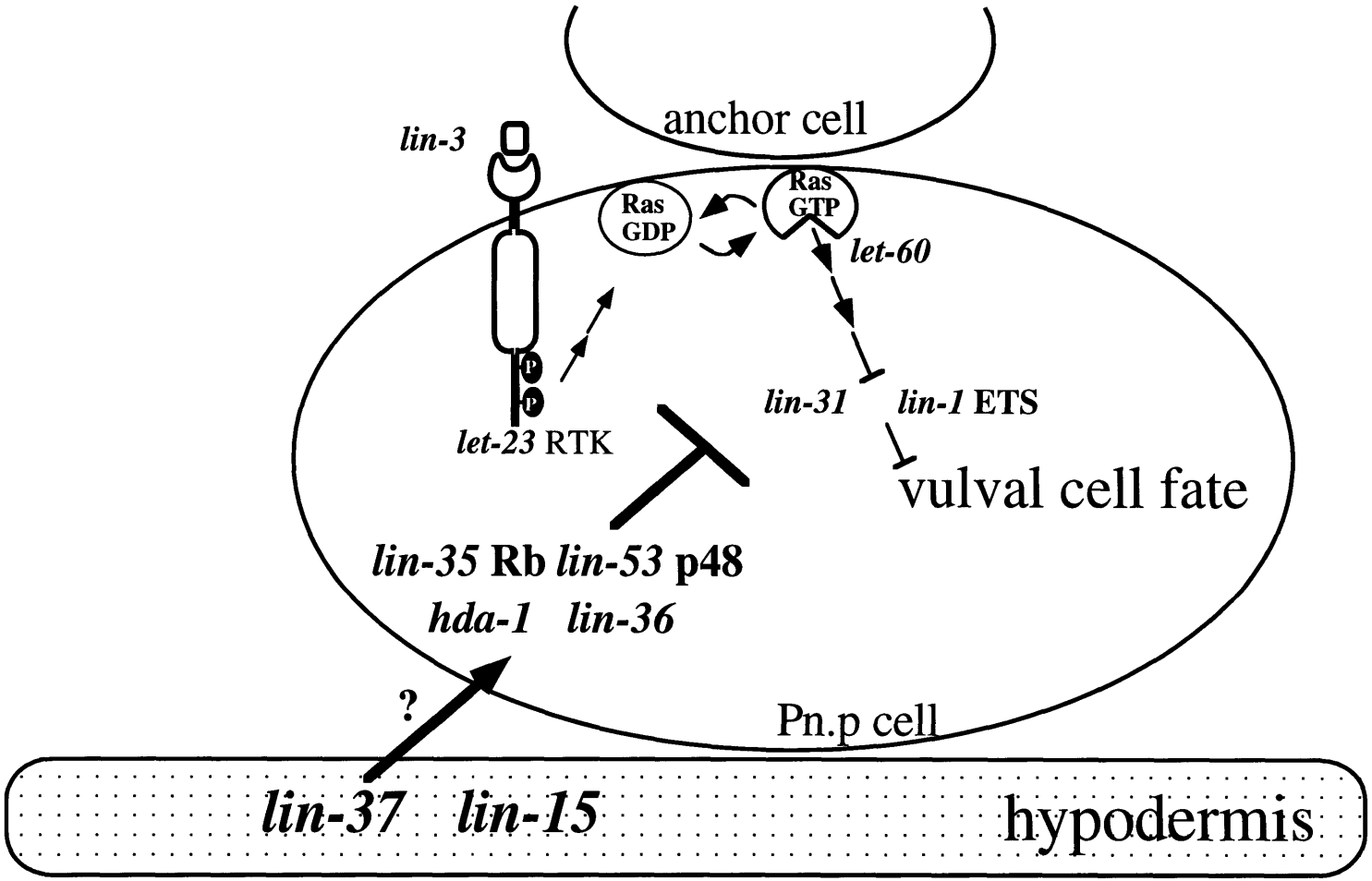
anchor cell
lin-3
Ras GDP
Ras GTP
let-60
P
P
let-23 RTK
lin-31
lin-1 ETS
vulval cell fate
lin-35 Rb lin-53 p48
hda-1 lin-36
?
Pn.p cell
lin-37 lin-15
hypodermis

Chapter 4

Ongoing experiments and future directions

Xiaowei Lu

Howard Hughes Medical Institute, Massachusetts Institute of Technology
Cambridge, MA 02139

Ongoing Experiments

Analysis of LIN-37 expression by immunocytochemistry

To analyze expression pattern of the endogenous LIN-37 protein, we have generated and affinity-purified polyclonal antibodies against LIN-37. We plan to first confirm the specificity of the affinity-purified antibodies on Western blots of total proteins of wild type and *lin-37* mutant strains. Next we will examine whole-mount staining of wild type and other synMuv mutants to identify pattern and subcellular localization in wild type and changes in mutants. These antibodies could also potentially be used in immunoprecipitation analysis of *C. elegans* protein extract to evaluate proteins that interact with LIN-37.

Cloning of the C. *briggsae lin-35* homolog

We identified a putative E2F binding site in the *C. elegans lin-35* promoter (TTGCGCGC) (Figure 1). Expression of a LIN-35::GFP reporter driven by the 400 bp *lin-35* promoter was diminished in a *lin-55*DP mutant strain (data not shown). Furthermore, mutating the E2F site (from TTGCGCGC to TTGCTAGC) also diminished expression of the GFP reporter (data not shown). Taken together, these results suggest that transcription of *lin-35* is normally positively regulated by E2F.

To understand how *lin-35* activity is regulated, which may shed light on how the LIN-35 Rb repressor complex might be regulated by other synMuv genes as well as other vulval signaling systems, we have cloned the *lin-35* homolog from a closely related nematode species *C. briggsae*. It has been shown that regulatory and coding sequences are highly conserved between *C. briggsae* and *C. elegans,* which diverged from each other some 50 million years ago. The identity of the *C. briggsae lin-35* gene is confirmed by the genomic syntony between the two species, i.e., the chromosomal organization of *lin-35* with respect to neighboring loci have also been conserved (data not shown).

Comparison of coding sequences reveal that the two LIN-35 proteins are 67% identical to each other (Figure 2), relatively low in comparison with the high degree of conservation seen in a

number of proteins analyzed to date (S. Shaham, M. M. Metzstein, G. Stanfield and H. R. Horvitz, personal communications), suggesting that the structural constraint on primary sequences of LIN-35 is not tight. Although we do not know whether LIN-35 Rb is regulated by phosphorylation, LIN-35 Rb has seven potential CDK phosphorylation sites (S/T-P motifs), 3 located N-terminal to the A pocket, 2 in the A pocket, 2 in the spacer region (Figure 2). The third site in the N-terminal region are present in both species but at a slightly different position with respect to neighboring residues. All remaining six are conserved between the two species. Only one of these sites (S685 in *C. elegans* LIN-35) is conserved in human Rb (S567), which has not been shown to be phophorylated in *vivo* (Knudsen and Wang, 1997). However, it should be noted that phosphorylation sites in Rb do not appear to be well conserved among Rb-related proteins, even in p107 and p130.

The only conserved portion in the promoter region is a stretch of sequence of approximately 40 basepairs, including the E2F site (Figure 3A). Interestingly, the orientation of the E2F site is flipped in *C. briggsae*. A search of potential transcription factor binding sites against the eukaryotic promoter database (EPD) identified putative binding sites for heat shock factor (Sorger, 1991) and CdxA, a caudal-family homeodomain protein (Margalit et al., 1993). Curiously, we observed that rescue of the *lin-35* mutant phenotype by the minimal rescuing fragment was greatly reduced when transgenic animals were raised at 25°C instead of 20°C, suggesting that expression of *lin-35* might be negatively regulated as temperature increases (data not shown). Intron-exon structure of the two *lin-35* loci is conserved, and none of the intron sequences are conserved except for intron 2. Intron 2 is greater than 3 kb in size in both species, considerably larger than normal size of *C. elegans* introns (Riddle et al., 1997). Determination of the sequence of the *C. briggsae* intron 2 is in progress. Preliminary results indicate that there exists at least one conserved element (Figure 3B). This 20-bp element contains a potential GATA factor binding site. Homeodomain proteins involved in vulval development include the *sex comb reduced*-related *lin-39* (Maloof and Kenyon, 1998), the *antennapedia*-related *mab-5* (Clandinin et al., 1997) and the *extradenticle*-related *ceh-20* (E. Chen and M. J. Stern, personal communications). At present, it remains to be tested if and how any *C. elegans* homeodomain proteins regulate *lin-35* transcription.

Isolation of deletion mutants of *lin-53* and *hda-1*

We have shown that the null phenotypes of *lin-53* p48 and the histone deacetylase gene *hda-1* are embryonic lethality by RNAi, which has also been reported by others (Shi and Mello, 1998); and that they act later in development in the class B synMuv pathway by tissue-specific antisense expression (Lu and Horvitz, 1998 and Chapter 2 of this thesis). Isolation of null alleles in these genes would greatly facilitate characterization of their functions in postembryonic development, including their roles in vulval development. Therefore, we sought to isolate null mutations in these two genes by PCR screening for mutants carrying germline deletions in these genes from a library of mutagenized animals.

After screening 1.7×10^6 haploid genomes, we have identified two candidate deletion mutants for each gene. One of the *lin-53* deletions removes 0.75 kb sequences in the coding region of *lin-53*, truncating the protein after the first WD domain, and is not expected to affect the second gene (Figure 4A). Interestingly, the second, 1.7 kb deletion spans part of *lin-53* and part of the downstream K07A1.11, resulting in in-frame fusion of the fifth WD domain of *lin-53* to corresponding position of K07A11.1, generating a chimera 7 WD-repeat protein (Figure 4A). Preliminary characterization of one of the candidate *hda-1* deletions revealed that the coding sequences of *hda-1* were completely removed by the 2.4 kb deletion and should represent a null allele (Figure 4B). Recovery of mutant animals and phenotypic analyses will soon be underway.

Future directions

Identification of new synMuv genes and characterization of the synMuv A pathway

Based on the findings that some synMuv genes function outside the P(3-8).p cells, we propose that a LIN-35 Rb/LIN-53 p48/HDA-1 nuclear complex responds to the intercellular signaling pathway encoded by other class B synMuv genes to regulate transcription during vulval development in *C. elegans*. The primal components of the proposed signal transduction pathway, such as the ligand, receptor and signal transducers, remain to be identified. In addition, there might be additional corepressor proteins recruited by LIN-35 Rb. The dominant-negative LIN-53(L292F) protein is still capable of interacting with LIN-35 Rb and HDA-1 in GST pull-down assays, suggesting that it might be defective in binding other protein component of the

repressor complex (Lu and Horvitz, 1998 and Chapter 2 of this thesis). Furthermore, little is known about the nature of the class A synMuv pathway, making it difficult to interpret the interaction between the synMuv genes and the Ras pathway. Some of the class A genes identified are represented by only one allele, indicating that the screen has not reached saturation yet and that additional synMuv A genes may exist. Cloning of the remaining synMuv genes and identification of new synMuv genes should help piece the puzzles together.

Previous synMuv genetic screens were designed to isolate homozygous viable and fertile mutations therefore relied entirely on the isolation of partial loss-of-function mutations to identify synMuv genes that are also required for viability or fertility. This is exemplified by the failure of these screens to isolate loss-of-function mutations in *lin-53* and *hda-1*, which result in embryonic lethality, and in *lin-9*, which results in sterility. In the future, genetic screens done in a clonal fashion should allow sib recovery of sterile synMuv mutants. A screen for synthetic lethal or sterile mutants in a *synMuv A or B* mutant background might identify new genes that functions redundantly with the synMuv genes in development including vulval development. Isolation of temperature-sensitive synMuv mutants by shifting temperature after embryogenesis should bypass lethality early in development thereby allowing identification of synMuv genes required for viability. Partial maternal-effect has been observed with a number of previously isolated synMuv mutants (Thomas, 1997), suggesting that there might exist strict maternal-effect synMuv genes. An F3 synMuv screen may identify such genes missed by previous F2 screens. Lastly, new synMuv genes may be identified by screening for enhancers of weak synMuv mutants.

The genetic screens can also be complemented by reverse genetic approach. With the completion of the genomic sequence and the increasing number of tools for the analysis of gene function, candidate synMuv genes identified by homology or protein-protein interaction can be genetically characterized. Experiments to identify protein-protein interactions with cloned synMuv genes are already underway in collaboration with other researchers (M. Vidal, personal communications). This approach will also be instrumental in elucidating functions of novel synMuv genes cloned to date, such as LIN-15A, LIN-15B, LIN-36 and LIN-37.

Identification of *lin-35* Rb target genes

Our molecular and genetics analyses of the class B synMuv genes suggest that they act to repress transcription of E2F-dependent vulval cell fates genes. Identification of target genes regulated by the synMuv genes not only validates the model but also is central to understanding the nature of antagonism between the synMuv genes and the Ras signaling pathway. Preliminary results indicate that *lin-35* transcription is activated by E2F, although it is not known whether it is auto-regulated by the LIN-35 Rb repressor complex. Systematic analysis of gene expression patterns by the *C. elegans* genome project will likely identify genes that are dynamically expressed in the P(3-8).p cells during vulval development. Furthermore, newly developed technology such as mRNA differential display using DNA microarrays (e.g., Affymetrix, Genome Systems) can be applied to identify genes that become derepressed in synMuv mutants. These approaches combined with identification of potential E2F sites with an initial focus on the proximal promoter regions should identify candidate *lin-35* target genes that can then be subject to genetic analysis. In addition, previously identified suppressor mutations of synMuv mutants that by themselves do not cause any vulval phenotype, might define candidate vulval cell fate genes regulated by the synMuv activity thus are worth further pursuit (S. G. Clark and H. R. Horvitz, unpublished results).

Determining the interface of the Rb pathway and the Ras pathway

Interactions between SynMuv genes and *lin-3*

Previous results suggest that the synMuv phenotype is independent of the anchor cell inductive signal encoded by the gene *lin-3,* as reducing *lin-3* activity by weak mutations or laser killing of the anchor cell in synMuv mutants did not block the expression of the Muv phenotype (Ferguson et al., 1987; Thomas, 1997). However, upon closer examination, we recently found that synMuv phenotype can be partially suppressed by weak mutations in *lin-3* (*lin-3* null mutations could not be tested because they result in L1 lethality) (X. Lu and H. R. Horvitz, unpublished results). It has been suggested that *lin-1* defines one branch downstream of the inductive signal as the Muv phenotype caused by *lin-1* loss of function is less severe in the absence of the signal (Beitel et al., 1995). Could the other branches downstream of inductive signal be mediated by the synMuv activities? This hypothesis predicts that the absence of *lin-3* would have no effect on the Muv

phenotype when synMuv A, B and *lin-1* are all inactivated (Figure 5). Experiments are underway to test this prediction.

Interactions between SynMuv genes and Ras pathway

The Vul phenotypes of the Ras pathway mutants have been shown to be epistatic to the synMuv phenotype. It has been interpreted to mean that the synMuv genes genetically act upstream of or in parallel to the Ras pathway, assuming Ras acts in a more or less linear pathway. However, accumulating evidence indicates that the Ras pathway mediating vulval induction is likely to have multiple branches (Beitel et al., 1995; Kornfeld et al., 1995; Sundaram and Han, 1995; Sieburth et al., 1998), making it difficult to interpret the epistasis interactions. For example, an extreme scenario that completely contradicts previous interpretation would now makes sense in the context of a nonlinear Ras pathway: both class A and B synMuv genes can act downstream of Ras, in parallel to the main branch mediated by *lin-1*. In this scenario, most of Ras signaling is going through the *lin-1* branch such that inactivation of synMuv genes would not affect the Vul phenotype of Ras signaling mutants as a result of unregulated *lin-1* activity (Figure 6, right panel). This hypothesis can be tested by examining whether there is an effect of loss of function *let-60*Ras mutation on the expressivity of the *lin-1* Muv phenotype, and if so, whether this effect can be accounted for by either class A or B synMuv activity. In addition, since both Rb and Ras pathway appears to regulate expression of vulval fate genes, identification of target genes regulated by either pathway is a critical step toward understanding their genetic interactions. Systematic analysis of expression of genes in one pathway in mutants of the other pathway has not yet been done. In any case, although epistasis analysis has not been very informative in revealing how the Rb pathway interfaces with the Ras pathway, it is not inconsistent with recent findings in mammalian cells, which suggest that Rb acts downstream of or in parallel to Ras (Leone et al., 1997; Mittnacht et al., 1997; Peeper et al., 1997).

Searching for mammalian genes related to the novel synMuv genes

The class B synMuv pathway implicates components and mechanisms that are highly conserved in evolution, indicating that there may be mammalian counterparts of other components of the synMuv pathway with conserved functions. Therefore, information gleaned from studies of *C. elegans* synMuv genes not only is interesting from the point of view of developmental biology,

but also can be generalized and applied to biology and disease in humans. Identification and characterization of mammalian genes related to the as yet novel synMuv genes may serve as an entry point to discover novel regulatory circuits and networks important for normal growth control and tumorigenesis, in particular those that involve Rb. For example, although it is well established that Rb exerts most of its effect by regulating transcription, the exact mechanisms by which Rb acts as a transcriptional repressor of some genes and a coactivator of other genes are not well understood. Study of Rb-mediated pathways in a simple organism amenable to genetic analysis such as *C. elegans* should help identify the key regulators and effectors that influence the broad spectrum of functions carried out by Rb.

Experimental procedures

Generation of polyclonal antisera to LIN-37

Purified bacterially produced 6xHis::LIN-37 fusion protein was used to immunize rabbits. Antisera were batch-purified against GST::LIN-37 fusion protein bound to nitrocellulose filter strips. Bound antibodies were then preabsorbed against *lin-37(n758)* mutant animals.

Cloning of the *C. briggsae lin-35* homolog

C. briggsae genomic fosmid filters (Genome Systems) were probed with a *lin-35* cDNA at low stringency. Four overlapping fosmid clones were isolated: G05D24, G06C09, G13I16 and G47E18. An 11 kb Hind III- Pst I fragment from G06C09 that spans the entire *C. briggsae lin-35* locus was subcloned into the Bluesript SK(+) vector (Strategene) and determination of its sequence is in progress.

PCR screening of deletion library

450 genomic DNA samples representing 1.7×10^6 haploid genomes were screened by nested PCR using 96-well plates in a MJ Research tetrad PCR machine. PCR reactions were carried out with 0.5 U Taq DNA polymerase (GIBCO BRL) in 20 ul volumn.

Conditions for *lin-53* deletion screen:

1^{st} round

primer sequences

F0: 5' GAA ATG GCC ACT CTT GAA G 3'

R9: 5' AAC GTT CAT TGA TAG GAA TGT G 3'

cycling condition: 94°C for 30s, 60°C for 60s, 72°C for 60s; 40 cycles

2nd round

primer sequences

F1: 5' AAG ATC GCG TCG CAA ATG ATG 3'

R8: 5' ATC CAC TAC TAG CCA GAA CAG 3' or

R6: 5' TCG TCG AAT TCT GGT GTG TCT G 3'

cycling condition: 94°C for 30s, 60°C for 60s, 72°C for 25s; 40 cycles

Conditions for *hda-1* deletion screen:

1st round

primer sequences

F3: 5' ACT AAA GGT CAA TCA TGG GAG GAG CC 3'

R2: 5' AGC ACA CCA TCC AAC ATC AGA TGA AGA C 3'?

2nd round

primer sequences

F4: 5' TCA AAA GCC ATG TGG CCT GTG CGA TTG 3'

R3: 5' ATA TGA GAC CAC ATG CGT AGT CAT C 3'

cycling condition for both rounds: 94°C for 30s, 60°C for 60s, 72°C for 80s; 40 cycles

References

Beitel, G. J., Tuck, S., Greenwald, I., and Horvitz, H. R. (1995). The *Caenorhabditis elegans* gene *lin-1* encodes an ETS-domain protein and defines a branch of the vulval induction pathway. Genes Dev *9*, 3149-3162.

Clandinin, T. R., Katz, W. S., and Sternberg, P. W. (1997). *Caenorhabditis elegans* HOM-C genes regulate the response of vulval precursor cells to inductive signal. Dev Biol *182*, 150-161.

Ferguson, E. L., Sternberg, P. W., and Horvitz, H. R. (1987). A genetic pathway for the specification of the vulval cell lineages of *Caenorhabditis elegans*. Nature *326*, 259-267.

Knudsen, E. S., and Wang, J. Y. (1997). Dual mechanisms for the inhibition of E2F binding to RB by cyclin- dependent kinase-mediated RB phosphorylation. Mol Cell Biol *17*, 5771-5783.

Kornfeld, K., Hom, D. B., and Horvitz, H. R. (1995). The *ksr-1* gene encodes a novel protein kinase involved in Ras-mediated signaling in *C. elegans*. Cell *83*, 903-913.

Leone, G., DeGregori, J., Sears, R., Jakoi, L., and Nevins, J. R. (1997). Myc and Ras collaborate in inducing accumulation of active cyclin E/Cdk2 and E2F. Nature *387*, 422-426.

Lu, X., and Horvitz, H. R. (1998). *lin-35* and *lin-53*, two genes that antagonize a *C. elegans* Ras pathway, encode proteins similar to Rb and its binding protein RbAp48. Cell *95*, 981-991.

Maloof, J. N., and Kenyon, C. (1998). The Hox gene *lin-39* is required during *C. elegans* vulval induction to select the outcome of Ras signaling. Development *125*, 181-190.

Margalit, Y., Yarus, S., Shapira, E., Gruenbaum, Y., and Fainsod, A. (1993). Isolation and characterization of target sequences of the chicken CdxA homeobox gene. Nucleic Acids Res *21*, 4915-4922.

Mittnacht, S., Paterson, H., Olson, M. F., and Marshall, C. J. (1997). Ras signalling is required for inactivation of the tumour suppressor pRb cell-cycle control protein. Curr Biol *7*, 219-221.

Peeper, D. S., Upton, T. M., Ladha, M. H., Neuman, E., Zalvide, J., Bernards, R., DeCaprio, J. A., and Ewen, M. E. (1997). Ras signalling linked to the cell-cycle machinery by the retinoblastoma protein. Nature *386*, 177-181.

Riddle, D. L., Blumenthal, T., Meyer, B. J., and Priess, J. R. (1997). *C. elegans* II (Cold Spring Harbor, New York: Cold Spring Harbor Press).

Shi, Y., and Mello, C. (1998). A CBP/p300 homolog specifies multiple differentiation pathways in *Caenorhabditis elegans*. Genes Dev *12*, 943-955.

Sieburth, D. S., Sun, Q., and Han, M. (1998). SUR-8, a conserved Ras-binding protein with leucine-rich repeats, positively regulates Ras-mediated signaling in *C. elegans*. Cell *94*, 119-130.

Sorger, P. K. (1991). Heat shock factor and the heat shock response. Cell *65*, 363-366.

Sundaram, M., and Han, M. (1995). The *C. elegans ksr-1* gene encodes a novel Raf-related kinase involved in Ras-mediated signal transduction. Cell *83*, 889-901.

Thomas, J. H. (1997). Genetic and Molecular Analysis of Synthetic Multivulva Genes in *Caenorhabditis elegans*. Ph.D. Thesis. Massachusetts Institute of Technology, Cambridge, MA.

Figure 1. The *lin-35* promoter contains a putative E2F binding site. The putative E2F site is shaded. The SL1 *trans*-splice site is indicated. Initiation methionine is boxed. Numbers on the right indicate positions relative to the translation start site. The E2F site mutation engineered in the *lin-35*::GFP reporter construct is indicated on the bottom.

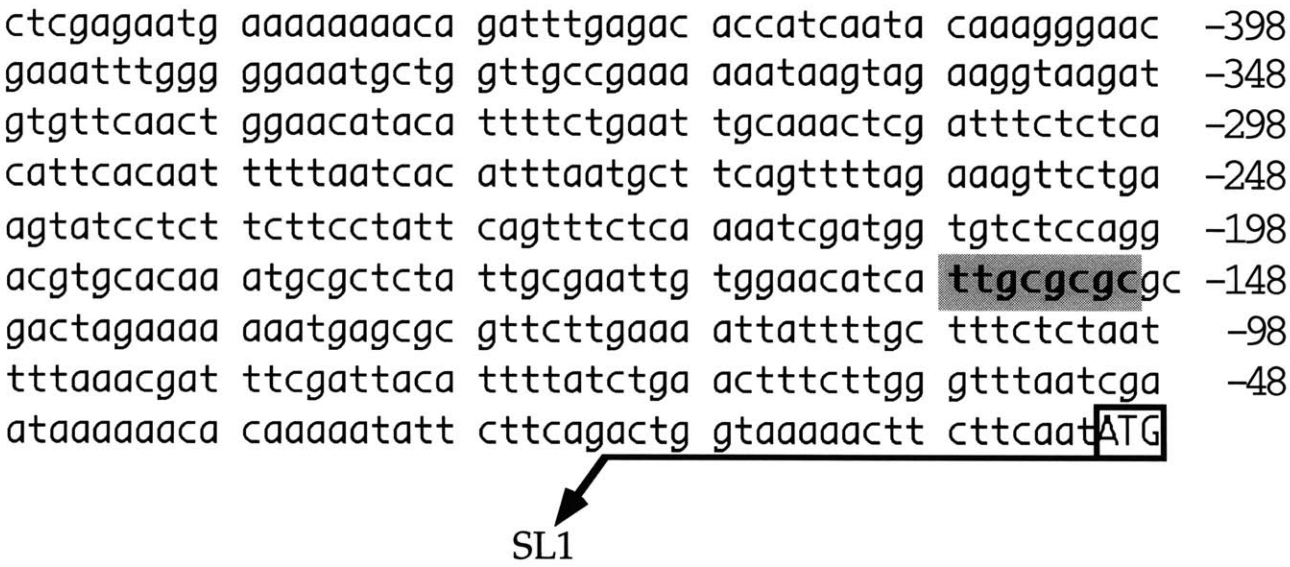

E2F site mutation: **ttgcgcgc** ⟶ **ttgctagc**

Figure 2. Alignment of *C. elegans* and *C. briggsae* LIN-35. Identities are shaded. The A and B pocket domains are underlined. Putative CDK phosphorylation sites are indicated by asterisks. Note that the third site is offset by 8 amino acids in the two proteins.

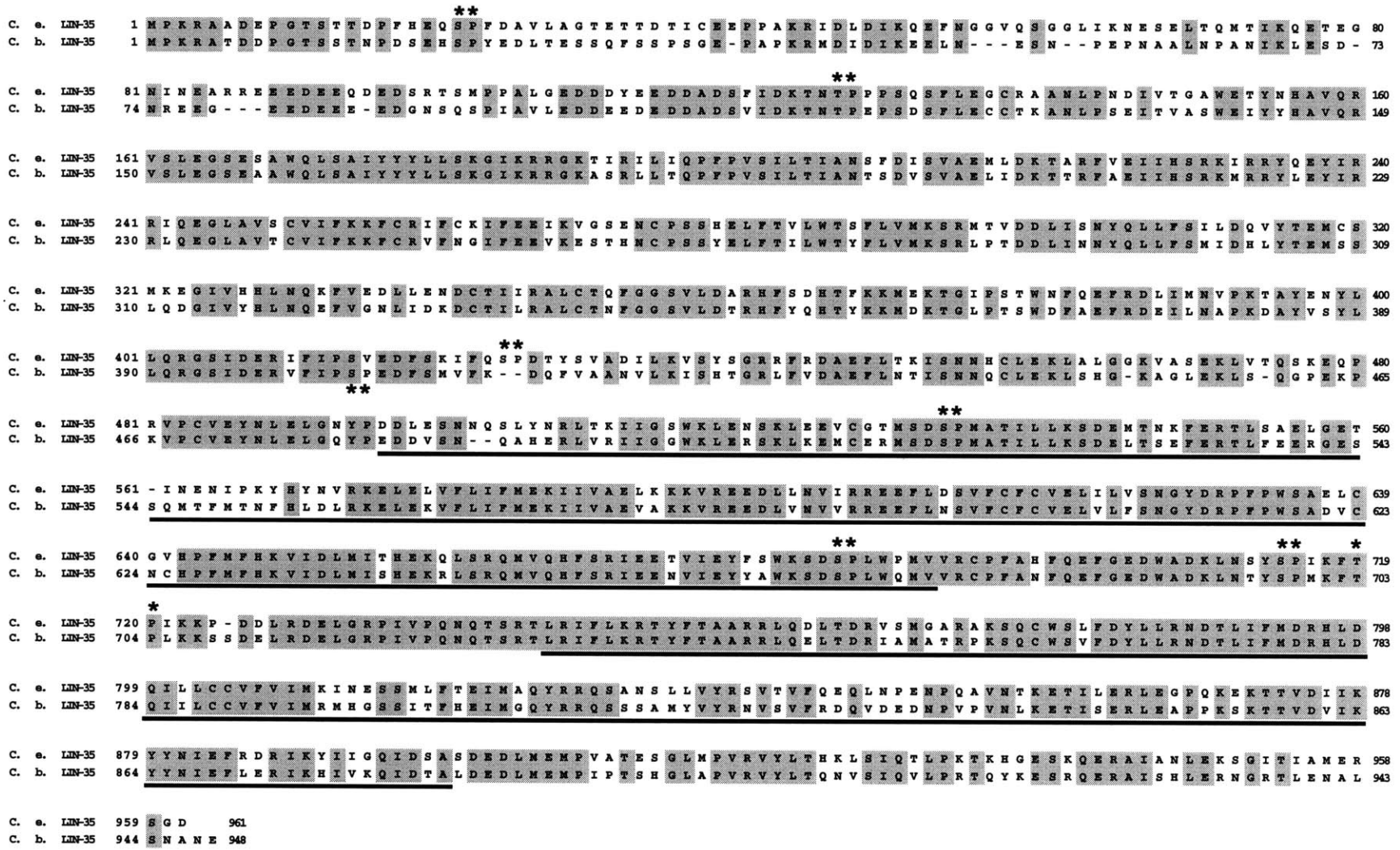
C. e. LIN-35 1 MPKRAADEPGTSTTDPFHEQSPFDAVLAGTETTDTICEEPPAKRIDLDIKQEFNGGVQSGGLIKNESELTQMTIKQETEG 80
C. b. LIN-35 1 MPKRATDDPGTSSTNPDSEHSPYEDLTESSQFSSPSGE-PAPKRMDIDIKEELN---ESN--PEPNAALNPANIKLESD- 73
C. e. LIN-35 81 NINEARREEEDEEQDEDSRTSMPPALGEDDDYEEDDADSFIDKTNTPPPSQSFLEGCRAANLPNDIVTGAWETYNHAVQR 160
C. b. LIN-35 74 NREEG---EEDEEE-EDGNSQSPIAVLEDDEEDEDDADSVIDKTNTPEPSDSFLECCTKANLPSEITVASWEIYYHAVQR 149
C. e. LIN-35 161 VSLEGSESAWQLSAIYYYLLSKGIKRRGKTIRILIQPFPVSILTIANSFDISVAEMLDKTARFVEIIHSRKIRRYQEYIR 240
C. b. LIN-35 150 VSLEGSEAAWQLSAIYYYLLSKGIKRRGKASRLLTQPFPVSILTIANTSDVSVAELIDKTTRFAEIIHSRKMRRYLEYIR 229
C. e. LIN-35 241 RIQEGLAVSCVIFKKFCRIFCKIFEEIKVGSENCPSSHELFTVLWTSFLVMKSRMTVDDLISNYQLLFSILDQVYTEMCS 320
C. b. LIN-35 230 RLQEGLAVTCVIFKKFCRVFNGIFEEVKESTHNCPSSYELFTILWTYFLVMKSRLPTDDLINNYQLLFSMIDHLYTEMSS 309
C. e. LIN-35 321 MKEGIVHHLNQKFVEDLLENDCTIIRALCTQFGGSVLDARHFSDHTFKKMEKTGIPSTWNFQEFRDLIMNVPKTAYENYL 400
C. b. LIN-35 310 LQDGIVYHLNQEFVGNLIDKDCTILRALCTNFGGSVLDTRHFYQHTYKKMDKTGLPTSWDFAEFRDEILNAPKDAYVSYL 389
C. e. LIN-35 401 LQRGSIDERIFIPSVEDFSKIFQSPDTYSVADILKVSYSGRRFRDAEFLTKISNNHCLEKLALGGKVASEKLVTQSKEQP 480
C. b. LIN-35 390 LQRGSIDERVFIPSPEDFSMVFK--DQFVAANVLKISHTGRLFVDAEFLNTISNNQCLEKLSHG-KAGLEKLS-QGPEKP 465
C. e. LIN-35 481 RVPCVEYNLELGNYPDDLESNNQSLYNRLTKIIGSWKLENSKLEEVCGTMSDSPMATILLKSDEMTNKFERTLSAELGET 560
C. b. LIN-35 466 KVPCVEYNLELGQYPEDDVSN--QAHERLVRIIGGWKLERSKLKEMCERMSDSPMATILLKSDELTSEFERTLFEERGES 543
C. e. LIN-35 561 -INENIPKYHYNVRKELELVFLIFMEKIIVAELKKKVREEDLLNVIRREEFLDSVFCFCVELILVSNGYDRPFFPWSAELC 639
C. b. LIN-35 544 SQMTFMTNFHLDLRKELEKVFLIFMEKIIVAEVAKKVREEDLVNVVRREEFLNSVFCFCVELVLFSNGYDRPFFPWSADVC 623
C. e. LIN-35 640 GVHPFMFHKVIDLMITHEKQLSRQMVQHFSRIEETVIEYFSWKSDSPLWPMVVRCPFAHFQEFGEDWADKLNSYSPIKFT 719
C. b. LIN-35 624 NCHPFMFHKVIDLMISHEKRLSRQMVQHFSRIEENVIEYYAWKSDSPLWQMVVRCPFANFQEFGEDWADKLNTYSPMKFT 703
C. e. LIN-35 720 PIKKP-DDLRDELGRPIVPQNQTSRTLRIFLKRTYFTAARRLQDLTDRVSMGARAKSQCWSLFDYLLRNDTLIFMDRHLD 798
C. b. LIN-35 704 PLKKSSDELRDELGRPIVPQNQTSRTLRIFLKRTYFTAARRLQELTDRIAMATRPKSQCWSVFDYLLRNDTLIFMDRHLD 783
C. e. LIN-35 799 QILLCCVFVIMKINESSMLFTEIMAQYRRQSANSLLVYRSVTVFQEQLNPENPQAVNTKETILERLEGPQKEKTTVDIIK 878
C. b. LIN-35 784 QILCCVFVIMRMHGSSITFHEIMGQYRRQSSSAMYVYRNVSVFRDQVDEDNPVPVNLKETISERLEAPPKSKTTVDVIK 863
C. e. LIN-35 879 YYNIEFRDRIKYIIGQIDSASDEDLMEMPVATESGLMPVRVYLTHKLSIQTLPKTKHGESKQERAIANLEKSGITIAMER 958
C. b. LIN-35 864 YYNIEFLERIKHIVKQIDTALDEDLMEMPIPTSHGLAPVRVYLTQNVSIQVLPRTQYKESRQERAISHLERNGRTLENAL 943
C. e. LIN-35 959 SGD 961
C. b. LIN-35 944 SNANE 948

Figure 3. Conserved *lin-35* regulatory elements between *C. elegans* and *C. briggsae.* Potential transcription factor binding sites and their orientations are indicated by arrows. A, a conserved element in the *lin-35* promoter region. Numbers indicate positions from the translation start site. B, a conserved element in *lin-35* intron 2. Numbers indicate positions from the start of the next exon.

A

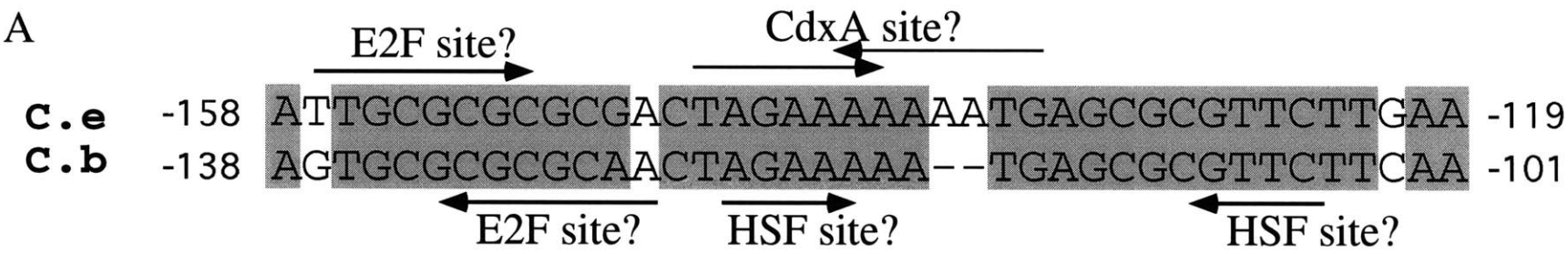
E2F site?
CdxA site?
C.e -158 ATTGCGCGCGCGACTAGAAAAAAATGAGCGCGTTCTTGAA -119
C.b -138 AGTGCGCGCGCAACTAGAAAAA--TGAGCGCGTTCTTCAA -101
E2F site?
HSF site?
HSF site?

B


GATA site?
C.e -555 ACATACGACTGATATGGTCG -534
C.b -1365 ACACACGACTGATATGGTTG-1344

Figure 4. Identification of *lin-53* and *hda-1* deletion alleles. A, positions of the two candidate deletions in *lin-53* are indicated relative to the cDNAs. Their predicted effects on translation are shown on the bottom. PCR primers and their orientations are indicated by the small arrows. B, a 2.4 kb deletion removes all coding sequences of *hda-1*. The position of the deletion are indicated relative to the *hda-1* cDNA. PCR primers are indicated as in A.

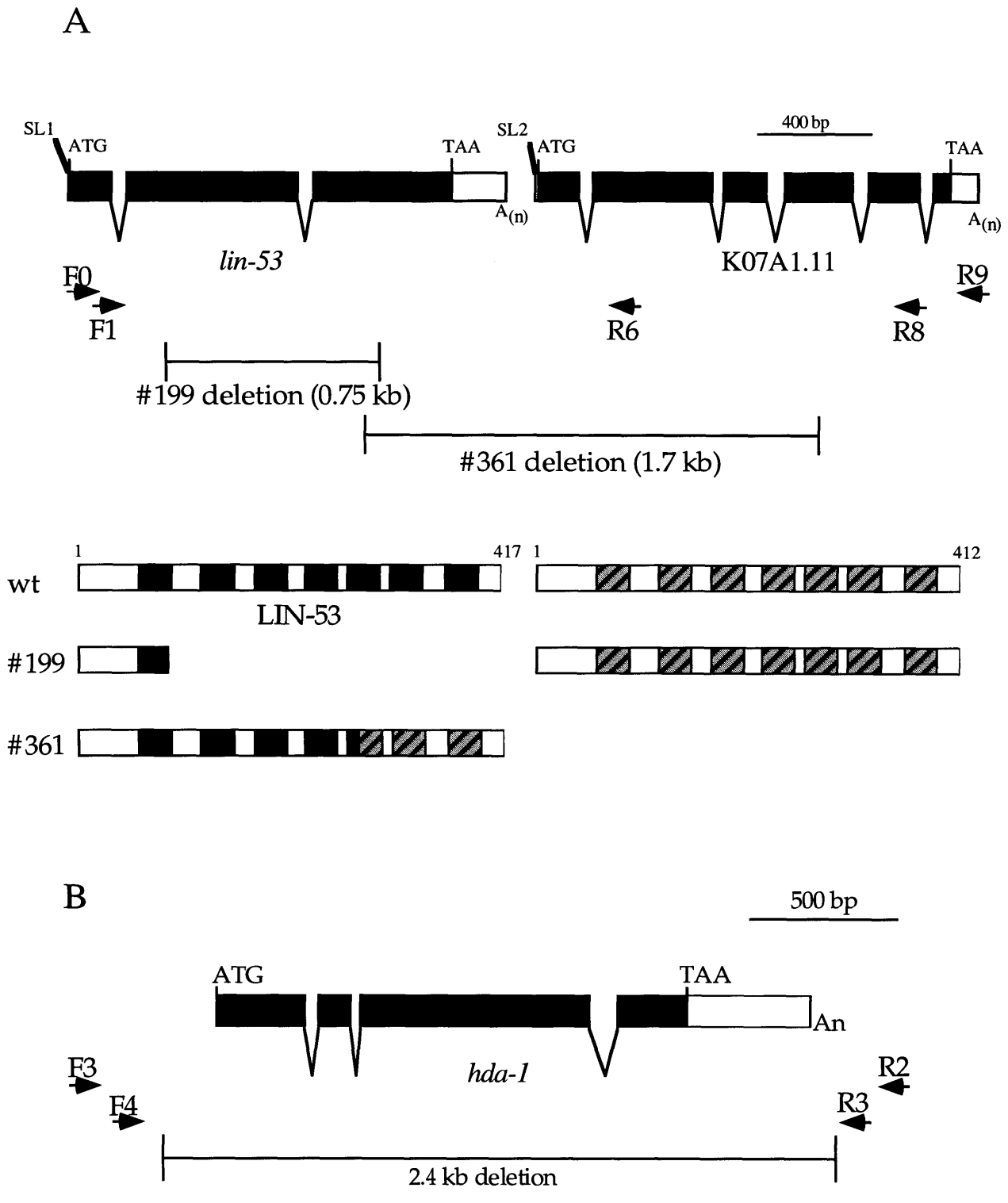
A
SL1
ATG
TAA
A(n)
lin-53
SL2
ATG
400 bp
TAA
A(n)
K07A1.11
F0
F1
R6
R8
R9
#199 deletion (0.75 kb)
#361 deletion (1.7 kb)
wt
1
417
LIN-53
1
412
#199
#361
B
500 bp
ATG
TAA
An
hda-1
F3
F4
R2
R3
2.4 kb deletion

Figure 5. Could synMuv genes act downstream of *lin-3*? Beitel et al. (1995) proposed that there is a branch downstream of the inductive signal LIN-3 and in parallel to the ETS transcription fator LIN-1, indicated by 'X' in the top panel. If 'X' is the synMuv genes, then the presence or absence of *lin-3* activity should have no effect on the Muv phenotype of a *synMuv AB; lin-1* triple mutant, as illustrated in the bottom panels. Black indicates the presence of gene activities and grey indicates the absence of gene activities.

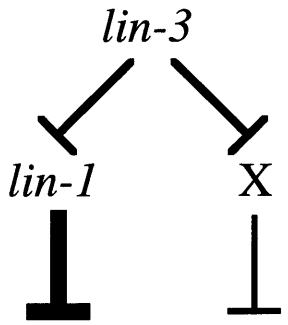
lin-3
lin-1
X
vulval cell fates

X= synMuv???

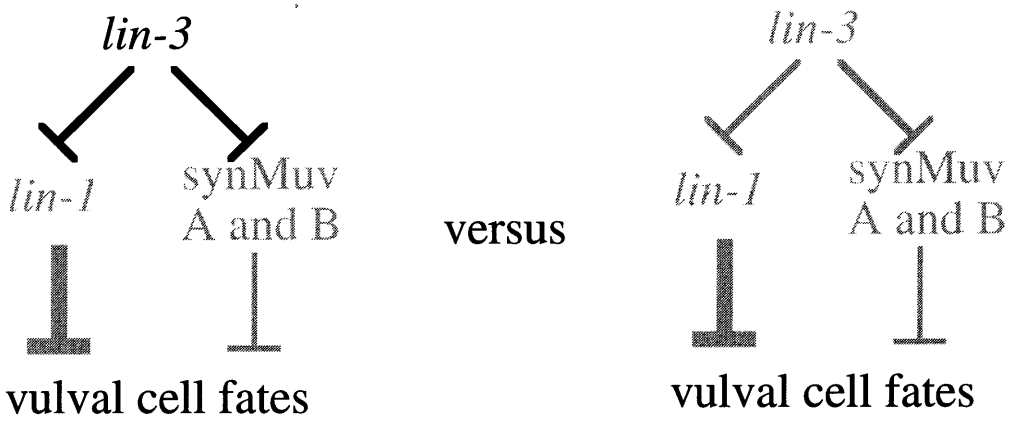
lin-3
lin-1
synMuv
A and B
vulval cell fates
versus
lin-3
lin-1
synMuv
A and B
vulval cell fates

Figure 6. The interface between the synMuv genes and the Ras pathway is unknown. Either class of synMuv genes, class A or B, could act upstream of, downstream of or in parallel to the Ras pathway. For simplicity, the A and B genes are shown at a unit, but they could interface the Ras pathway at different points. Further characterization of the synMuv A genes and identification of the target genes regulated by the synMuv B genes should help understand the nature of the antagonism between the synMuv genes and the Ras pathway.

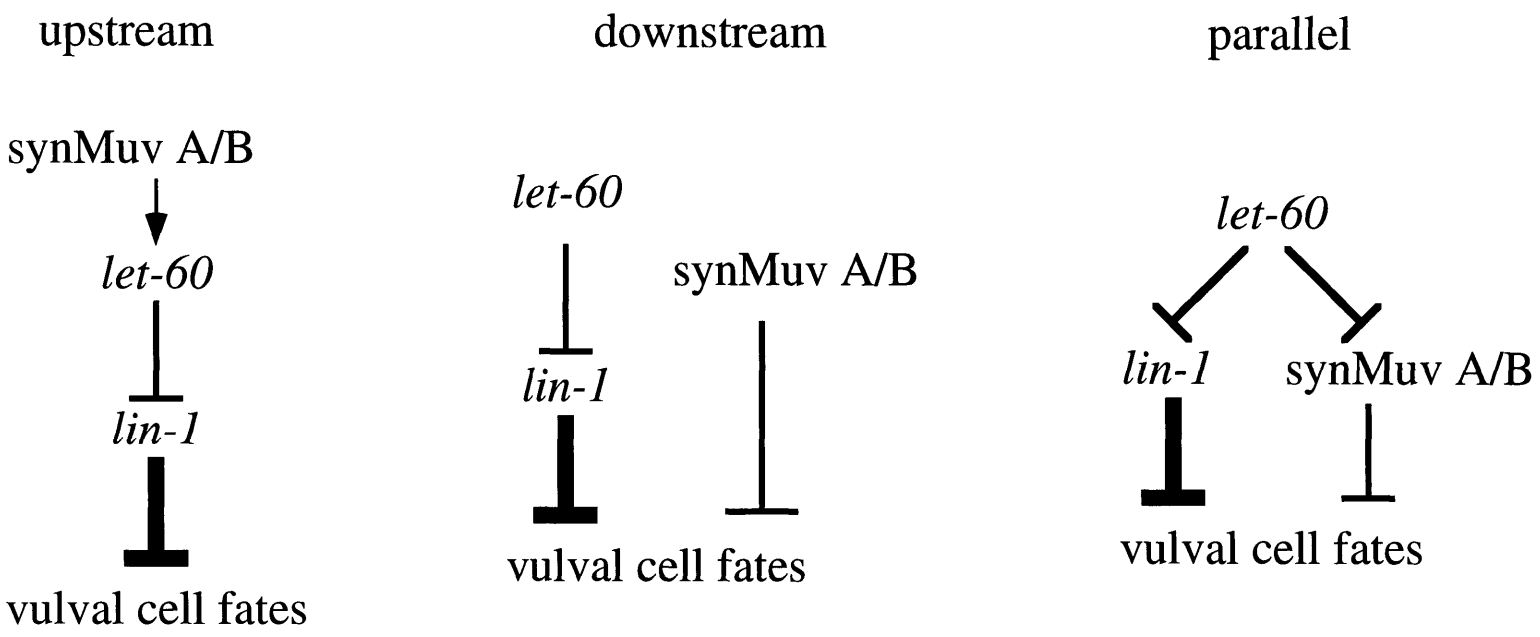
upstream
synMuv A/B
let-60
lin-1
vulval cell fates
downstream
let-60
lin-1
synMuv A/B
vulval cell fates
parallel
let-60
lin-1
synMuv A/B
vulval cell fates

Chapter 5

The *C. elegans* locus *lin-15*, a negative regulator of a tyrosine kinase signaling pathway, encodes two different proteins

reprinted from Genetics *137*, 987-997 (1994)

Scott G. Clark, Xiaowei Lu and H. Robert Horvitz
Howard Hughes Medical Institute, Massachusetts Institute of Technology
Cambridge, MA 02139

The *Caenorhabditis elegans* Locus *lin-15*, a Negative Regulator of a Tyrosine Kinase Signaling Pathway, Encodes Two Different Proteins

Scott G. Clark,[1] Xiaowei Lu and H. Robert Horvitz

Howard Hughes Medical Institute, Department of Biology, Massachusetts Institute of Technology, Cambridge, Massachusetts 02139

Manuscript received February 14, 1994
Accepted for publication April 18, 1994

ABSTRACT

The *Caenorhabditis elegans* locus *lin-15* negatively regulates an intercellular signaling process that induces formation of the hermaphrodite vulva. The *lin-15* locus controls two separate genetic activities. Mutants that lack both activities have multiple, ectopic pseudo-vulvae resulting from the overproduction of vulval cells, whereas mutants defective in only one *lin-15* activity appear wild-type. *lin-15* acts non-cell-autonomously to prevent the activation of a receptor tyrosine kinase/*ras* signaling pathway. We report here the molecular characterization of the *lin-15* locus. The two *lin-15* activities are encoded by contiguous genomic regions and by two distinct, non-overlapping transcripts that may be processed from a single mRNA precursor by *trans*-splicing. Based on the DNA sequence, the 719- and 1,440-amino acid *lin-15* proteins are not similar to each other or to known proteins. *lin-15* multivulva mutants, which are defective in both *lin-15* activities, contain deletions and insertions that affect the *lin-15* genomic region.

THE vulva of the *Caenorhabditis elegans* hermaphrodite is formed by the 22 descendants of three ectodermal blast cells, P5.p, P6.p and P7.p (SULSTON and HORVITZ 1977) (Figure 1A). Three other cells, P3.p, P4.p and P8.p, also have the potential to produce vulval cells. Since all six of these cells are able to express any of three alternative cell lineages (referred to as 1°, 2° and 3°) and are equivalent in their developmental potential, they are considered to define the vulval equivalence group (SULSTON and WHITE 1980; KIMBLE 1981; STERNBERG and HORVITZ 1986). Cells that adopt the 1° and 2° cell fates generate eight and seven descendants, respectively, that together form the vulva, whereas those that express the 3° fate generate two non-vulval descendants that fuse with the syncytial hypoderm that envelops the animal.

Cell interactions determine the fates of the cells of the vulval equivalence group (see HORVITZ and STERNBERG (1991) for review). A signal from the gonadal anchor cell induces the nearest Pn.p cells to express vulval cell lineages: P6.p adopts a 1° cell fate, while P5.p and P7.p adopt 2° cell fates (Figure 1B). The more distant cells P3.p, P4.p and P8.p adopt 3° cell fates. The elimination of the anchor cell causes all six cells to express a non-vulval 3° fate, resulting in a vulvaless (Vul) phenotype (KIMBLE 1981) (Figure 1C). Genetic experiments suggest that an inhibitory signal from the syncytial hypoderm prevents the expression of vulval cell fates (HERMAN and HEDGECOCK 1990). The removal of the hypodermal inhibitory signal allows all six cells to express vulval cell fates, resulting in a multivulva (Muv) phenotype (Figure 1D). These results suggest that during wild-type development, the anchor cell signal promotes the expression of vulval cell fates by overcoming the hypodermal inhibitory signal. In addition, interactions among the induced Pn.p cells prevent adjacent cells from both expressing a 1° fate (STERNBERG 1988).

Many mutants with altered vulval cell lineages have been characterized (HORVITZ and SULSTON 1980; FERGUSON and HORVITZ 1985, 1989; BEITEL *et al.* 1990; HAN *et al.* 1990; KIM and HORVITZ 1990; AROIAN and STERNBERG 1991; CLARK *et al.* 1992; HAN *et al.* 1993; MILLER *et al.* 1993). Some mutations cause all six cells P3.p–P8.p to express a 3° cell lineage, and no vulva is formed. As this Vul phenotype is identical to that of animals lacking the anchor cell, these mutations define genes that could be involved in the signaling process required for vulval induction. Five such Vul genes encode proteins similar to those involved in intercellular signaling in other organisms: *lin-3* encodes a molecule related to TGFα (HILL and STERNBERG 1992), *let-23* encodes a receptor tyrosine kinase (AROIAN *et al.* 1990), *sem-5* encodes an adaptor protein with SH2 and SH3 domains (CLARK *et al.* 1992), *let-60* encodes a *ras* protein (HAN and STERNBERG 1990) and *lin-45* encodes a *raf* serine/threonine kinase (HAN *et al.* 1993). Recently, mutations in the *mpk-1/sur-1* gene, which encodes a mitogen-activated protein (MAP) kinase, have been identified as suppressors of activated *let-60 ras* mutations, suggesting that *mpk-1/sur-1* also functions in the signaling pathway required for vulval induction (LACKNER *et al.* 1994; WU and HAN 1994). Other mutations, including some *lin-15* mutations, cause all six cells P3.p-P8.p to express 1° and 2° cell lineages, resulting in a multivulva phenotype (FERGUSON *et al.* 1987).

[1] Current address: Department of Anatomy, University of California, San Francisco, California 94143.

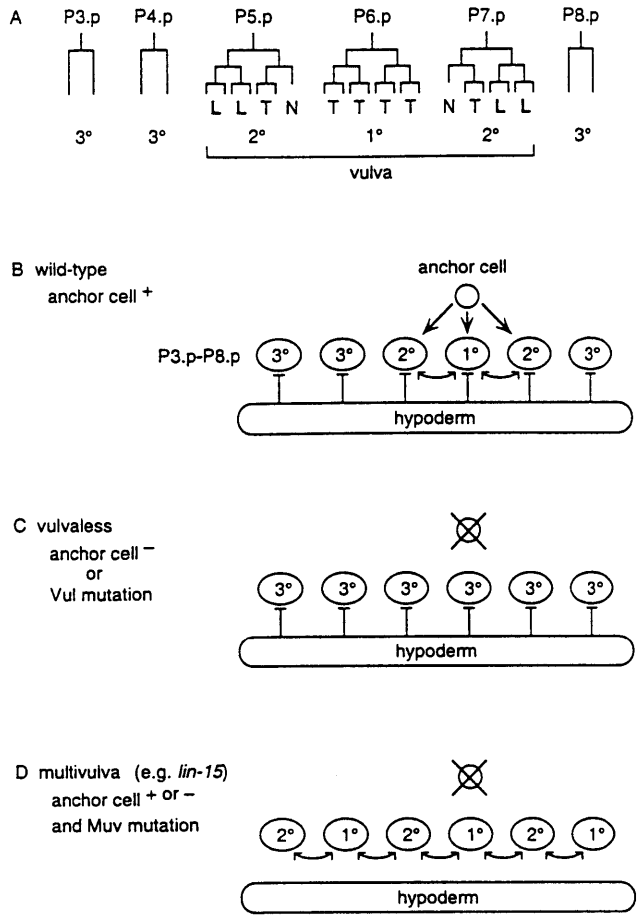

FIGURE 1.—Vulval cell lineages and models for vulval formation (adapted from SULSTON and HORVITZ 1977; BEITEL *et al.* 1990). (A) Cell lineages that generate the vulva. Each P3.p–P8.p cell expresses one of three lineages, referred to as 1°, 2° and 3°. P6.p normally expresses a 1° cell lineage, which produces eight descendants; P5.p and P7.p normally express a 2° cell lineage, which produces seven descendants; and P3.p, P4.p and P8.p normally express a 3° cell lineage, which produces two descendants. The vulva is formed by the 22 descendants of the 1° and 2° cell lineages, while the 3° cell lineage generates non-vulval hypodermal cells. The lineages are, in part, defined by the axis of the final cell division; L, longitudinal, T, transverse, N, non-dividing (STERNBERG and HORVITZ 1986). (B) Wild-type. An inductive signal from the gonadal anchor cell causes the nearest Pn.p cells to express a 1° or 2° cell lineage, while the more distant Pn.p cells express a 3° cell lineage. An inhibitory signal from the hypoderm prevents the expression of the 1° and 2° vulval cell lineages and is overridden by the anchor cell inducing signal. Interactions among the induced cells prevent adjacent Pn.p cells from both expressing a 1° cell lineage. (C) Vulvaless. In the absence of the anchor cell signal or of the response to that signal, the hypodermal inhibitory signal prevents all six Pn.p cells of the vulval equivalence group from expressing a 1° or 2° cell fate, so that no vulva is formed. (D) Multivulva. In the absence of the hypodermal inhibitory signal, all six Pn.p cells express a 1° or 2° cell lineage, and multiple vulva-like ventral protrusions are formed. Even after the elimination of the anchor cell, multivulva mutants such as *lin-15* have a multivulva phenotype.

The multivulva phenotype of many mutants requires mutations in two genes (HORVITZ and SULSTON 1980; FERGUSON and HORVITZ 1985, 1989; J. THOMAS and H. R. HORVITZ, unpublished results). Over 70 such "synthetic Muv" mutations have been identified and divided into two classes, referred to as A and B. Hermaphrodites carrying a class A and a class B mutation have a multivulva phenotype, while hermaphrodites carrying only one mutation or two mutations of the same class have a wild-type vulval phenotype. Thus, these class A and class B genes appear to define two functionally redundant genetic pathways both of which must be disrupted to cause the expression of vulval cell fates.

The first synthetic Muv mutations were discovered when the Muv phenotype of the strain CB1322 was found to require mutations in two unlinked genes, *lin-8 II* and *lin-9 III* (HORVITZ and SULSTON 1980). Five additional synthetic Muv mutations were fortuitously obtained after mutagenesis of a strain that contained an undetected class A mutation (FERGUSON and HORVITZ 1989). Subsequent mutageneses of existing class A and class B single mutants, which are phenotypically wild-type, allowed the systematic isolation of further synthetic Muv mutants (FERGUSON and HORVITZ 1989; J. THOMAS and H. R. HORVITZ, unpublished results). Two genes, *lin-8* and *lin-38*, are defined only by class A mutations, and six genes, including *lin-35*, *lin-36* and *lin-37*, are defined only by class B mutations (FERGUSON and HORVITZ 1989).

Of the mutations that caused a synthetic Muv phenotype, six mapped to the same small interval as the gene *lin-15*, which had been defined previously by single mutations that cause a Muv phenotype (FERGUSON and HORVITZ 1985, 1989). Three of these mutations were in class A, and three were in class B. Complementation tests established that both the class A and class B mutations failed to complement *lin-15* multivulva mutations, indicating that *lin-15* is a complex locus with three distinct types of alleles: Muv, class A synthetic Muv and class B synthetic Muv. These observations indicate that the *lin-15* locus controls two separate activities, one that acts in the class A pathway and one that acts in the class B pathway, and that both of these activities are disrupted in the *lin-15* Muv mutants.

A *lin-15* Muv mutant lacking an anchor cell still has a multivulva phenotype, suggesting that its Muv phenotype does not result from the overproduction of the anchor cell signal and that *lin-15* functions elsewhere than in the anchor cell to regulate the expression of vulval cell lineages (FERGUSON *et al.* 1987). Genetic mosaic analysis indicates that *lin-15* acts non-cell-autonomously and likely functions in the syncytial hypoderm that surrounds the Pn.p cells (HERMAN and HEDGECOCK 1990). These observations suggest that *lin-15* acts in the hypoderm to inhibit the expression of vulval cell lineages and that the absence of *lin-15* function allows the six cells P3.p–P8.p to express vulval cell lineages. Loss-of-function mutations in the receptor tyrosine kinase *let-23* gene, the SH3-SH2-SH3 adaptor protein *sem-5* gene, *let-341*, *let-60 ras* and *lin-45 raf* suppress the Muv phenotype conferred by *lin-15* mutations, indicating that *lin-15* acts upstream of these five genes in the genetic

pathway for vulval induction (FERGUSON *et al.* 1987; BEITEL *et al.* 1990; HAN *et al.* 1990; CLARK *et al.* 1992, 1993; HAN *et al.* 1993). The action of *lin-15* within the surrounding hypodermis may negatively regulate the *let-23* receptor tyrosine kinase signaling pathway.

We cloned the *lin-15* locus by identifying polymorphisms associated with *lin-15* mutations and by rescuing the *lin-15* mutant phenotype by germline transformation. Two adjacent transcripts of 2.3 and 4.6 kb encode the *lin-15* class A and class B genetic activities, respectively. We show that these transcripts are *trans*-spliced and provide evidence that supports the hypothesis (SPIETH *et al.* 1993) that these transcripts are processed from a single mRNA precursor. The 719- and 1,440-amino acid *lin-15* proteins are not highly similar to any known proteins and thus may represent new types of molecules involved in intercellular signaling.

MATERIALS AND METHODS

Standard methods for culturing and handling *C. elegans* were used (BRENNER 1974).

Strains: The following mutations were used in our studies.

Linkage group (LG) II: lin-8(n111).

LGIII: lin-9(n112), lin-36(n766).

LGX: lin-15(e1763, n309, n374, n433, n743, n744, n749, n765, n767, n1139, n1296, n1331, n1344, n2141) n1296, n1331 and *n1344* were identified as spontaneous Muv mutants (KIM and HORVITZ 1990) in the mutator strain TR679 (COLLINS *et al.* 1987). *n1139* was isolated after γ-irradiation (FERGUSON and HORVITZ 1985). *n2141* (C. BARGMANN, personal communication) as well as the other nine *lin-15* mutations (FERGUSON and HORVITZ 1985, 1989) were recovered following treatment with ethyl methanesulfonate (EMS). The *n433, n749* and *n767* mutations belong to the A class and cause a Muv phenotype in the presence of a class B mutation, such as *lin-9(n112)* or *lin-36(n766)*. The *n374, n743* and *n744* mutations belong to the B class and cause a Muv phenotype in association with a class A mutation, such as *lin-8(n111)*. *n765*ts mutants have a temperature-sensitive Muv phenotype because they lack class B function and have a temperature-sensitive defect in class A function. The remaining *lin-15* mutants lack both class A and B function and have a Muv phenotype that is independent of other synthetic Muv mutations.

Analysis of *lin-15*-associated polymorphisms: Genomic DNA was prepared from *lin-15* mutants raised on 1.5% agarose NGM plates seeded with HB101 essentially as described (SULSTON and HODGKIN 1988). Approximately 5 μg of genomic DNA from each mutant was digested with *Eco*RI, separated by agarose gel electrophoresis and blotted to nylon filters. The filters were probed with cosmid or plasmid ^{32}P-labeled DNA. All eight *lin-15* multivulva mutants examined and one *lin-15* class A mutant, *n767*, contained *Eco*RI restriction fragment length polymorphisms. Based on our *Eco*RI restriction map, we determined the approximate positions and lengths of the deletions and insertions within each *lin-15* mutant (see Figure 5).

Germline transformation and analysis of *lin-15* genomic region: Germline transformation (MELLO *et al.* 1991) of *lin-8* and *lin-15*, of *lin-9* and *lin-15*, of *lin-36* and *lin-15* and of *lin-15* Muv mutants was performed by coinjecting test DNA (10–50 μg/ml) and the dominant *rol-6(su1008)* roller marker (plasmid pRF4 at 80 μg/ml). Transgenic animals typically carry coinjected DNAs as extrachromosomal arrays (MELLO *et al.* 1991) and are identified by the roller phenotype conferred by pRF4. A rescued F_2 population was defined as an F_2 roller population (derived from F_1 rollers) in which at least 50% of the animals were not multivulva in phenotype. The overlapping cosmids C29B12 and ZC436 each rescued the *lin-15(n765)* Muv phenotype, suggesting that the *lin-15* gene is located in the region common to these cosmids. A number of genomic DNA fragments were subcloned from C29B12 and were similarly tested for the rescue of the Muv phenotype of *lin-15(n765*ts*), of lin-8(n111); lin-15(n374)* and of *lin-9(n112); lin-15(n433), lin-9(n112); lin-15(n749)* or *lin-36(n766); lin-15(n767)* (see Figure 2B). We determined the DNA sequences of both strands of the 11.7-kb *Eag*I-*Eco*RI fragment (see Figure 2B) of C29B12 using Sequenase 2.0 (U.S. Biochemical Corp.) or using the ABI Prism cycle sequencing kit and an ABI 373A DNA Sequencer (Applied Biosystems, Inc.), essentially according to the manufacturers' instructions. Based on the sequences of the two cDNAs (see below), the *lin-15* coding regions are completely contained in this genomic DNA fragment.

Isolation and characterization of *lin-15* cDNAs: The 10.5-kb *Bam*HI-*Eco*RI fragment from C29B12 (see Figure 2B) was used to screen approximately 400,000 plaques of a λZAP cDNA library derived from mixed-stage poly(A)$^+$ RNA (BARSTEAD and WATERSTON 1989). Eleven positive clones were identified; four were from the *Eag*I-*Sal*I region, and seven were from the *Sal*I-*Eco*RI region. We determined the complete DNA sequences of one strand of the longest clone derived from the *Eag*I-*Sal*I region as well as partial sequences of the remaining 10 clones. As none of the cDNAs was full length, we used the method of reverse transcription-polymerase chain reaction (RT-PCR) to clone the 5′ regions of the *lin-15* transcripts. To amplify the 5′ region of the 2.3-kb transcript, we used a primer corresponding to sequences of the *lin-15* A cDNA (5′CAGATTCCATTGACTGGGTAGG) and a primer corresponding to sequences of either the *C. elegans trans*-spliced leaders SL1 (5′GTTTAATTACCCAAGTTTGAG) (KRAUSE and HIRSH 1987) or SL2 (5′GGTTTTAACCCAGTTACTCAAG) (HUANG and HIRSH 1989). DNA was amplified from 250 ng of mixed-stage RNA using the GeneAmp Thermostable r*Tth* Reverse Transcriptase RNA PCR Kit (Perkin Elmer) and then cloned using the TA Cloning Kit (Invitrogen). We determined the DNA sequences of both strands of two independent clones obtained using the SL1 primer and one strand of three independent clones recovered using the SL2 primer. These RT-PCR-derived clones contained the *trans*-spliced leader sequences and lacked putative intron sequences, indicating that they were derived from a processed transcript and not from genomic DNA. The DNA sequence of the 5′ region of the 4.6-kb *lin-15* B transcript was assembled from the sequences of four overlapping DNA fragments (referred to as B1, B2, B3 and B4) amplified using multiple sets of primers. Fragments B2 and B3 were amplified directly from mixed-stage RNA using RT-PCR, whereas fragments B1 and B4 were generated by a second round of PCR amplification from DNA produced by RT-PCR of RNA. The following primers were used: B1, 5′CACACGATGCCTTGCAAACG (1st round), 5′CATTGATCGAAGAAGGTGCTCC (2nd round) and 5′GCAGGTTCACCTTGGTCTTTATGC (both rounds); B2, 5′GTGGAATGTCATAGTTTGCAACTG and 5′CAAATTTAGAAGAATGCAAGTT; B3, 5′CATGATGGCTGGCACAACTTGAG and 5′ATCTGCGGAAATTGCTACTTACC; B4, 5′GTTTGTGAGGAGACTGTTGCT (1st round), 5′GCAATTTCCGCAGATAAATCGC (2nd round) and SL1 primer (both rounds). We determined the complete DNA sequences of one strand of one independent clone for each fragment as well as partial sequences of additional clones.

Construction of frameshift mutation clones: To establish that the *lin-15* A and B activities are encoded by the two identified genes, we introduced a frameshift mutation into the predicted coding region of each gene within the *Spe*I-*Nru*I

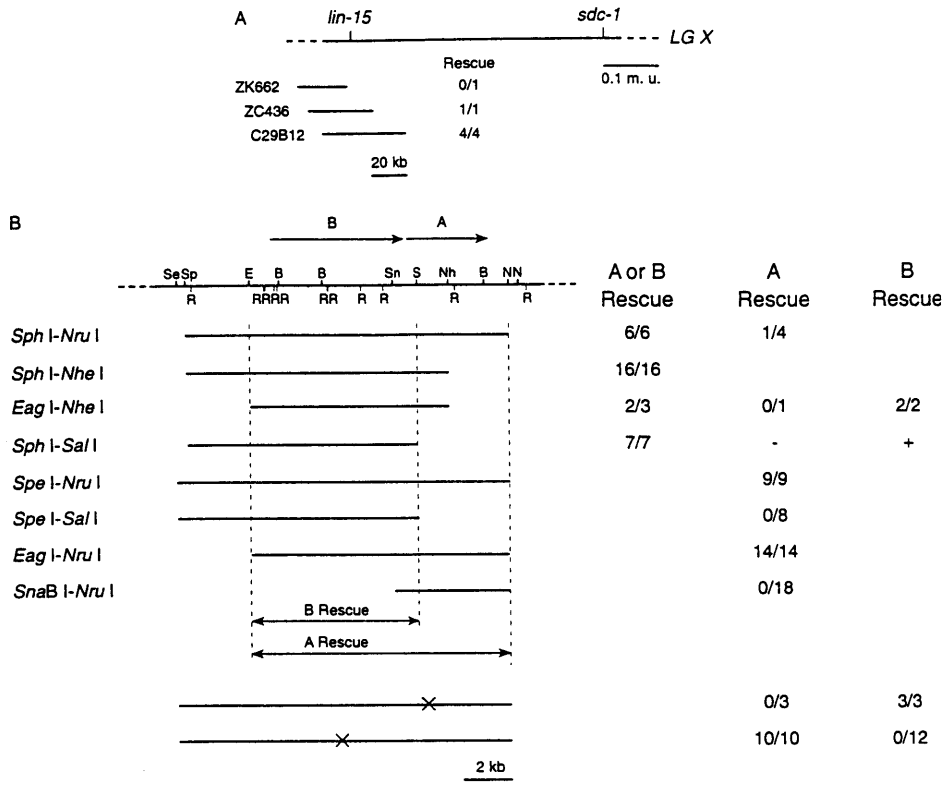

FIGURE 2.—Genetic and physical maps of the *lin-15* region of the *X* chromosome. (A) Genetic map with cosmid clones representing this region shown below. Cosmids were tested for the rescue of the Muv phenotype of the *lin-15(n765ts)* mutant when maintained as extrachromosomal arrays after germline transformation. The fraction of independently derived transformed F_2 populations rescued for the Muv phenotype of *lin-15(n765)* animals is listed for each clone. (B) Restriction map of the central region of C29B12 and structures of genomic subclones. Genomic subclones were tested for rescue of the Muv phenotype of *lin-15(n765)* animals; a subclone containing either *lin-15* A or *lin-15* B function could rescue the Muv phenotype of *lin-15(n765)*. Subclones were also tested for the rescue of the Muv phenotype of strains defective in either *lin-15* A activity [*lin-9(n112); lin-15(n433)*, *lin-9(n112); lin-15(n749)* or *lin-36(n766); lin-15(n767)*] or *lin-15* B activity [*lin-8(n111); lin-15(n374)*]. Specifically, we used *lin-9(n112); lin-15(n433)* for the *Eag*I-*Nhe*I and *Sph*I-*Sal*I fragments, and *lin-36(n766); lin-15(767)* for the *Sph*I-*Nru*I, *Spe*I-*Nru*I and *Spe*I-*Sal*I fragments. The fraction of independently derived transformed F_2 populations rescued for the Muv phenotype of *lin-15(n765)* animals (A or B Rescue), for *lin-15* A activity (A Rescue) and for *lin-15* B activity (B Rescue) are listed for each clone. +, rescue of *lin-15* B activity was observed in 32/33 transformed F_1 animals, but no stably transformed F_2 animals were recovered. −, 0/20 transformed F_1 animals were rescued for *lin-15* A activity, and no stably transformed F_2 animals were obtained. Frameshift mutations (denoted by ×) were introduced in the coding regions of the 2.3- and 4.6-kb transcripts present in the *Spe*I-*Nru*I genomic fragment (see MATERIALS AND METHODS), and these clones were then tested for the rescue of *lin-15* A and *lin-15* B function. Arrows represent the lengths and directions of transcription of the *lin-15* A and B transcripts. Abbreviations are as follows: Se (*Spe*I), Sp (*Sph*I), E (*Eag*I), B (*Bam*HI), Sn (*Sna*BI), S (*Sal*I), Nh (*Nhe*I), N (*Nru*I) and R (*Eco*RI).

genomic DNA fragment and tested these altered clones for the rescue of *lin-15* A activity in *lin-9(n112); lin-15(n433)* and B activity in *lin-8(n111); lin-15(n374)* or *lin-8(n111); lin-15(n744)* by germline transformation. For the putative *lin-15* A coding region, an 8-bp *Nco*I linker (5′CCCATGGG) was ligated into a *Msc*I site corresponding to nucleotide 757 of the 2.3-kb cDNA (see Figure 4A). This alteration is predicted to produce a truncated *lin-15* A protein consisting of residues 1–243 of the native protein and an additional 18 amino acids (PWATLEWQLQRKRFVMRG) derived from the linker sequences and the altered reading frame. For the putative *lin-15* B coding region, the 8-bp *Nco*I linker was ligated into a *Sca*I site corresponding to position 2352 of the 4.6-kb cDNA (see Figure 4B). This alteration is expected to generate a truncated *lin-15* B protein containing residues 1–775 of the native protein and an additional 32 amino acids (PWDWPQNYPRRKAHHHQLQLLHKLDPMLPLRN) derived from the linker sequences and the altered reading frame.

To verify that the failure to rescue the *lin-15* gene activity resulted from the frameshift mutation, we restored the reading frame in each modified clone by digesting with *Nco*I and then filling in the 5′ overhang using DNA polymerase I large (Klenow) fragment. This treatment produced a 12-bp insertion (CCCATGCATGGG) at the original site and is predicted to result in the insertion of 4 amino acids (PMHG). The constructs containing the restored reading frames rescued *lin-15* gene activity. We confirmed the DNA sequences of the modified region for all four clones.

RESULTS

Identification of *lin-15*-specific polymorphisms: We cloned the *lin-15* gene on the basis of its map position near the *sdc-1* gene on the *X* chromosome (Figure 2A). Based upon a physical map of the *C. elegans* genome consisting of overlapping cosmids and yeast artificial

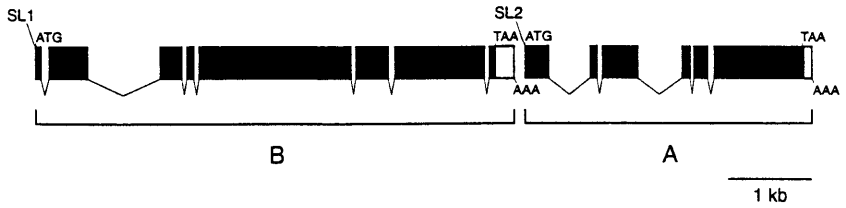

FIGURE 3.—*lin-15* genomic structure deduced from cDNA and genomic DNA sequences. The protein coding regions are denoted as solid boxes and the 3′ untranslated regions are shown as open boxes. SL1 and SL2, the *trans*-spliced SL1 and SL2 leader sequences, respectively. The downstream *lin-15* A cDNA is also processed with SL1 (not shown). ATG and TAA, the predicted start and stop sites of translation, respectively. AAA, poly(A) addition sites.

chromosomes (YACs) (COULSON *et al.* 1986, 1988; A COULSON and J. SULSTON, personal communication), we obtained cosmids that covered a small region left of the *sdc-1* gene (NONET and MEYER 1991). Genomic DNA prepared from four *lin-15* Muv mutants (*n1139, n1296, n1331, n1344*) was probed with these cosmids to detect possible *lin-15*-associated DNA rearrangements (see MATERIALS AND METHODS). *n1139* was recovered following mutagenesis by γ-irradiation (FERGUSON and HORVITZ 1985), and the other three alleles were isolated as spontaneous mutants in the mutator strain TR679 (KIM and HORVITZ 1990). As γ-irradiation often causes chromosomal rearrangements (ROSENBLUTH *et al.* 1985) and TR679-derived mutants often result from transposon insertions (COLLINS *et al.* 1987), these four mutants seemed likely to have readily detectable *lin-15* polymorphisms. All four *lin-15* Muv strains were found to contain *Eco*RI restriction fragment length polymorphisms (RFLPs) in a region covered by two overlapping cosmids, C29B12 and ZK662 (see below). Subsequently, five *lin-15* strains (*e1763, n309, n765, n767, n2141*) that were recovered following treatment with EMS were also shown to have *Eco*RI RFLPs in this region (see below and Figure 5 for description). These results suggest that at least part of the *lin-15* gene is located within the region shared by these two cosmids.

Germline rescue of *lin-15* mutants: We tested C29B12, ZK662 and a third cosmid, ZC436, in germline transformation experiments (MELLO *et al.* 1991) and found that C29B12 and ZC436 each rescued the Muv phenotype of *lin-15(n765*ts*)* animals (Figure 2A). A 14-kb genomic fragment (*Sph*I-*Nru*I) as well as shorter fragments derived from the region common to C29B12 and ZC436 also rescued the Muv phenotype of *lin-15(n756*ts*)* mutants (Figure 2B). As the Muv phenotype of *lin-15* mutants requires the loss of both A and B activities, the recovery of either A or B activity alone would be sufficient to rescue the Muv phenotype of *lin-15(n765*ts*)* animals or other *lin-15* Muv mutants. To assay specifically for *lin-15* A function, genomic DNA subclones were tested for the rescue of the Muv phenotype of a double mutant strain containing a class B mutation, *lin-9(n112)* or *lin-36(n766)*, and a *lin-15* A mutation. As these strains do not lack *lin-15* B function, the rescue of the Muv phenotype would indicate that the tested genomic DNA fragment had *lin-15* A rescuing activity. We found that the 11-kb *Eag*I-*Nru*I and longer fragments contained *lin-15* A activity because they rescued the Muv phenotype of the *lin-9(n112); lin-15(n433), lin-9(n112); lin-15(n749)* or *lin-36(n766); lin-15(n767)* double mutant (Figure 2B). No rescued transformants were recovered using a fragment (*Sph*I-*Sal*I or *Spe*I-*Sal*I) that lacked the 3.8-kb *Sal*I-*Nru*I region, suggesting that this region is needed for the rescue of *lin-15* A function. However, this region alone is not sufficient for *lin-15* A rescue, because no rescued transformants were obtained using the 4.9-kb *Sna*BI-*Nru*I fragment. To assay specifically for the rescue of *lin-15* B function, we used a double mutant strain containing a class A mutation, *lin-8(n111)*, and a *lin-15* B mutation. In contrast to the results for *lin-15* A rescue, the *Eag*I-*Nhe*I and *Sph*I-*Sal*I fragments rescued the Muv phenotype of the *lin-8(n111); lin-15(n374)* double mutant (Figure 2B). These results indicate that the 7.2-kb region common to these two fragments is sufficient for the rescue of the *lin-15* B defect in the *lin-8(n111); lin-15(n374)* double mutant and, by inference, in the *lin-15(n765*ts*)* Muv mutant. Together, these data indicate that the 11-kb *Eag*I-*Nru*I genomic DNA fragment contains both *lin-15* A and B gene activities. While the *Eag*I-*Sal*I region is needed for the rescue of both *lin-15* functions, the 3.8-kb *Sal*I-*Nru*I region is essential for only the rescue of *lin-15* A activity.

***lin-15* encodes two different polypeptides:** We determined the DNA sequences of the 11.7-kb *Eag*I-*Eco*RI genomic fragment and of multiple cDNAs derived from this region (see MATERIALS AND METHODS). As none of the cDNAs isolated from a mixed-stage cDNA library was full length, the DNA sequences of cDNAs obtained by the method of RT-PCR were also determined (see MATERIALS AND METHODS). From our analysis of the cDNA and genomic DNA sequences, we determined that there are two separate, similarly oriented transcripts that are 2.3 and 4.6 kb in length (Figures 3 and 4). cDNAs for the downstream 2.3-kb transcript were generated by RT-PCR using an oligonucleotide primer for either the SL1 or SL2 *trans*-spliced leader (KRAUSE and HIRSH 1987; HUANG and HIRSH 1989). These results show that SL1 and SL2 are used for the processing of the 2.3 kb transcript, but do not indicate the relative abundances of

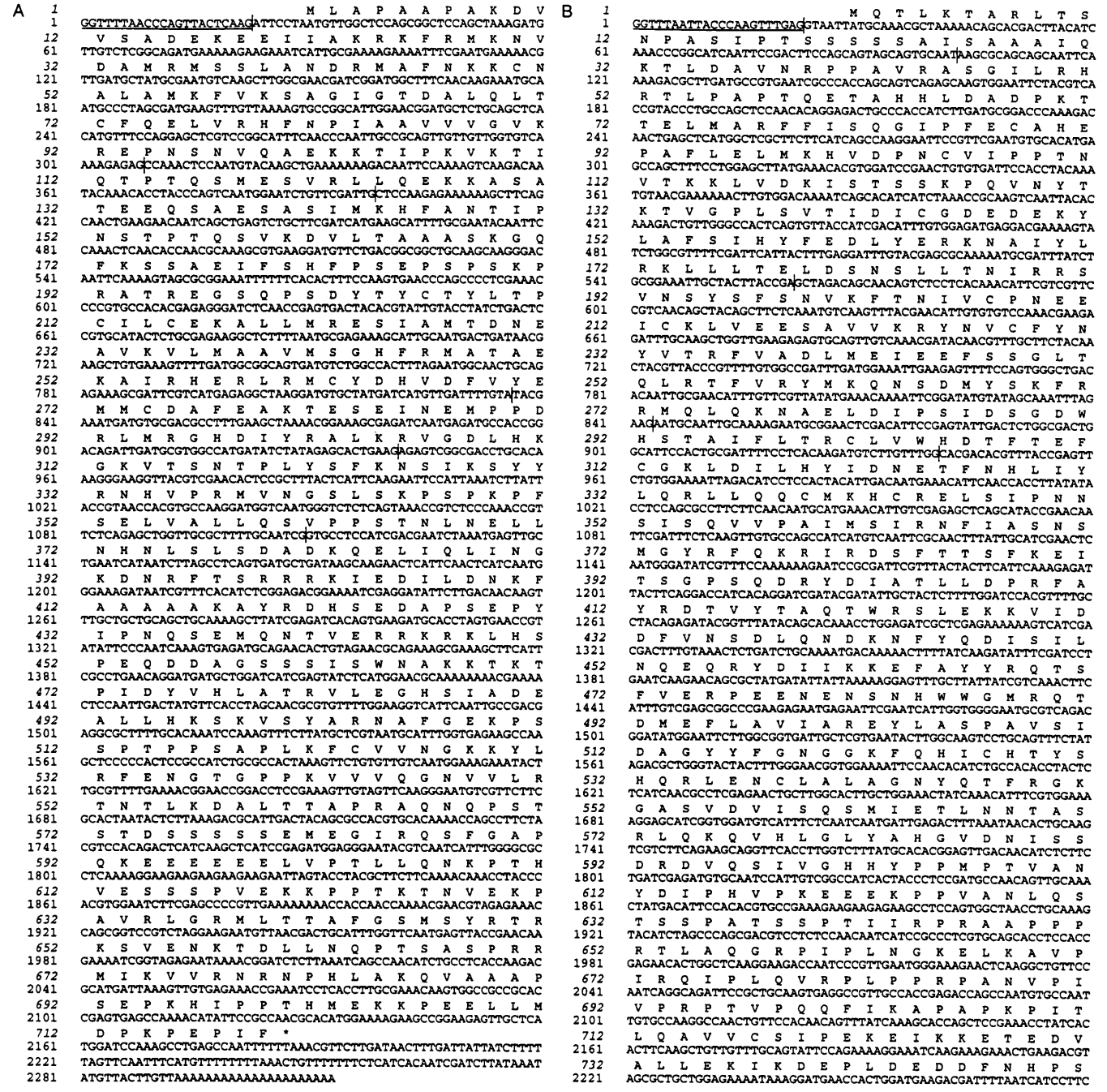

FIGURE 4.—Nucleotide and deduced amino acid sequences (single-letter code) corresponding to *lin-15* cDNAs. (A) Nucleotide sequence of a composite *lin-15* A cDNA assembled from sequences of cDNAs obtained by RT-PCR (nucleotides 1–337) and cDNAs isolated from a λ cDNA library (nucleotides 338–2,313) (see MATERIALS AND METHODS). The nucleotides derived from the 22-nucleotide *trans*-spliced leader SL2 (HUANG and HIRSH 1989) are underlined. Nucleotides are numbered on the left beginning with the SL2 sequences. Amino acids are numbered on the left in italics beginning with the first predicted methionine. The positions of splice sites as determined by comparison with genomic sequences are marked with vertical lines. The ochre termination codon is denoted as an asterisk. (B) Nucleotide sequence of a composite *lin-15* B cDNA assembled from sequences of cDNAs generated by RT-PCR (nucleotides 1–2554) and cDNAs isolated from a λ cDNA library (nucleotides 2554–4623) (see Materials and Methods). The nucleotides derived from the 22-nucleotide *trans*-spliced leader SL1 (KRAUSE and HIRSH 1987) are underlined. The ochre termination codon is denoted as an asterisk. (C) Nucleotide sequence of the *lin-15* A and B intragenic region. The sequence shown begins at the polyadenylation site of the *lin-15* B transcript and ends at the splice leader acceptor site of the *lin-15* A transcript.

SL1- and SL2-containing transcripts. cDNAs for the upstream 4.6 kb transcript were generated using an oligonucleotide primer for SL1 but could not be recovered using a primer for SL2, suggesting that this transcript is processed with SL1 and not with SL2. There are 110 nucleotides between the polyadenylation site of the 4.6-kb transcript and the splice-leader acceptor site of the 2.3-kb downstream transcript (Figure 4C).

```
 752  T D P V P N R T T A S S Q G P S S Y P R
2281  AACTGATCCGGTGCCAAACCGAACGACTGCTTCTTCACAAGGACCATCTTCGTATCCACG
 772  K I V V L A S K L P T S Q S S S P S T A
2341  GAAAATTGTAGTACTGGCCTCAAAACTACCCACGTCGCAAAGCTCATCACCATCAACTGC
 792  T S A Q A R S H V T T A Q L I R C G P S
2401  AACTTCTGCACAAGCTAGATCCCATGTTACCACTGCGCAACTGATCCGATGTGGGCCAAG
 812  E G T V P Q K I H S H N F V Q K F A Q K
2461  TGAAGGCACCGTTCCACAAAAAATTCATTCACACAACTTTGTGCAGAAGTTTGCTCAAAA
 832  Q N F V H K Y A L N S Q D H T G R L N Q
2521  GCAAAATTTTGTTCACAAGTATGCACTGAACTCACAAGACCACACAGGCAGGCTCAACCA
 852  T V P M R A A L R L P N S E Q K S G A P
2581  AACTGTACCCATGAGAGCTGCGCTGAGGCTTCCAAACAGCGAACAAAAGTCAGGAGCACC
 872  S S I N G K V Q R D D F K L E P L D D F
2641  TTCTTCGATCAATGGAAAAGTACAGAGGGATGACTTCAAATTGGAACCACTGGACGATTT
 892  N G E P D Y D N L I G A Q R L M Y S D N
2701  CAACGGAGAACCCGACTATGACAATTTAATTGGGGCTCAACGGCTTATGTACAGTGATAA
 912  L N D A S A E D A F A R H R V T M E F Q
2761  TCTCAATGACGCATCGGCAGAAGATGCGTTTGCAAGCATCGTGTGACTATGGAATTCCA
 932  K R R A C N R R C A V C G H L E I H E R
2821  GAAGCGCAGAGCTTGCAACCGTCGCTGTGCAGTATGTGGTCACTTGGAAATCCACGAGCG
 952  L K N V T I E N E K L L I M L G C I Y R
2881  TCTGAAGAATGTGACGATTGAAAATGAAAAGCTGTTGATTATGTTGGGCTGTATTTATCG
 972  G E F T L G Q A Q L F M A R E S K T Y I
2941  CGGAGAATTTACTCTAGGACAGGCACAGCTTTTCATGGCGCGTGAGAGCAAAACGTACAT
 992  C R L H F L E T L D E I Y Q M L R L K S
3001  TTGCCGTCTCCATTTCCTGGAGACCCTCGACGAGATCTACCAGATGCTACGTCTGAAATC
1012  A D D I L I C P L D L I Q N A L I T V S
3061  TGCCGATGATATTCTGATTTGCCCATTGGACTTGATTCAGAACGCATTGATCACTGTTTC
1032  A L R P H I I A S Q L R K I L H D F A E
3121  CGCCCTCCGTCCACACATTATTGCTTCACAACTTCGAAAGATTCTTCACGATTTTGCCGA
1052  R N N H L R E T P A E L K K L G Q Q Y F
3181  AAGAAATAATCATCTTCGTGAAACGCCAGCGGAATTGAAGAAACTTGGACAACAATACTT
1072  D Y R E P E P E P E R N D V D E Q E I I
3241  TGACTACCGCGAGCCCGAACCTGAGCCAGAGAGAAACGATGTGGATGAGCAAGAAATCAT
1092  P K L F R Q P R K Q V L E A D Q H D G T
3301  ACCGAAACTCTTTCGCCAGCCACGCAAGCAAGTTCTGGAAGCTGATCAGCATGACGGAAC
1112  V K V I E Q E D F K L P T V K P S E N E
3361  TGTCAAGGTTATAGAGCAGGAAGATTTCAAGCTCCCAACTGTCAAACCGTCTGAAAATGA
1132  E C D N P G V C C F C S K R G D R G G M
3421  GGAATGCGACAATCCGGGCGTTTGCTGCTTCTGTTCGAAACGTGGCGACCGAGGTGGAAT
1152  L R V P R S E E R L A R W V D K L G P E
3481  GCTTCGTGTCCCGAGAAGTGAGGAACGTTTGGCTAGATGGGTGGATAAGCTTGGACCAGA
1172  F E A R L H T N T E N L I C R S H F P D
3541  ATTTGAAGCCCGACTTCACACCAATACGGAAAACCTAATTTGCCGAAGCCATTTCCCAGA
1192  A A F S S R G R L L K G M I P D A A P E
3601  TGCAGCGTTCAGCAGTCGTGGTAGACTTTTGAAAGGAATGATTCCAGATGCTGCTCCAGA
1212  K V E T T Y I I Q G N N F L K L K E R K
3661  AAAAGTTGAGACCACGTATATCATTCAAGGGAACAACTTCCTCAAACTCAAAGAGCGCAA
1232  S G T D K N S A I D L A N M L N P D G V
3721  GTCTGGAACTGATAAGAATTCAGCCATTGATTTGGCGAATATGTTAAACCCCGACGGTGT
1252  E Y T Q E E E E E E E Y E E M S R S P T
3781  TGAATATACTCAGGAAGAAGAAGAAGAAGAGGAATATGAAGAAATGTCAAGATCCCCAAC
1272  E E T S D D E P S Q A A V Y N N A P V I
3841  GGAAGAGACTTCAGACGACGAGCCCAGTCAAGCAGCAGTTTACAACAATGCTCCAGTGAT
1292  K R T Y R K R E L S N E D G P L N L V T
3901  AAAACGTACCTATAGAAAGCGGGAGTTGTCAAACGAGGATGGACCTCTTAACTTGGTAAC
1312  P P A H T P N P R G R P R K Y P K N S V
3961  ACCACCTGCTCATACTCCGAACCCAAGAGGGCGCCCAAGGAAGTATCCCAAGAATAGTGT
1332  T P E A E K S L T D Y D Y N P G T S Q R
4021  AACACCAGAAGCTGAAAAAAGCCTCACCGACTACGACTACAATCCGGGAACATCTCAACG
1352  R A L K K G Y V Q L E D G E I V G E D C
4081  ACGTGCACTTAAGAAAGGTTACGTACAACTCGAAGACGGAGAAATTGTCGGCGAAGATTG
1372  E Y V P E K T P S G R L I R Q A V A R R
4141  CGAATACGTGCCTGAAAAAACACCAAGTGGAAGATTGATTCGACAAGCTGTTGCTAGACG
1392  S F A F A D E E E E E E E Y E E S P I V
4201  AAGCTTTGCTTTTGCTGATGAGGAAGAGGAGGAGGAAGAGTATGAAGAATCTCCAATTGT
1412  K K P K I A G R P V G R P R K D A N K L
4261  TAAAAAGCCCAAGATTGCTGGAAGACCAGTCGGACGACCGCGCAAAGATGCTAATAAGCT
1432  P T P T P P S N E *
4321  GCCAACCCCCACACCACCCAGCAACGAATAAGTGGAAATATTTTCATCCACCGTTCCTGA
4381  TTGTTGTTTTTATATATAATTTTTTCTCCATTGATGTTTTTGATGATTAAGTCATACGCA
4441  TAGTTTTACCCTGTTACTTTGATTGCCCTTAAAATTACCACTTTTATTTTACCTATTTAT
4501  TTTAATCATCATTCATCTGAAACCTCACAATGATGAGATGATCTCATCATTTTTATATTT
4561  TGTAGTTTTATATCAGTTTTATAAATGTTCACCGAAAAAAAAAAAAAAAAAAAAAAAAA
4621  AAA
```

```
C    1 TTTGATGCCA ACTGGTTTTT TTCTAATTCT TTCCAAATGG TTTCACATCA
    51 CCAAATGACA ATTTTCCTTT ACTTTCCTAT CTTGCTTATC ATACACTATC
   101 ACTTATTCAG
```

FIGURE 4.—*continued*

DNA sequences encoding the 4.6-kb transcript are located within the 7.2-kb *Eag*I-*Sal*I fragment sufficient for rescue of *lin-15* B function, while DNA sequences encoding the 2.3-kb transcript, except for the first exon and part of the first intron, are present within the 3.8-kb *Sal*I-*Nru*I fragment required only for rescue of *lin-15* A activity. In addition, the *lin-15* A mutant *n767* contains a 300-bp deletion within the 3-kb *Eco*RI fragment that contains part of the coding region for the 2.3-kb transcript (see below). These observations suggest that the 2.3-kb transcript encodes *lin-15* A gene activity and that the 4.6-kb transcript encodes *lin-15* B activity.

To confirm that these two transcripts encode the two *lin-15* proteins, we introduced frameshift mutations into the putative *lin-15* coding regions within the *Spe*I-*Nru*I genomic DNA clone and then tested these modified clones for the rescue of *lin-15* A and B function by germline transformation (see MATERIALS AND METHODS). We found that a *Spe*I-*Nru*I genomic clone containing a frameshift mutation within the predicted coding region for the downstream 2.3-kb transcript rescued *lin-15* B but not *lin-15* A function (Figure 2B). A clone altered to restore the appropriate reading frame rescued *lin-15* A function in 6/6 transformed F_2 populations, indicating that the introduced frameshift mutation within the coding region of the 2.3-kb transcript caused the loss of *lin-15* A rescuing activity. By contrast, a *Spe*I-*Nru*I genomic clone possessing a frameshift mutation within the coding region for the 4.6-kb transcript rescued *lin-15* A but not *lin-15* B activity. A clone modified to restore the proper reading frame rescued *lin-15* B function in 16/16 transformed F_2 populations, demonstrating that the frameshift mutation within the coding region of the 4.6-kb transcript eliminated the *lin-15* B rescuing activity. Together, these results establish that the 2.3-kb transcript encodes *lin-15* A activity and that the 4.6-kb transcript encodes *lin-15* B activity.

Based on the DNA sequences, the 2.3-kb *lin-15* A cDNA encodes a 719-amino acid protein and the 4.6-kb *lin-15* B cDNA encodes a 1,440-amino acid protein (Figure 4, A and B). The two *lin-15* proteins are not obviously similar in sequence to each other, and a search of the GenBank, PIR and SWISS-PROT databases using BLAST (ALTSCHUL and LIPMAN 1990) failed to identify any protein highly similar to either. Thus, the *lin-15* proteins define new types of molecules involved in intercellular signaling.

***lin-15* Muv mutations are rearrangements:** To investigate the molecular basis of the different classes of *lin-15* mutations, we analyzed genomic DNA prepared from *lin-15* Muv mutants as well as from *lin-15* mutants defective for either class A or class B activity (see MATERIALS AND METHODS). All eight *lin-15* Muv mutants analyzed, including four carrying EMS-induced alleles, had chromosomal rearrangements in the *lin-15* coding regions: seven mutants (*e1763*, *n309*, *n765*ts, *n1139*, *n1296*, *n1331*, *n1344*, *n2141*) contained deletions and one, *n1296*, had a deletion and a 1.6-kb insertion (Figure 5). The lengths of the deletions varied from about 200 bp in the *n765* mutant to at least 15 kb in the *e1763*, *n309* and *n1344* mutants. The *e1763*, *n309*, *n1139*, *n1344* and *n2141* Muv mutants had deletions that affected all or most of the genomic region encoding the two *lin-15* transcripts.

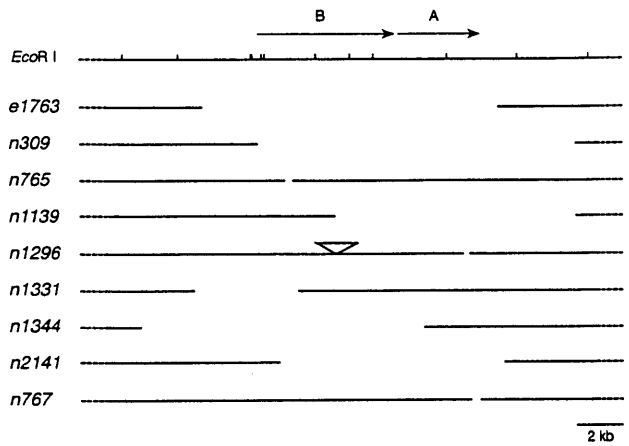

FIGURE 5.—*lin-15* Muv mutants contain chromosomal rearrangements that affect both the *lin-15* A and B coding regions. Based on the analysis of *Eco*RI restriction fragment length polymorphisms, the approximate position of the deletion and insertion is shown for each Muv mutant and for the *lin-15* A mutant *n767*. For example, the *n765*ts mutant contains a 200-bp deletion within the 2.1-kb *Eco*RI fragment; a 200-bp gap is shown within the center of the region, as the precise location within the 2.1-kb fragment was not determined. The genomic region not analyzed is depicted as a dotted line.

The 4-kb deletion present in the *n1331* mutant removed part of the *lin-15* B coding region and sequences 5′ of the *lin-15* B gene. Unless a second, undetected mutation exists in the *n1331* strain, this alteration caused the loss of *lin-15* A and *lin-15* B function. The requirement for the region deleted in the *n1331* strain for the expression of both *lin-15* activities is consistent with our germline transformation results, which indicate that this region is essential for the rescue of both *lin-15* A and B function. The *n1296* mutant had a 1.6-kb insertion within a region encoding the *lin-15* B gene and a 200-bp deletion in the 3-kb *Eco*RI fragment that contains part of the *lin-15* A gene. *n1296* was identified as a spontaneous Muv mutant in the mutator strain TR679 (KIM and HORVITZ 1990). The 1.6-kb insertion might be either a *Tc1* or a *Tc4* transposon, both of which are about 1.6 kb in size (ROSENZWEIG *et al.* 1983; YUAN *et al.* 1991).

The *n765*ts mutant has a temperature-sensitive defect in *lin-15* A activity and lacks *lin-15* B activity, resulting in a temperature-sensitive Muv phenotype (FERGUSON and HORVITZ 1989). The 200-bp deletion in the *n765*ts mutant is within the genomic region encoding the *lin-15* B transcript and likely disrupts *lin-15* B function; it is unclear whether this deletion or another lesion, perhaps a point mutation within the *lin-15* A gene, confers the temperature-sensitive defect in *lin-15* A function. This deletion might lead to a temperature-dependent loss of *lin-15* A function if it caused the elimination of the *lin-15* B protein and if the *lin-15* A protein were unstable at higher temperatures in the absence of *lin-15* B protein. If so, the three *lin-15* class B mutations (*n374, n743, n744*) must not eliminate the *lin-15* B protein, as they do not cause a temperature-dependent loss of *lin-15* A function.

In short, the alterations within all *lin-15* Muv mutants examined, except possibly *n765*ts, affected regions defined by germline rescue experiments to be required for both *lin-15* A and B activity. No obvious chromosomal alterations were found in two of three EMS-induced *lin-15* class A mutants (*n433, n749*) or in three EMS-induced *lin-15* class B mutants (*n374, n743, n744*) (data not shown). The *lin-15* class A mutant *n767* had a 300-bp deletion within the 3-kb *Eco*RI fragment that encodes part of the *lin-15* A gene (Figure 5).

DISCUSSION

lin-15 is a complex locus that encodes two separate genetic activities involved in the negative regulation of vulval induction (FERGUSON and HORVITZ 1989). We identified an 11-kb genomic fragment that complemented the loss of both of these activities when maintained as an extrachromosomal array following germline transformation. The analysis of cDNAs and genomic DNA sequences indicated that two distinct, non-overlapping and similarly oriented transcripts of lengths 2.3 and 4.6 kb encode the two *lin-15* gene activities. The 4.6-kb transcript encodes *lin-15* B function and is processed by the addition of the SL1 *trans*-spliced leader. The 2.3-kb transcript encodes *lin-15* A function, is processed by the addition of the SL1 and SL2 *trans*-spliced leaders and is located 110 bp downstream of the polyadenylation site of the 4.6-kb transcript.

The mRNAs of six *C. elegans* genes are *trans*-spliced to SL2, and each of these genes is located between 96 and 294 bp downstream of a similarly oriented gene (SPIETH *et al.* 1993). In particular, SPIETH *et al.* reported the unpublished conclusions of L. HUANG and P. STERNBERG that the *lin-15* A gene is located downstream of the *lin-15* B gene and that the *lin-15* A transcript is *trans*-spliced to SL2. HUANG *et al.* (1994) independently cloned and characterized the *lin-15* locus and obtained results similar to ours. SPIETH *et al.* proposed that those gene clusters are transcribed as a single polycistronic mRNA precursor and that the mature transcript for the downstream gene is formed by cleavage at the polyadenylation site and by *trans*-splicing to SL2.

The results of our germline rescue experiments and the site of the deletion in the *lin-15* Muv mutant *n1331* are consistent with the cotranscription model proposed by SPIETH *et al.* for the expression of the two *lin-15* transcripts. For example, if the *lin-15* A and *lin-15* B genes were transcribed as a single mRNA precursor, the expression of the downstream *lin-15* A gene would require expression of the upstream *lin-15* B gene. We found that rescue of *lin-15* A gene activity required the 7-kb region upstream of the *lin-15* A coding region that alone rescued only *lin-15* B function and contained the *lin-15* B gene. A frameshift mutation within the *lin-15* B gene eliminated the rescue of only *lin-15* B gene function and not the rescue of *lin-15* A gene activity, suggesting that

the expression of the downstream *lin-15* A gene required the transcription but not the translation of the upstream *lin-15* B gene. The deletion present in the Muv mutant *n1331* removed part of the *lin-15* B coding region and sequences 5′ of the *lin-15* B gene. Unless another lesion exists in the *n1331* strain, this deletion confers the loss of both *lin-15* A and B activities, indicating that this region is required for the expression of both *lin-15* functions. Together, these results support the cotranscription model proposed by SPIETH *et al.* (1993) but do not exclude the possibility that the promoter for the *lin-15* A gene is present within the *lin-15* B gene.

Using the technique of RT-PCR, we recovered cDNAs for the *lin-15* A gene using primers for sequences of either SL1 or SL2. These results indicate that the downstream *lin-15* A transcript is processed by *trans*-splicing using SL1 and SL2, although the relative abundances cannot be estimated from our data. Similar results were reported for transcripts of the downstream *gpd-3* gene and were suggested to reflect a variability in the selectivity of the *trans*-splicing process for polycistronic precursors (SPIETH *et al.* 1993). The *lin-15* A transcript might also be alternatively *trans*-spliced in this way. On the other hand, the SL1-containing transcripts might originate from another promoter located within the *lin-15* B gene and not be derived from a polycistronic precursor.

The class A and class B synthetic multivulva genes define redundant genetic pathways involved in the negative regulation of vulval induction (FERGUSON and HORVITZ 1989). Although multiple class B genes are located on chromosome *III*, the class A and class B genes are not clustered, except for the *lin-15* locus. Our analysis provides a molecular basis for understanding the *lin-15* complex locus but fails to explain why the *lin-15* A and B genes are clustered and apparently cotranscribed. Perhaps the cotranscription of the *lin-15* A and B genes ensures that both genes are expressed within the same cell and at similar levels.

The *lin-15* null phenotype is Muv: The phenotype caused by *lin-15* mutations in *trans* to a deficiency of the locus suggests that the known *lin-15* Muv alleles may not completely eliminate *lin-15* gene function (FERGUSON and HORVITZ 1985). Specifically, the phenotype of *lin-15(n765*ts*)/mnDf4* animals at 25° is more severe than that of *lin-15(n765*ts*)* homozygotes at 25°. *lin-15(n765*ts*)* animals raised at 25° have a highly penetrant Muv phenotype similar to that of *lin-15(n309)* and other strong Muv alleles; most *n765/mnDf4* animals raised at 25° grow to the size of L3 larvae and are sterile, which is a phenotype only occasionally exhibited by *lin-15(n765*ts*)* animals grown at 25°. At 20°, the deficiency does not enhance the *lin-15* phenotype. A null mutation in *trans* to a deficiency uncovering that locus is likely to cause the same phenotype as a homozygous null mutation, which suggested that the strong *lin-15* alleles may not be null. However, deficiencies often remove large chromosomal regions containing many genes, so haplo-insufficiency could cause strains heterozygous for a particular mutation and a deficiency to have a more severe phenotype than homozygous mutants even if the mutation is null. Our molecular analysis revealed that some Muv mutations delete the complete *lin-15* coding region and thus cannot possess any *lin-15* function. For example, the *e1763* mutation deletes the entire *lin-15* genomic region, while the *n309*, *n1139*, *n1344* and *n2141* mutations remove most of this region. Thus, *e1763* and most likely the other strong *lin-15* mutations are true null alleles.

Although the class A and class B pathways are redundant for the formation of the vulva, some mutations in the class B pathway affect viability and fertility in the presence of a functional class A pathway, indicating that some genes in the class B pathway may have unique functions outside of vulval formation (FERGUSON and HORVITZ 1989). In particular, three class B mutations *lin-9(n112)*, *lin-35(n745)* and *lin-37(n758)* cause a reduction in fertility and body size at 25°, and a double mutant carrying *lin-9(n112)* and *lin-35(n745)* is sterile. By contrast, the complete elimination of *lin-15* A and B activity causes few defects in fertility and body size at 25° and fewer defects at 20°. Although *lin-15* B activity is required in the class B pathway for vulval formation, *lin-15* B function is largely dispensable in the class B pathway for other processes.

Possible roles for the *lin-15* A and *lin-15* B proteins: The expression of vulval cell fates depends upon the activation of a tyrosine kinase/*ras* signaling cascade that during wild-type development is triggered by a signal from the gonadal anchor cell (for review, see HORVITZ and STERNBERG 1991) (Figures 1B and 6A). The removal of *lin-15* function causes the activation of this signaling pathway even in the absence of the anchor cell inductive signal. A signal involving *lin-15* from the surrounding hypoderm might normally prevent the activation of this signaling pathway, since mosaic analysis suggests that *lin-15* functions in the hypoderm (HERMAN and HEDGECOCK 1990) (Figures 1D and 6A). As loss-of-function mutations in the receptor tyrosine kinase *let-23* gene, the SH3-SH2-SH3 adaptor protein *sem-5* gene, *let-341*, *let-60 ras* and *lin-45 raf* suppress the Muv phenotype induced by *lin-15* mutations, *lin-15* acts upstream of these five genes in the genetic pathway for vulval induction (FERGUSON *et al.* 1987; BEITEL *et al.* 1990; HAN *et al.* 1990; CLARK *et al.* 1992, 1993; HAN *et al.* 1993). Preliminary data suggest that *let-23* and *let-60* are expressed in P3.p–P8.p (M. KOGA and Y. OHSHIMA; J. DENT, L. AVERY and M. HAN, personal communications), suggesting that these genes as well as *sem-5*, *let-341* and *lin-45* act in these cells to induce the differentiation of vulval cell types. Thus, the action of *lin-15* within

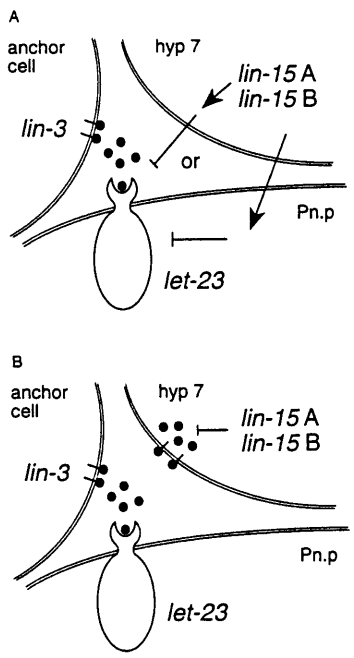

FIGURE 6.—Two models for the negative regulation of the tyrosine kinase/*ras* signaling cascade by *lin-15*. (A) A signal from the hypoderm involving the two *lin-15* proteins may inhibit the receptor tyrosine kinase *let-23* by direct interactions. The products of other class A and class B synthetic multvulva genes might mediate these intercellular interactions because the *lin-15* A and B proteins lack hydrophobic signal sequences. Alternatively, the hypoderm might signal to factors within the Pn.p cells that block the action of *let-23*. These factors may be encoded by other synthetic multivulva genes. (B) The action of the *lin-15* proteins may prevent the hypoderm from producing or releasing molecules related to the *lin-3* product that would inappropriately activate the vulval inductive pathway.

the hypoderm may negatively regulate the *let-23* receptor tyrosine kinase signaling pathway within the cells P3.p–P8.p.

The sequences of the 719- and 1,440-amino acid *lin-15* proteins do not suggest how *lin-15* A and *lin-15* B might function. One possibility is that a hypodermal signal involving *lin-15* directly inhibits the *let-23* receptor tyrosine kinase (Figure 6A). Since neither of the *lin-15* proteins contains a hydrophobic signal sequence, this hypothesis would suggest that products of other synthetic Muv genes of both the A and B classes directly mediate these intercellular interactions. The inhibition of *let-23* activity could be either directly from the hypoderm or indirectly from within the cells P3.p–P8.p, in which case we expect some synthetic Muv genes to act within these cells. The inhibitory signal from the hypoderm might be similar to the signal involving the Drosophila gene *argos* (FREEMAN *et al.* 1992). Mutations in the *argos* gene cause the overproduction of photoreceptors within the developing fly eye analogously to the proliferation of vulval cells that occurs in *lin-15* mutants. *argos* functions non-cell-autonomously, and, based upon its DNA sequence, is predicted to encode a secreted protein.

Alternatively, the *lin-15* A and B proteins might act in parallel to prevent the hypoderm from expressing a signal that inappropriately causes vulval induction. For example, in the absence of *lin-15* function, the hypoderm might release a factor similar to the *lin-3* protein, which is related to TGF-α (Figure 6B).

The *lin-15* A and B genes encode unfamiliar molecules involved in intercellular signaling. Receptor tyrosine kinase/*ras* signaling pathways highly conserved with the *C. elegans* vulval induction pathway have been identified in both Drosophila and mammals, suggesting that molecules similar to the *lin-15* A and B proteins exist in these organisms. The further study of *lin-15* and other synthetic Muv genes may lead to a greater understanding of *C. elegans* vulval induction as well as of the regulation of other tyrosine kinase/*ras* signaling pathways.

We are grateful to STUART KIM for providing the TR679-derived *lin-15* mutants, to MIKE NONET and BARBARA MEYER for sharing unpublished results regarding the location of the *sdc-1* gene and to TOM BLUMENTHAL for suggestions concerning possible *trans*-splicing of the *lin-15* transcripts. We thank CORI BARGMANN, ANDREW CHISHOLM, ERIK JORGENSEN, KERRY KORNFELD, VILLU MARICQ and PIALI SENGUPTA for critically reading the manuscript. This work was supported by U.S. Public Health Service grants GM24663 and GM24943 to H.R.H. and by the Howard Hughes Medical Institute. S.G.C. was a Research Associate of the Howard Hughes Medical Institute during part of this work. H.R.H. is an Investigator of the Howard Hughes Medical Institute. The Genbank accession numbers for the *lin-15* A cDNA, *lin-15* B cDNA and 11.7-kb *lin-15* genomic DNA fragment are U10411, U10412 and U10413, respectively.

LITERATURE CITED

ALTSCHUL, S. F., and D. J. LIPMAN, 1990 Protein database searches for multiple alignments. Proc. Natl. Acad. Sci. USA **87:** 5509–5513.

AROIAN, R. V., and P. W. STERNBERG, 1991 Multiple functions of *let-23*, a *Caenorhabditis elegans* receptor tyrosine kinase gene required for vulval induction. Genetics **128:** 251–267.

AROIAN, R. V., M. KOGA, J. E. MENDEL, Y. OHSHIMA and P. W. STERNBERG, 1990 The *let-23* gene necessary for *Caenorhabditis elegans* vulval induction encodes a tyrosine kinase of the EGF receptor subfamily. Nature **348:** 693–699.

BARSTEAD, R. J., and R. H. WATERSTON, 1989 The basal component of the nematode dense-body is vinculin. J. Biol. Chem. **264:** 10177–10185.

BEITEL, G. J., S. G. CLARK and H. R. HORVITZ, 1990 *Caenorhabditis elegans ras* gene *let-60* acts as a switch in the pathway of vulval induction. Nature **348:** 503–509.

BRENNER, S., 1974 The genetics of *Caenorhabditis elegans*. Genetics **77:** 71–94.

CLARK, S. G., M. J. STERN and H. R. HORVITZ, 1992 *C. elegans* cell-signalling gene *sem-5* encodes a protein with SH2 and SH3 domains. Nature **356:** 340–344.

CLARK, S. G., M. J. STERN and H. R. HORVITZ, 1993 Genes involved in two *Caenorhabditis elegans* cell-signaling pathways. Cold Spring Harbor Symp. Quant. Biol. **57:** 363–373.

COLLINS, J., B. SAARI and P. ANDERSON, 1987 Activation of a transposable element in the germ line but not the soma of *Caenorhabditis elegans*. Nature **328:** 726–728.

COULSON, A., J. SULSTON, S. BRENNER and J. KARN, 1986 Toward a physical map of the genome of the nematode *Caenorhabditis elegans*. Proc. Natl. Acad. USA **83:** 7821–7825.

COULSON, A., R. WATERSTON, J. KIFF, J. SULSTON and Y. KOHARA, 1988 Genome linking with yeast artificial chromosomes. Nature **335:** 184–186.

FERGUSON, E. L., and H. R. HORVITZ, 1985 Identification and characterization of 22 genes that affect the vulval cell lineages of the nematode *Caenorhabditis elegans*. Genetics **110:** 17–72.

FERGUSON, E. L., and H. R. HORVITZ, 1989 The multivulva phenotype of certain *Caenorhabditis elegans* mutants results from defects in two functionally redundant pathways. Genetics **123:** 109–121.

FERGUSON, E. L., P. W. STERNBERG and H. R. HORVITZ, 1987 A genetic pathway for the specification of the vulval cell lineages of *Caenorhabditis elegans*. Nature **326:** 259–267.

FREEMAN, M., C. KLAMBT, C. S. GOODMAN and G. M. RUBIN, 1992 The *argos* gene encodes a diffusible factor that regulates cell fate decisions in the Drosophila eye. Cell **69:** 963–975.

HAN, M., and P. W. STERNBERG, 1990 *let-60*, a gene that specifies cell fates during C. elegans vulval induction, encodes a *ras* protein. Cell **63:** 921–931.

HAN, M., R. V. AROIAN and P. W. STERNBERG, 1990 The *let-60* locus controls the switch between vulval and nonvulval cell fates in *Caenorhabditis elegans*. Genetics **126:** 899–913.

HAN, M., A. GOLDEN, Y. HAN and P. W. STERNBERG, 1993 *C. elegans lin-45 raf* gene participates in *let-60 ras*-stimulated vulval differentiation. Nature **363:** 133–139.

HERMAN, R. K., and E. M. HEDGECOCK, 1990 Limitation of the size of the vulval primordium of *Caenorhabditis elegans* by *lin-15* expression in surrounding hypodermis. Nature **348:** 169–171.

HILL, R. J., and P. W. STERNBERG, 1992 The gene *lin-3* encodes an inductive signal for vulval development in *C. elegans*. Nature **358:** 470–476.

HORVITZ, H. R., and P. W. STERNBERG, 1991 Multiple intercellular signalling systems control the development of the *Caenorhabditis elegans* vulva. Nature **351:** 535–541.

HORVITZ, H. R., and J. E. SULSTON, 1980 Isolation and genetic characterization of cell-lineage mutants of the nematode *Caenorhabditis elegans*. Genetics **96:** 435–454.

HUANG, L. S., P. TZOU and P. W. STERNBERG, 1994 The *lin-15* locus encodes two negative regulators of *C. elegans* vulval development. Mol. Biol. Cell **5:** 395–412.

HUANG, X. Y., and D. HIRSH, 1989 A second trans-spliced RNA leader sequence in the nematode *Caenorhabditis elegans*. Proc. Natl. Acad. Sci. USA **86:** 8640–8644.

KIM, S. K., and H. R. HORVITZ, 1990 The *Caenorhabditis elegans* gene *lin-10* is broadly expressed while required specifically for the determination of vulval cell fates. Genes Dev. **4:** 357–371.

KIMBLE, J., 1981 Alterations in cell lineage following laser ablation of cells in the somatic gonad of *Caenorhabditis elegans*. Dev. Biol. **87:** 286–300.

KRAUSE, M., and D. HIRSH, 1987 A trans-spliced leader sequence on actin mRNA in C. elegans. Cell **49:** 753–761.

LACKNER, M. R., K. KORNFELD, L. M. MILLER, H. R. HORVITZ and S. KIM, 1994 A MAP kinase homolog, *mpk-1*, is involved in *ras*-mediated induction of vulval cell fates in *Caenorhabditis elegans*. Genes Dev. **8:** 160–173.

MELLO, C. C., J. M. KRAMER, D. STINCHCOMB and V. AMBROS, 1991 Efficient gene transfer in *C. elegans*: extrachromosomal maintenance and integration of transforming sequences. EMBO J. **10:** 3959–3970.

MILLER, L. M., M. E. GALLEGOS, B. A. MORISSEAU and S. K. KIM, 1993 *lin-31*, a *Caenorhabditis elegans* HNF-3/*fork head* transcription factor homolog, specifies three alternative cell fates in vulval development. Genes Dev. **7:** 933–947.

NONET, M. L., and B. J. MEYER, 1991 Early aspects of *Caenorhabditis elegans* sex determination and dosage compensation are regulated by a zinc-finger protein. Nature **351:** 65–68.

ROSENBLUTH, R. E., C. CUDDEFORD and D. L. BAILLIE, 1985 Mutagenesis in *Caenorhabditis elegans*. II. A spectrum of mutational events induced with 1500 r of γ-radiation. Genetics **109:** 493–511.

ROSENZWEIG, B., L. W. LIAO and D. HIRSH, 1983 Sequence of the *C. elegans* transposable element *Tc1*. Nucleic Acids Res. **11:** 4201–4209.

SPIETH, J., G. BROOKE, S. KUERSTEN, K. LEA and T. BLUMENTHAL, 1993 Operons in C. elegans: Polycistronic mRNA precursors are processed by trans-splicing of SL2 to downstream coding regions. Cell **73:** 521–532.

STERNBERG, P. W., 1988 Lateral inhibition during vulval induction in *Caenorhabditis elegans*. Nature **335:** 551–554.

STERNBERG, P. W., and H. R. HORVITZ, 1986 Pattern formation during vulval development in C. elegans. Cell **44:** 761–772.

SULSTON, J., and J. HODGKIN, 1988 Methods, pp. 587–606 in *The Nematode Caenorhabditis elegans*, edited by W. B. WOOD. Cold Spring Harbor Laboratory, Cold Spring Harbor, N.Y.

SULSTON, J. E., and H. R. HORVITZ, 1977 Post-embryonic cell lineages of the nematode *Caenorhabditis elegans*. Dev. Biol. **56:** 110–156.

SULSTON, J. E., and J. G. WHITE, 1980 Regulation and cell autonomy during postembryonic development of *Caenorhabditis elegans*. Dev. Biol. **78:** 577–597.

WU, Y., and M. HAN, 1994 Suppression of activated Let-60 Ras protein defines a role of *Caenorhabditis elegans* Sur-1 MAP kinase in vulval differentiation. Genes Dev. **8:** 147–159.

YUAN, J. Y., M. FINNEY, N. TSUNG and H. R. HORVITZ, 1991 *Tc4*, a *Caenorhabditis elegans* transposable element with an unusual foldback structure. Proc. Natl. Acad. Sci. USA **88:** 3334–3338.

Communicating editor: R. K. HERMAN

Appendix

Attempts to clone *let-341* and isolation of suppressors of *let-341(n1613ts)*

Xiaowei Lu

Howard Hughes Medical Institute, Massachusetts Institute of Technology
Cambridge, MA 02139

Introduction

The gene *let-341* was previously identified as a Ras signaling gene required for vulval development (Clark et al., 1992). Loss-of-function mutations in *let-341* cause a variable larval lethal and vulvaless phenotype, which is completely suppressed by gain-of-function mutations in *let-60* Ras, suggesting that *let-341* genetically acts upstream of or in parallel to *let-60* to positively regulate the activity of *let-60*. One candidate gene for *let-341* is a guanine nucleotide exchange factor for Ras (Lowy and Willumsen, 1993). Ras proteins are membrane-bound GTPases and cycle between the active GTP-bound form and the inactive GDP-bound form. Guanine nucleotide exchange factors promote the conversion of Ras from the GDP-bound form to the GTP-bound form. The CDC25 gene of *S. cerevisiae* (Broek et al., 1987) and the *Son of Sevenless* (*Sos*) gene of *Drosophila* (Simon et al., 1991), both of which encode guanine nucleotide exchanges factors, have been shown to be essential upstream activators of Ras by genetic analyses. Furthermore, mammalian genes closely related to *Sos* have been identified and shown to have conserved functions in RTK/Ras signaling (Chardin et al., 1993). The *C. elegans* genome project has recently identified a putative Sos homolog in the *let-341* region, as predicted from genomic sequences (see below). Whether or not *let-341* encodes this Sos homolog is currently being tested (S. Clark, personal communication). To understand the role of *let-341* in vulval signaling, we attempted to identify this gene by positional cloning. In addition, to seek new genes in the Ras signaling pathway, we screened for mutations that suppress the temperature-sensitive lethality of *let-341(n1613ts)*.

Results

Mapping of *let-341*

let-341 was previously mapped to linkage group V, closely linked to *unc-62* (S. G. Clark and H. R. Horvitz, personal communications). We first positioned *let-341* on the physical map between the Tc1 polymorphism *stP3* on the left (Williams et al., 1992), and the restriction fragment length polymorphism (RFLP) associated with the cosmid R02F11, or *nPR* for short, on the right

(Figure 1). None of the cosmid clones from the region available at the time rescued the temperature-sensitive lethality of *let-341(n1613ts)* animals in germline transformation experiments, nor did any detect allele-specific polymorphisms associated with nine independently isolated *let-341* mutants (data not shown). These results indicated that *let-341* is probably located in the 'gap' regions that are represented only by yeast artificial chromosome (YAC) clones.

To further map *let-341* on the physical map, we used cosmid DNA from the region to identify new RFLPs. We identified only one new RFLP using the cosmid C18G1 but subsequent mapping revealed that it was not linked to *let-341* (see Experimental Procedures for details). Since the RFLP mapping approach was uninformative, we turned to map physically the breakpoints of deficiencies that define the genetic region of *let-341*. *let-341* was deleted by *sDf27* but not *sDf50*, indicating that it lies in between the right breakpoints of *sDf50* and *sDf27*. We tested for the presence or absence of DNA from the region in deficiency homozygotes by PCR. At the time, cosmid sequences from the region were not yet available, so we focused on several YAC clones in the region whose end sequences were determined by the genome project (A. Coulson, personal communication). We found by PCR that the YAC clone Y54H12 overlaps with Y7E8, Y58D4 and Y47D10. Furthermore, the right end of Y7E8 extends into a gap to the right of the cosmid cluster represented by C10D4. The right end of Y54H12 is deleted by *sDf27* but not *sDf50*, and therefore falls into the same region as *let-341*. Importantly, the right end of Y7E8 is not deleted by either *sDf27* or *sDf50*, and therefore defines the right boundary of *let-341*. Taken together, these data indicate that *let-341* lies in the region from *stP3* to the right end of Y7E8, which is spanned by two overlapping YAC clones Y54H12 and Y7E8. Since it is not known to what extent there is overlap between these two clones, which are about 430 kb and 175 kb in size, respectively, it is difficult to estimate the size of the region to which *let-341* has been localized. Attempts to test Y54H12 and Y7E8 for rescue of the temperature-sensitive lethality of *let-341(n1613ts)* animals were unsuccessful (see Experimental Procedures for details). Interestingly, the YAC clone Y47D7, which overlaps with Y54H12 (Figure 1), has recently been shown by the *C. elegans* genome project to contain sequences with predicted similarities to *Drosophila* and mammalian Sos proteins. It remains to be tested whether *let-341* indeed is this Sos-related gene. In short, we have localized *let-341* to a region spanned by

Y54H12 and Y7E8, which likely contains an Sos-related gene. However, the molecular identity of *let-341* remains unproved.

Isolation of suppressors of *let-341(n1613ts)*

To identify novel genes in the Ras signaling pathway, we took advantage of the temperature-sensitive lethality of *let-341(n1613)* animals. These animals are healthy with wild-type vulvae at 15°C, but die as L1 larvae with almost 100% penetrance at 25°C. We were interested in suppressor mutations that not only suppress the lethality, but also cause a Muv phenotype, which are more likely to identify genes in the vulval induction pathway. We hoped to isolate gain-of-function mutations in positive regulators or effectors of the Ras pathway, or loss-of-function mutations in negative regulators of the Ras pathway.

We screened 150,000 haploid genomes for F2 suppressors and isolated 24 Muv suppressors and 50 non-Muv suppressors. Of the Muv suppressors, 21 (*n2692-n2696, n2698-n2701, n2703-n2705, n2708, n2712, n2714-n2716, n2748-n2750, n2753*) are *lin-1* loss-of-function alleles based upon complementation tests. Two (*n2792* and *n2794*) are *let-60* mutations carrying the G13E mutation identical to previously isolated *let-60* gain-of-function alleles (Beitel et al., 1990). One allele, *n2799*, mapped very close to *let-60* but conferred a much stronger Muv phenotype than *let-60*(G13E) mutants, therefore is likely a novel allele of *let-60* (Table 1). The non-Muv suppressors are *n2754-n2791, n2793, n2795-n2798, n2800-n2806.*

To increase the chance of getting rare Muv mutations, we next screened 1.2 million haploid genomes for F1 suppressors and isolated 21 Muv suppressors and 60 non-Muv suppressors. Of the Muv suppressors, 11 (*n2930, n2961, n2964, n2965, n2967, n2975, n3000* and the rest discarded) are recessive *lin-1* alleles. The isolation of *lin-1* mutations was probably because some F1 animals of the genotype *lin-1/+; n1613* survived and propagated at the restrictive temperature as a result of the leakiness of the lethal phenotype of the *n1613* mutation. Six are *let-60* G13E mutations, 3 caused a strong dominant Muv phenotype, and incompletely penetrant recessive embryonic lethality (Table 1). These alleles, *n2892*, *n2896* and *n2940* also mapped very close to *let-60*. *n2940* had a C to T transition resulting in a missense mutation that changes an alanine at position 146 to threonine (A146V). This mutation has been previously isolated in

screens for activating Ras mutation by random mutagenesis and has been shown to have high nucleotide exchange rate (Lowy and Willumsen, 1993). The failure to isolate Muv suppressors resulting from activating mutations in signaling genes downstream of Ras may be due to the limited mutational spectrum of EMS, the mutagen used in both screens. The non-Muv suppressors include *n2893-n2895, n2897-n2905, n2907-n2912, n2926-n2929, n2931, n2933, n2935, n2937-n2939, n2942-n2947, n2950-n2952, n2955-n2960, n2962, n2966, n2968, n2969, n2974*. The remaining non-Muv suppressors suppressed the lethality of *n1613* only weakly at the restrictive temperature and therefore were discarded.

Non-Muv suppressors from both screens were not systematically characterized. Interestingly, one recessive non-Muv suppressors, *n2905*, can suppress the lethality but not the vulvaless phenotype caused by *let-23(n2020)* and *sem-5(n2030)* (Table 3), suggesting that it may act in the RTK/Ras pathway for viability but not for vulval development. This mutation maps to linkage group IV. *n2754*, *n2772*, *n2774* and *n2911* are strong, dominant suppressors and map to linkage group V. They might be intragenic revertants of *let-341(n1613ts)* (Table 2).

Experimental Procedures

Mapping with *stP3*

stP3 was mapped to the left of *unc-62* by picking Unc non-Dpy and Dpy non-Unc recombinants from *unc-62 dpy-11/stP3* hermaphrodites and scoring the progeny of these recombinants for *stP3*. 54/54 Dpy non-Unc recombinant had *stP3*, and 0/31 Unc non-Dpy recombinants had *stP3*. *let-341* was mapped to the right of *unc-62* by picking at restrictive temperature Unc non-Let recombinants from *unc-62 let-341(n1613ts)/stP3* hermaphrodites and scoring the progeny of these recombinants for *stP3*. None of the eleven Unc non-Let recombinants had *stP3*.

Mapping with RFLPs

To map *let-341* with respect to RFLPs, we mated *let-341 unc-46/let-341* or *let-341 dpy-11/let-341* males into RW7000 hermaphrodites and selected cross progeny of the genotype *let-341 unc-46/nPR eP74* and *let-341 dpy-11/nPR eP74*, respectively. 41 Unc non-Let and 19 Dpy non-Let

recombinants were picked and homozygozed. DNA was extracted from these recombinants, digested with appropriate restriction enzyme, Southern blotted and probed with appropriate cosmid. Of the 41 Unc non-Let recombinants, 9 were nPR eP74, 10 were nPR, and 22 were non-nPR non-eP74. Of the 19 Dpy non-Let recombinants, 13 were nPR eP74, 2 were nPR, and 4 were non-nPR non-eP74. The RFLP detected by C18G1 appeared to be unlinked to linkage group V, based on the following observations. First, the above Dpy non-Let and Unc non-Let homozygous recombinants are frequently found to be heterozygous for the C18G1 polymorphism. Second, the C18G1 polymorphism segregated independently of either *dpy-11*, *unc-46*, *eP74* or *nPR*. It is likely that C18G1 contains a repetitive element that is polymorphic elsewhere in the genome, or that C18G1 itself is unlinked to linkage group V and was misplaced on the physical map.

PCR on deficiency homozygotes

sDf27/+ and *sDf50/+* hermaphrodites were picked individually to a plate, allowed to lay eggs for an hour, and removed from the plate. After 24 to 48 hours, embryos that remained unhatched and appeared dead, presumably homozygous for the defiencency, were subject to duplex PCR using a pair of test primers and a pair of 'internal control' primers, which amplify from a non-deleted region. The size of the control PCR product was designed to be bigger than that of the test product so as to not outcompete the test product when PCRed from wild type. We concluded that a test DNA was deleted by the deficiency when the control product but not the test product was amplified in multiple samples tested.

Determination of overlap among YAC clones in the *let-341* region

The possible overlap between the YAC Y54H12 on the left and Y7E8, Y54D8 and Y47D10 on the right was determined by PCR of miniprep DNA from yeast strains carrying individual YAC using primers that amplify the right ends of Y54H12 and Y7E8, respectively. Y54H12 was found to overlap with Y7E8 and Y54D8 and Y47D10. Furthermore, the right end of Y54H12 appeared to extend into a gap since it could not be amplified from DNA of cosmids left of the gap. Similarly, the right end of Y7E8 also was found to extend into a gap.

Rescue attempts with Y54H12 and Y7E8

To test the YAC clones Y54H12 and Y7E8 for rescue of the *let-341* phenotype, we separated the YAC DNA from yeast chromosomal DNA by pulsed field gel electrophoresis in 1% agarose gel. The YAC DNA was cut out of the gel and electroeluted and ethanol precipitated. YAC DNA was coinjected with the *rol-6* DNA marker pRF4 into *let-341(n1613ts)* animals. However although F1 transgenic animals can occasionally be obtained, no transgenic lines were established after multiple attempts. It is likely that the YAC DNA are toxic or extrachromosomal array containing the YAC is unstable.

Suppressor screen of *let-341(n1613ts)*

let-341(n1613ts) hermaphrodites were mutagenized with ethyl methanesulfonate (EMS) (Brenner, 1974). In the F2 screen, mutagenized *let-341(n1613ts)* animals were picked to separate large petri plates and their F1 progeny were allowed to grow at 20°C until L4. The plates were then shifted to 25°C. After 3 days at 25°C surviving F2 adults were picked to separate petri plate. Those that propagated at 25°C were kept as suppressors (Figure 2). Only one isolate from each original plate was kept to ensure independent isolation.

In the F1 screen, mutagenized *let-341(n1613ts)* animals were picked to separate petri plates and allowed to recover overnight at 20°C and then shifted to 25°C. Survivors were picked a week later to a new plate. Again those that propagated at 25°C were kept and only one isolate from each original plate was kept (Figure 2).

Mapping of the strong dominant Muv mutations

To test whether *n2799*, *n2892*, *n2896* and *n2940*, which conferred a strong dominant Muv phenotype, are novel *let-60* mutations, we constructed strains of the genotype *unc-24 dpy-20/sup; let-341(n1613ts)* and *dpy-20 unc-30/sup; let-341(n1613ts),* where *sup* is one of the four Muv mutations. The strains were maintained at 25°C and Dpy Muv and Unc Muv recombinants were screened for. While Unc Muv animals were readily identified, no Dpy Muv recombinants were found, indicating that they are tightly linked to *dpy-20*, and by inference to *let-60.*

References

Beitel, G. J., Clark, S. G., and Horvitz, H. R. (1990). *Caenorhabditis elegans ras* gene *let-60* acts as a switch in the pathway of vulval induction. Nature *348*, 503-509.

Brenner, S. (1974). The genetics of *Caenorhabditis elegans*. Genetics *77*, 71-94.

Broek, D., Toda, T., Michaeli, T., Levin, L., Brichmeier, C., Zoller, M., Powers, S. and Wigler, M. (1987). The *S. cerevisiae* CDC25 gene product regulates the RAS/adenylate cyclase pathway. Cell *48*, 789-799.

Chardin, P., Camonis, J. H., Gale, N. W., Van Aelst, L., Schlessinger, J., Wigler, M. H. and Bar-Sagi, D. (1993). Human Sos1: a guanine nucleotide exchange factor for Ras that binds to GRB2. Science *260*, 1338-1343.

Clark, S. G., Stern, M. J., and Horvitz, H. R. (1992). Genes involved in two *Caenorhabditis elegans* cell-signaling pathways. Cold Spring Harb Symp Quant Biol *57*, 363-373.

Lowy, D. R., and Willumsen, B. M. (1993). Function and regulation of ras. Annu Rev Biochem *62*, 851-891.

Simon, M. A., Bowtell, D. D. L., Dodson, G. S., Laverty, T. R. and Rubin, G. M. (1991). Ras1 and a putative guanine nucleotide exchange factor perform crucial steps in signaling by the Sevenless protein tyrosine kinase. Cell *67*, 701-716.

Williams, B. D., Schrank, B., Huynh, C., Shownkeen, R., and Waterston, R. H. (1992). A genetic mapping system in *Caenorhabditis elegans* based on polymorphic sequence-tagged sites. Genetics *131*, 609-624.

Figure 1. Genetic and physical maps of the *let-341* region. Genetic map is shown on the top. Physical map is shown on the bottom. cosmid and YAC clones are indicated by horizontal lines. All 'gap' regions except the one left of the C10D4 cosmid cluster are indicated by double vertical lines. The gap left of the C10D4 cosmid cluster is magnified to indicate the overlap of Y54H12 with Y7E8 and other YAC clones. The corresponding positions of the RFLPs flanking *let-341* on both maps are indicated by dotted lines. *let-341* is located in between *stP3* and the left end of Y7E8 on the physical map.

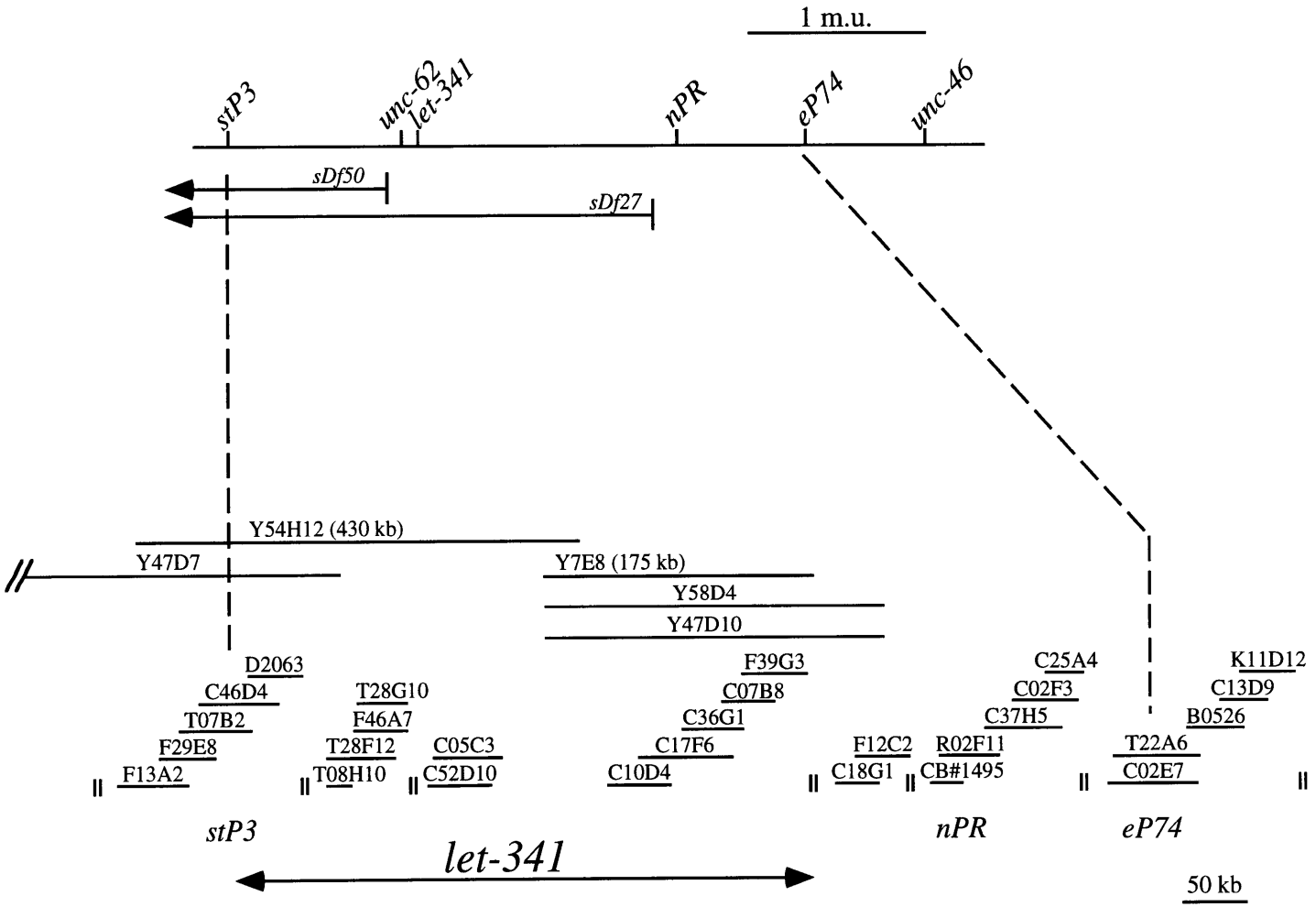
1 m.u.
stP3
unc-62
let-341
nPR
eP74
unc-46
sDf50
sDf27
Y54H12 (430 kb)
Y47D7
Y7E8 (175 kb)
Y58D4
Y47D10
D2063
C46D4
T07B2
F29E8
F13A2
T28G10
F46A7
T28F12
T08H10
C05C3
C52D10
F39G3
C07B8
C36G1
C17F6
C10D4
C25A4
C02F3
C37H5
F12C2
C18G1
R02F11
CB#1495
K11D12
C13D9
B0526
T22A6
C02E7
stP3
nPR
eP74
let-341
50 kb

Figure 2. Summary of *let-341(n1613ts)* suppressor screens. In the F2 screen, mutagenized P0 animals were raised at 20°C until their F1 progeny growed to L4. Then the plates were shifted to 25°C and surviving F2 animals were isolated and allowed to propagate at 25°C. Only one isolate from each P0 plate was kept. In the F1 screen, mutagenized P0 animals were allowed to recover at 20°C overnight before shifting to 25°C. Survivors at 25°C were isolated a week later. Only one isolate from each P0 plate was kept. The results of the screens are summarized on the bottom.

F2 screen

EMS

P0 — *let-341(n1613ts)* at 20°C

↓

F1 — grow to L4 at 20°C, then shift to 25°C

↓

F2 — recover surviving L4 animals at 25°C

↓

Keep at 25°C and discard *n1613* escapers

F1 screen

EMS

P0 — *let-341(n1613ts)* at 25°C

↓

F1 — A week later, clone out survivors

↓

Keep at 25°C and discard *n1613* escapers

Results:

sreen	#haploid genomes screened	#suppressors isolated	
		#Muv	#non-Muv
F2	150,000	24 *lin-1(lf)* 3 *let-60(gf)*	50
F1	1,200,000	11 *lin-1(lf)* 9 *let-60(gf)*	60

Table 1. *let-60* mutations isolated as *let-341(n1613)* suppressors

Allele	Mutation in *let-60*	screen
n2792	G13E	F2
n2794	G13E	F2
n2906	G13E	F1
n2932	G13E	F1
n2934	G13E	F1
n2936	G13E	F1
n2941	G13E	F1
n2963	G13E	F1
n2799	ND	F2
n2892	ND	F1
n2896	ND	F1
n2940	A146V	F1

Table 2. Mapping data for some of the non-Muv *let-341* suppressors

Allele	Linkage Group	Linked Marker
n2905	IV	*unc-5* (1/37)
n2754	V	*dpy-11* (6/20)
n2772	V	*dpy-11* (6/24)
n2774	V	*dpy-11* (9/21)
n2908	V	*dpy-11*
n2910	V	*dpy-11*
n2911	V	*dpy-11*

Numbers in parentheses indicate number of homozygous suppressors that segregated the linked marker.

Table 3. *n2905* suppresses the lethality of *let-23(n2020)* and *sem-5(n1619)*

Genotype	Phenotype		
	Let	Vul	WT
n2020	90%	10%	0%
n2020; n2905	<1%	99%	<1%
n1619	91%	9%	0%
n2905; n1619	1%	76%	23%